



2012-11-02

# Regulation of Sensory Neurogenesis in the Trigeminal Placode: Notch Pathway Genes, Pax3 Isoforms, and Wnt Ligands

Jason Samuel Adams  
*Brigham Young University - Provo*

Follow this and additional works at: <https://scholarsarchive.byu.edu/etd>

 Part of the [Cell and Developmental Biology Commons](#), and the [Physiology Commons](#)

---

## BYU ScholarsArchive Citation

Adams, Jason Samuel, "Regulation of Sensory Neurogenesis in the Trigeminal Placode: Notch Pathway Genes, Pax3 Isoforms, and Wnt Ligands" (2012). *All Theses and Dissertations*. 3144.  
<https://scholarsarchive.byu.edu/etd/3144>

This Dissertation is brought to you for free and open access by BYU ScholarsArchive. It has been accepted for inclusion in All Theses and Dissertations by an authorized administrator of BYU ScholarsArchive. For more information, please contact [scholarsarchive@byu.edu](mailto:scholarsarchive@byu.edu), [ellen\\_amatangelo@byu.edu](mailto:ellen_amatangelo@byu.edu).

Regulation of Sensory Neurogenesis in the Trigeminal Placode: Notch Pathway Genes,  
Pax3 Isoforms, and Wnt Ligands

Jason S. Adams

A dissertation submitted to the faculty of  
Brigham Young University  
in partial fulfillment of the requirements for the degree of

Doctor of Philosophy

Michael R. Stark, Chair  
Sterling N. Sudweeks  
R. Paul Evans  
Paul R. Reynolds  
Robert E. Seegmiller

Department of Physiology and Developmental Biology  
Brigham Young University

September 2012

Copyright © 2012 Jason S. Adams

All Rights Reserved

## ABSTRACT

### Regulation of Sensory Neurogenesis in the Trigeminal Placode: Notch Pathway Genes, Pax3 Isoforms, and Wnt Ligands

Jason S. Adams

Department of Physiology and Developmental Biology, BYU  
Doctor of Philosophy

This dissertation is divided into three chapters, each discussing the study of different regulatory molecules involved in sensory neurogenesis occurring in the trigeminal placode.

Chapter one is a spatiotemporal description of Notch pathway genes in chick opV placode by stage-specific expression analysis, showing expression of many Notch pathway genes and effectors in the opV placode. Notch pathway gene expression is primarily confined to the ectoderm with highest expression of these genes at the beginning stages of peak neuronal differentiation. This information preceded studies of the functional roles that Notch signaling has in the opV placode and how it may affect the transcription factor, Pax3.

Chapter two is a study of the transcription factor Pax3 and its role in opV placode development and sensory neuron differentiation. Pax3 is known to activate or repress gene transcription, and its activity may be dependent on the splice variant or isoform present. We show through RT-PCR that alternative splice forms of Pax3 are present at stages of chick development corresponding to cellular competence, cellular differentiation and ingression, and cellular aggregation. We have named these splice forms, Pax3V1 and Pax3V2.

Using quantitative RT-PCR we show that Pax3V2 is consistently expressed at lower levels compared to Pax3 during cellular competence and differentiation. In order to determine the function of the three splice forms, we misexpressed them in the opV placode and analyzed the effect on neurogenesis. We looked at markers for neuronal differentiation of targeted cells after *in ovo* electroporation of Pax3, Pax3V1, and Pax3V2, which showed a significant difference between the control and each construct, but not between the groups of constructs. To enhance the process of neurogenesis we exposed the electroporated embryos to DAPT, a Notch signaling inhibitor that enhances sensory neurogenesis. Using this method we found that misexpression of Pax3 and Pax3V1 resulted in cells failing to differentiate, while Pax3V2 misexpression more closely resembles the neuronal differentiation seen in controls. These results show that the Pax3V2 isoform allows for neuronal differentiation of opV placodal cells after misexpression, while the Pax3 isoform and the Pax3V1 isoform block neuronal differentiation.

Chapter three is a study of the necessity of Wnt signaling originating from the neural tube to induce Pax3 expression in the opV placode. A double knockout of Wnt1 and Wnt3a was produced to determine the necessity of these genes in opV placode development. Pax3 expression in the opV placode at E8.5 and E9.5 was markedly reduced in the double mutants when compared to wild type mice. This study shows that Wnt1 and Wnt3a genes are necessary for normal Pax3 expression, but that other signals may contribute to its induction.

Keywords: sensory neurogenesis, Notch signaling, Pax3, splice forms, isoforms, alternative splicing, ophthalmic trigeminal placode, Wnt signaling

## ACKNOWLEDGMENTS

I would like to thank Dr. Michael Stark for his direction, guidance, time, and counsel. He has always pushed me to succeed, and has had my interests and goals as a priority.

I am grateful to my committee for their support. Dr. Sterling Sudweeks has been essential in mentoring and helping me with quantitative PCR, and Dr. Paul Evans, Dr. Paul Reynolds, and Dr. Robert Seegmiller have facilitated my development as a graduate student with their teaching and guidance.

The members of the Stark lab have been great to work with and I appreciate their hard work during this research.

I would also like to thank Dr. Jeff Barrow and Aaron Smith for their help and counsel as I worked on the study using the mouse knockout models. I thank Dr. Ben Bikman as well for his help and expertise in experiments involving quantitative PCR.

I want my family to know that I appreciate their love, patience, and support for me during this time. Thank you Heather, Landon, Nathaniel, Andrew, and Harrison for being such a great family and strength. I would like to dedicate this work to my wife, Heather, and children Landon, Nathaniel, Andrew and Harrison.

This research was supported by the following source: NIH/NICHD grant #R01HD046475-01 to M.R.S.

## TABLE OF CONTENTS

TITLE PAGE.....	i
ABSTRACT.....	ii
ACKNOWLEDGMENTS.....	iii
TABLE OF CONTENTS.....	iv
LIST OF TABLES.....	xi
LIST OF FIGURES.....	xii
CHAPTER 1: Sensory Neuron Differentiation is Regulated by Notch Signaling in the Trigeminal Placode.....	1
Abstract.....	1
Introduction.....	1
Materials and methods.....	3
Chick.....	3
Whole-Mount <i>in situ</i> hybridization.....	3
Immunohistochemistry.....	5
Results.....	5
Figure 1.1 Notch signaling in the trigeminal placode.....	7-8
Figure 1.2 Notch signaling in the trigeminal placode, continued.....	9
Figure 1.3 <i>Delta1</i> gene expression domain overlaps with Pax3 protein expression.....	10
Figure 1.4 Notch pathway gene expression remains in the ectoderm at a later developmental stage.....	11

Table 1.1 Spatiotemporal expression of Notch signaling genes.....	12
Discussion.....	13
CHAPTER 2: Pax3 Splice Form Expression and Isoform Function in the Ophthalmic Trigeminal Placode.....	15
Introduction.....	15
Materials and methods.....	20
Chick.....	20
RNA isolation.....	20
RT-PCR.....	21
DNA sequencing.....	22
Mapping splicing enhancers and splicing silencers in the exon.....	22
Quantitative PCR.....	22
Plasmid constructs.....	24
Cellular transfections.....	24
Immunocytochemistry.....	25
<i>In ovo</i> electroporation.....	25
Electroporation in whole-embryo explants.....	25
Tissue culture.....	26
Immunohistochemistry.....	26
Statistical analysis.....	27
Results.....	28

Identification of Pax3 alternative splice forms.....	28
Figure 2.1 Predicted genomic structure of Pax3 in chick.....	30
Figure 2.2 N-terminal amplification of Pax3 gene.....	31
Figure 2.3 Predicted isoforms of Pax3 in chick.....	32
Figure 2.4 Pax3 sequence of exons 2, 4, and 5.....	33
Figure 2.5 C-terminal amplification of Pax3 gene.....	34
Figure 2.6 Pax3 sequence of exons 5, 6, 7, and 8.....	36
Figure 2.7 Amino acid sequence of Pax3 isoform.....	37
Figure 2.8 Predicted amino acid sequence of Pax3V1 isoform.....	38
Figure 2.9 Predicted amino acid sequence of Pax3V2 isoform.....	39
Quantitative analysis of the splice form Pax3 and the splice form Pax3V2.....	40
Figure 2.10 Fold expression change between the spatiotemporal expression of Pax3 and Pax3V2.....	42-43
Table 2.1 Analysis of variance between groups using the overall fold difference.....	44
Table 2.2 Tukey-Kramer analysis of individual fold differences.....	45-46
Table 2.3 Analysis of variance between groups using the sample's fold difference.....	47
Table 2.4 Tukey-Kramer analysis between sample pairs using the sample's fold difference.....	47
Misexpression of Pax3 and Pax3V1 may contribute to the maintenance of placodal cells, as Pax3V2 may contribute to the neuronal differentiation of placodal cells.....	48

Figure 2.11 Plasmid constructs.....	49
Figure 2.12 GFP expression and Pax3 antibody staining of cells transfected with plasmid constructs.....	50
Figure 2.13 Pax3 isoform electroporation at 6-8ss may contribute to neuronal differentiation.....	53-54
Figure 2.14 Pax3 isoform electroporation at 14-16ss may contribute to neuronal differentiation.....	55-56
Figure 2.15 <i>In ovo</i> misexpression of Pax3 constructs at 6-8ss and 14-16ss.....	57
Figure 2.16 <i>In ovo</i> misexpression of Pax3 constructs at 6-8ss and 14-16ss, continued.....	58
Figure 2.17 Pax3 isoform may contribute to neuronal Differentiation.....	62-63
Figure 2.18 Pax3 isoform contributes to neuronal differentiation with inhibition of Notch signaling.....	64-65
Figure 2.19 Misexpression of Pax3 constructs <i>in ovo</i> and <i>ex ovo</i> in culture.....	66
Table 2.5A and 2.5B Analysis of variance of Pax3/GFP cells in the ectoderm.....	67
Table 2.6A and 2.6B Tukey-Kramer analysis of Pax3/GFP cells in the ectoderm.....	68
Table 2.7A and 2.7B Analysis of variance of Pax3/GFP cells in the mesenchyme.....	69
Table 2.8A and 2.8B Tukey-Kramer analysis of Pax3/GFP cells in the mesenchyme.....	70
Table 2.9A and 2.9B Analysis of variance of Islet1 cells in the mesenchyme.....	71



Table 2.10A and 2.10B Tukey-Kramer analysis of Islet1 cells in the mesenchyme.....	72
Table 2.11A and 2.11B Analysis of variance of Pax3/GFP/Islet1 cells in the mesenchyme.....	73
Table 2.12A and 2.12B Tukey-Kramer analysis of Pax3/GFP/Islet1 cells in the mesenchyme.....	74
Table 2.13A, 2.13B, and 2.13C Analysis of variance of Pax3/GFP/Islet1 cells in the mesenchyme.....	75
Table 2.14A, 2.14B, and 2.14C Tukey-Kramer analysis of Pax3/GFP/Islet1 cells in the mesenchyme.....	76-77
Discussion.....	78
 CHAPTER 3: The Role of Wnt1 and Wnt3a in the Induction and Maintenance of Pax3 Expression in the Ophthalmic Trigeminal Placode.....	
Introduction.....	83
Materials and methods.....	85
Mice.....	85
Genotyping.....	86
Immunohistochemistry.....	87
$\beta$ -Galactosidase staining.....	87
Whole-mount <i>in situ</i> hybridization.....	88
Results.....	88
The effect of Wnt1;Wnt3a double knockout on Pax3 expression in the opV placode.....	88

Figure 3.1 Whole-mount embryos of Wnt1 and Wnt3a double mutant mice at E8.5 and E9.5.....	90
Figure 3.2 Expression of Pax3 and Islet1 in Wnt1 and Wnt3a double mutant mice during early opV placodal development.....	91-92
Conditional knockout of Wnt signaling using Cre recombinase.....	93
Figure 3.3 Whole-mount embryos of Sox1-Cre;Sry mice at E8.5 and E9.5.....	96
Figure 3.4 Expression of Pax3 and Islet1 in Sox1-Cre;Sry mice during early opV placodal development.....	97
Figure 3.5 Expression of Pax2 in Sox1-Cre;Sry mice during early otic placodal development.....	98
Figure 3.6 X-gal staining showing spatiotemporal Sox1-Cre expression in early mouse development.....	99
Figure 3.7 Staining of Axin2 expression showing spatiotemporal activity of Wnt signaling in Sox1-Cre;Sry mice.....	100
Discussion.....	101
REFERENCES.....	103
APPENDIX.....	113
Table 1 Predicted size of the Pax3 splice forms in chick.....	113
Table 2 Number of PESEs and PESSs per exon found in the Pax3 gene of chick.....	114
Table 3 Cell counts of <i>in ovo</i> misexpression embryos at 6-8ss.....	115
Table 4 Cell counts of <i>in ovo</i> misexpression embryos at 14-16ss.....	123
Table 5 Cell counts of cultured misexpression embryos in DMSO.....	130

Table 6 Cell counts of cultured misexpression embryos in DAPT.....	138
CURRICULUM VITAE.....	148

## LIST OF TABLES

Table 1.1	Spatiotemporal expression of Notch signaling genes.....	12
Table 2.1	Analysis of variance of the overall fold differences.....	44
Table 2.2	Tukey-Kramer analysis of individual fold differences.....	45-46
Table 2.3	Analysis of variance of the sample's fold difference.....	47
Table 2.4	Tukey-Kramer analysis of the sample's fold difference between other samples.....	47
Table 2.5A and 2.5B	Analysis of variance of Pax3/GFP cells in the ectoderm.....	67
Table 2.6A and 2.6B	Tukey-Kramer analysis of Pax3/GFP cells in the ectoderm.....	68
Table 2.7A and 2.7B	Analysis of variance of Pax3/GFP cells in the mesenchyme.....	69
Table 2.8A and 2.8B	Tukey-Kramer analysis of Pax3/GFP cells in the mesenchyme.....	70
Table 2.9A and 2.9B	Analysis of variance of Islet1 cells in the mesenchyme.....	71
Table 2.10A and 2.10B	Tukey-Kramer analysis of Islet1 cells in the mesenchyme.....	72
Table 2.11A and 2.11B	Analysis of variance of Pax3/GFP/Islet1 cells in the mesenchyme.....	73
Table 2.12A and 2.12B	Tukey-Kramer analysis of Pax3/GFP/Islet1 cells in the mesenchyme.....	74
Table 2.13A, 2.13B, and 2.13C	Analysis of variance of Pax3/GFP/Islet1 cells in the mesenchyme.....	75
Table 2.14A, 2.14B, and 2.14C	Tukey-Kramer analysis of Pax3/GFP/Islet1 cells in the mesenchyme.....	76-77

## LIST OF FIGURES

Figure 1.1	Notch signaling in the trigeminal placode.....	7-8
Figure 1.2	Notch signaling in the trigeminal placode, continued.....	9
Figure 1.3	<i>Delta1</i> gene expression domain overlaps with Pax3 protein expression.....	10
Figure 1.4	Notch pathway gene expression remains in the ectoderm at a later developmental stage.....	11
Figure 2.1	Predicted genomic structure of Pax3 in chick.....	30
Figure 2.2	N-terminal amplification of Pax3 gene.....	31
Figure 2.3	Predicted isoforms of Pax3 in chick.....	32
Figure 2.4	Pax3 sequence of exons 2, 4, and 5.....	33
Figure 2.5	C-terminal amplification of Pax3 gene.....	34
Figure 2.6	Pax3 sequence of exons 5, 6, 7, and 8.....	36
Figure 2.7	Amino acid sequence of Pax3 isoform.....	37
Figure 2.8	Predicted amino acid sequence of Pax3V1 isoform.....	38
Figure 2.9	Predicted amino acid sequence of Pax3V2 isoform.....	39
Figure 2.10	Fold expression change between the spatiotemporal expression of Pax3 and Pax3V2.....	42-43
Figure 2.11	Plasmid constructs.....	49
Figure 2.12	GFP expression and Pax3 antibody staining of cells transfected with plasmid constructs.....	50
Figure 2.13	Pax3 isoform electroporation at 6-8ss may contribute to neuronal differentiation.....	53-54

Figure 2.14	Pax3 isoform electroporation at 14-16ss may contribute to neuronal differentiation.....	55-56
Figure 2.15	<i>In ovo</i> misexpression of Pax3 constructs at 6-8ss and 14-16ss.....	57
Figure 2.16	<i>In ovo</i> misexpression of Pax3 constructs at 6-8ss and 14-16ss, continued.....	58
Figure 2.17	Pax3 isoform may contribute to neuronal differentiation.....	62-63
Figure 2.18	Pax3 isoform contributes to neuronal differentiation with inhibition of Notch signaling.....	64-65
Figure 2.19	Misexpression of Pax3 constructs <i>in ovo</i> and <i>ex ovo</i> in culture.....	66
Figure 3.1	Whole-mount embryos of Wnt1 and Wnt3a double mutant mice at E8.5 and E9.5.....	90
Figure 3.2	Expression of Pax3 and Islet1 in Wnt1 and Wnt3a double mutant mice during early opV placodal development.....	91-92
Figure 3.3	Whole-mount embryos of Sox1-Cre;Sry mice at E8.5 and E9.5.....	96
Figure 3.4	Expression of Pax3 and Islet1 in Sox1-Cre;Sry mice during early opV placodal development.....	97
Figure 3.5	Expression of Pax2 in Sox1-Cre;Sry mice during early otic placodal development.....	98
Figure 3.6	X-gal staining showing spatiotemporal Sox1-Cre expression in early mouse development.....	99
Figure 3.7	Staining of Axin2 expression showing spatiotemporal activity of Wnt signaling in Sox1-Cre;Sry mice.....	100

## CHAPTER 1: Sensory Neuron Differentiation is Regulated by Notch Signaling in the Trigeminal Placode

Rhonda N.T. Lassiter, Matthew K. Ball, Jason S. Adams,  
Brian T. Wright, Michael R. Stark

Department of Physiology and Developmental Biology, Brigham Young University,  
Provo, Utah 84602, USA

### *Abstract*

Characterizing Notch signaling in sensory neurogenesis had not been previously performed. The ophthalmic trigeminal placode (opV) contributes cells to its ganglion that differentiate only as sensory neurons, making this a good model system for our study. To begin this study, a spatiotemporal description of Notch pathway genes in chick opV placode by stage-specific expression analysis was performed, showing expression of many Notch pathway genes and effectors in the opV placode. Notch pathway gene mRNA expression was shown to be primarily confined to the ectoderm with highest expression of the Notch pathway genes at the beginning stages of peak neuronal differentiation. This information contributed to the study of functional roles that Notch signaling may have in the opV placode, which was published in 2010 (Lassiter et al., 2010).

### *Introduction*

The ophthalmic trigeminal placode is a bilateral thickening of ectodermal cells on either side of the midbrain and rostral hindbrain. These cells either remain as ectodermal cells or become induced to become sensory neurons (Baker and Bonner-Fraser, 2000; Schlosser, 2006). Induction of the opV placode begins as early as 4 somite stage (ss) in chick with the expression of the early placode marker, Pax3 (Stark et al., 1997). The induced cells become specified and

committed as sensory neurons by 8ss (Baker et al., 1999), and begin delaminating from the placode at 13ss with peak delamination and migration occurring between 18-26ss (Stark et al., 1997). During these stages of development, the Pax3+ cells begin differentiating into sensory neurons with the expression of Neurogenin2 (Ngn2) and Islet1, both of which are proneural transcription factors (Lassiter et al., 2007). The differentiating cells from the placode delaminate from the ectoderm and migrate to the opV ganglion contributing only sensory neurons to the ganglion, making this a good model system to study sensory neurogenesis.

Previous studies had identified ligands and receptors in the opV placode, which include FGFR4, Frizzled1, 2, and 7, and Delta1 (Stark et al., 1997; Stark et al., 2000; Begbie et al., 2002). This showed that multiple pathways are possibly involved in the development of the opV placode, including the Notch signaling pathway. Additional ligands had been identified and functional studies of these ligands had been performed, including Wnt, FGF, and PDGF (Canning et al., 2008; Lassiter et al., 2007; Lassiter et al., 2009; McCabe and Bronner-Fraser, 2008). Using knockdown techniques, these ligands were found to be necessary for normal opV placode development, but none had been shown to generate prolific neurogenesis. In this study, we wanted to investigate the Notch signaling pathway that may be necessary for terminal differentiation.

The Notch signaling pathway is known to contribute to CNS neural progenitor maintenance and differentiation (Lasky and Wu, 2005; Okamura and Saga, 2008). This was shown through real-time imaging of the embryonic brain confirming that a main function of Notch signaling is to coordinate with other cellular signaling in maintaining neural progenitor cells (Kageyama et al., 2008; Shimojo et al., 2008). In addition, functional studies to inhibit Notch signaling by the gamma-secretase inhibitor, DAPT, showed premature differentiation of



neurons (Abelló et al., 2007; Daudet et al., 2007; Nelson et al., 2007). Since the Notch signaling pathway in the CNS had been shown to function in progenitor cell maintenance and differentiation, we wanted to show its function in sensory neurogenesis using the opV placode. However, to do this it was necessary to characterize the expression of Notch ligands, receptors, and effectors in the opV placode. My efforts contributed to this data by characterizing the expression of many Notch pathway genes in the opV placode, allowing for a focused experimentation of the Notch pathway and facilitating the publication of this study.

A detailed spatiotemporal mRNA expression of Notch pathway genes in the opV placode showed that Notch ligands, receptors, and effectors were confined to the ectoderm, and their expression increased at the stage of placodal differentiation. This study showed the mRNA expression of the Notch pathway genes during opV development, which contributes to the hypothesis that Notch signaling may be involved in the terminal differentiation of sensory neurons.

### *Materials and methods*

#### Chick

Fertilized chick (*Gallus gallus domesticus*, White Leghorn) eggs were incubated at 37°C in a humidified incubator until the appropriate stage was reached as specified by Hamburger and Hamilton, 1951.

#### Whole-Mount *in situ* hybridization

Digoxigenin (DIG)-labeled RNA antisense probes were synthesized from plasmids containing fragments or complete cDNA of the following chicken genes: cDelta1, cLunatic Fringe, cNotch1, cJagged1 (Daudet et al. 2007), cHairy1, and cHairy2 (obtained from D.

Henrique, Universidade de Lisboa, Portugal). DIG-labeled RNA antisense probes were synthesized from PCR amplification of chick cDNA of the following chicken genes: cDelta4, cHes5, cNgn2 (Lassiter et al. 2009), and cNotch2. The following primers were used for the respective genes: cDelta4, outer primers (forward 5'-TGTGCCGAACAGAATGGATA-3' and reverse 5'-TACCTTGACCCACTTGACCT-3') and inner primers (forward 5'-GAGTGCATCTGTCGTTCTGG-3' and reverse 5'-TTGAACGACGAGAGTCCACC-3'), cHes5, outer primers (forward 5'-GAGCCAGCTTCGTGCTGA-3' and reverse 5'-TGTGACCACGTGTAAGGTCT-3') and inner primers (forward 5'-CTGACAGCAGCTCTCGGATA-3' and reverse 5'-AGTGGTAGTGGACCTGTGAC-3'), cNotch2, outer primers (forward 5'-ACCGAAGTGGACGTCAGAAC-3' and reverse 5'-GAACACGGTCCACACAGACA-3') and inner primers (forward 5'-CCAGGATGGAAATGAAGAACC-3' and reverse 5'-GAAGGAGCTCTGTGTGGACC-3').

Whole-mount *in situ* hybridization was performed in chick embryos as described by (Henrique et al. 1995). Briefly, formaldehyde-fixed embryos of appropriate developmental stages were buffered and exposed to a DIG-labeled anti-sense RNA probe, which recognized the specific mRNA transcripts. After removal of the non-specifically adhering probe, the embryos were incubated with anti-DIG alkaline-phosphatase (AP) antibody (1/2000; Roche, Indianapolis, IN), followed by a chromogenic substrate for AP. Whole-mount embryos stained for specific mRNA transcripts were cryosectioned as follows. Embryos were fixed in 4% formaldehyde, which were rinsed and washed two times before being stepped up into a 15% sucrose solution, embedded in 7.5% gelatin/15% sucrose/PBS and cryosectioned (12 µm). Sections of 12µm were mounted on Superfrost Plus Glass slides (Fisher Scientific, Pittsburgh, PA) and the gelatin removed from tissue in PBS at 37°C for ten minutes for section analysis or

immunohistochemistry. Whole-mount and sectional imaging was done with bright field microscopy.

### Immunohistochemistry

Embryo sections from the *in situ* hybridization experiments were incubated overnight at 4°C with a dilution 1:300 Pax3 primary antibody (Developmental Studies Hybridoma Bank, Iowa City, IA) in BSA/PBS buffer (0.1% bovine serum albumen, 0.1% Tween-20 (Equitech Bio, Inc., Kerrville, TX, Fisher Scientific, Pittsburgh, PA)). The primary antibody was rinsed and washed twice for ten minutes in PBS at room temperature. The tissue was then covered with Alexa 546-conjugated goat anti-mouse IgG2a (Invitrogen, Grand Island, NY). IgG2a was diluted 1:1000 in BSA/PBS buffer. The tissue was incubated with the secondary antibodies for one hour at room temperature, upon which it was rinsed and washed twice for ten minutes in PBS. Antibody staining was visualized using a BX-61 fluorescent microscope (Olympus, Center Valley, PA).

### *Results*

Prior to this study, a spatiotemporal description of the Notch pathway genes in the chick opV placode was not available. A stage-specific analysis of the Notch pathway genes was necessary in order to better understand this signaling pathway in the opV placode. To accomplish this we compared the mRNA expression of *Notch1*, *Notch2*, *Delta1*, *Delta2*, *Jagged1*, *Lunatic fringe*, *Hes1*, *Hes2*, and *Hes5* to *Ngn2* at different developmental stages. *Ngn2* is a proneural cell marker in the opV placode (Begbie et al., 2002) and functions in the Notch signaling pathway. *Ngn2* directly induces expression of *Delta1* (Castro et al., 2006) and its expression is repressed by the Notch effector, *Hes1* (Shimojo et al., 2008). *Ngn2* was first

expressed in the opV placode at Hamburger-Hamilton stages (HH) 10-11 (Fig 1.1aa) with more robust staining observed in a broader region by stages 12-13 (Figs 1.1bb, 1.1dd), and expression was less obvious by stage 17 (Fig 1.1cc). Other Notch signaling pathway genes were not expressed in the opV placode at stage 9 (Fig 1.1, Fig 1.2). However, by stages 10-11 (Fig 1.1b), *Notch1* was expressed in the opV domain within the field marked by *Ngn2*, and became more apparent by stages 12-13 (Figs 1.1c, 1.1e). At stage 17, *Notch1* expression was reduced (Fig 1.1d). *Notch2* was expressed in a similar pattern as *Notch1* (Figs 1.2a-1.2c). At stages 10-11 (Fig 1.1g), *Delta1* was highly expressed in a few individual cells. By stages 12-13 *Delta1* expression was diffuse throughout the placode, with strong expression in several individual cells (Figs 1.1h, 1.1j). Expression was less obvious by stage 17 (Fig 1.1i). *Lunatic fringe* expression was similar to the expression of *Delta1* (Figs 1.1q-1.1t). *Jagged1* was expressed caudal to the opV placode in the hindbrain ectoderm and never expressed in the trigeminal placode (Figs 1.1k-1.1o). *Delta4* was not expressed in the opV placode at any of the analyzed stages (Figs 1.2d-1.2f). Notch signaling has been shown to activate the transcription of *Hes1* and *Hes5* (Bailey and Posakony, 1995; Jarriault et al., 1995; Jarriault et al., 1998; Ohtsuka et al., 1999). *Hes1* was expressed in the opV placode at stage 10-11 (Fig 1.1v), expression increased and was scattered by stages 12-13 (Figs 1.1w, 1.1y) and became less obvious by stage 17 (Fig 1.1x). It had a similar pattern as *Notch1*. *Hes2* was expressed in the opV placode at stages 11-12 (Figs 1.2h, 1.2i), stage 13 (data not shown), and stage 17 (data not shown). *Hes5* was not expressed in the opV placode at any stage (Figs 1.2j-1.2l). A table describing the expression of each gene provides additional detail (Table 1.1). These data show that known effectors of Notch transcription are expressed in early trigeminal placode development.

Using Pax3 as a marker for the opV placode and ganglion, we showed that Pax3 protein

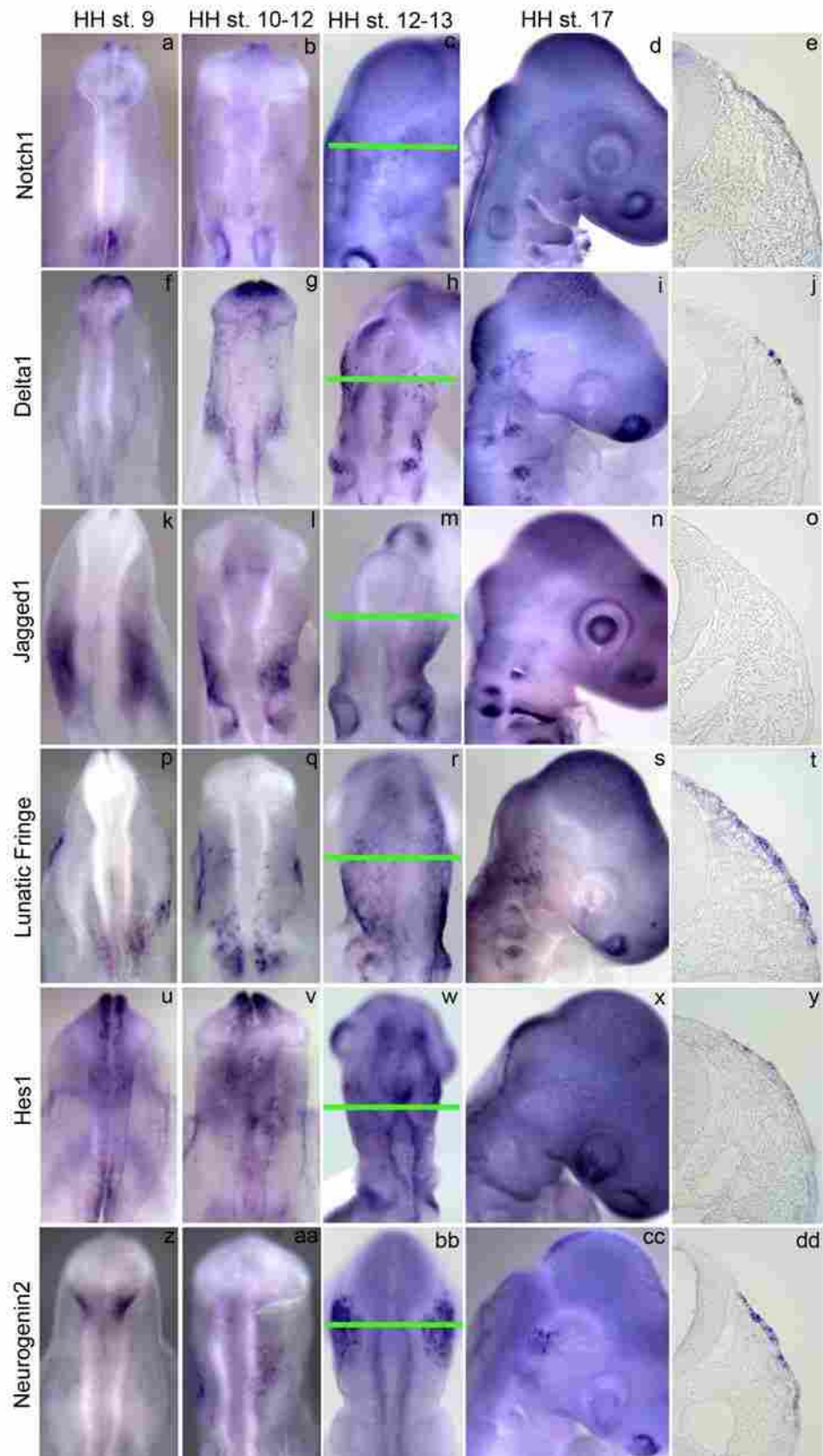


Figure 1.1 Notch signaling in the trigeminal placode (legend on page 8)

Figure 1.1 Notch signaling in the trigeminal placode

*Notch1* mRNA is expressed at low levels in ectodermal cells of the midbrain region at HH stage 10-11 (b). *Notch1* mRNA expression increased in ectodermal cells (e) at HH stage 12-13 (c) and the expression decreased by HH stage 17 (d). At HH stage 10-11, *Dll1* mRNA is expressed at low levels in ectodermal cells of the midbrain region (g). *Dll1* mRNA expression levels increased in ectodermal cells (j) at HH stage 12-13 (h) and this level of expression decreases slightly by HH stage 17 (i). *Jagged1* mRNA is not expressed in the ectodermal cells (k-o) of the trigeminal placode. *Lunatic fringe* mRNA is expressed at low levels in ectodermal cells of the midbrain region at HH stage 10-11 (q). At HH stage 12-13, *lunatic fringe* expression levels increased in ectodermal cells (r, t) and this level of expression is decreased by HH stage 17 (s). *Hes1* mRNA expression was detected at low levels in the midbrain ectoderm at HH stage 10-11 (v). *Hes1* expression increased in the midbrain ectoderm (y) at HH stage 12-13 (w) and faint expression was detected at HH stage 17 (x). *Ng2* mRNA expression was detected at moderate levels in the trigeminal placode at HH stage 10-11 (aa). *Ng2* mRNA expression levels increased at HH stage 12-13 (bb, dd) and decreased by stage 17 (cc). Notch signaling was not detected in the midbrain ectoderm at HH stage 9 (a, f, k, p, u).

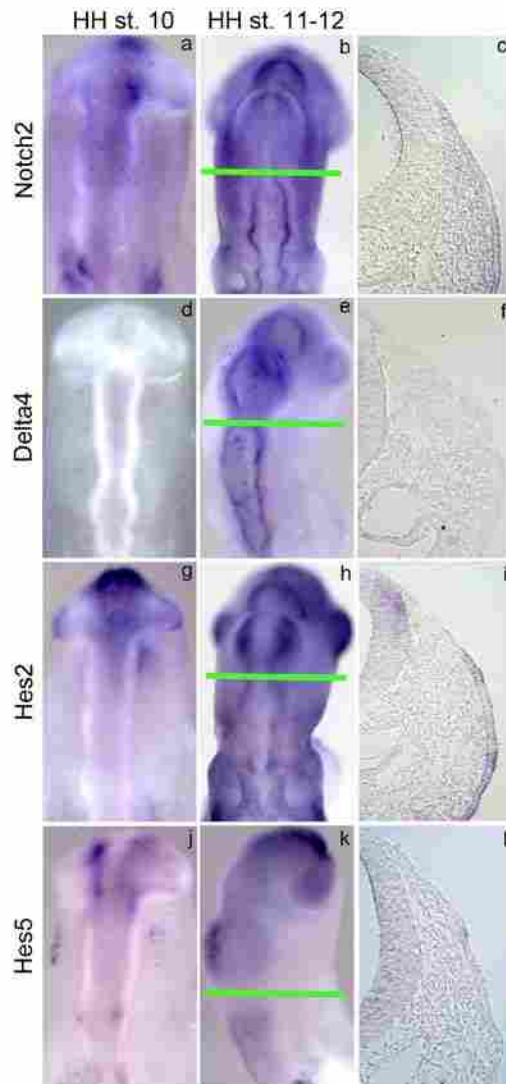


Figure 1.2 Notch signaling in the trigeminal placode, continued

*Notch2* mRNA is expressed at low levels in ectodermal cells (c) of the midbrain region at HH stage 10 (a) and HH stage 11-12 (b). *Dll4* mRNA is not expressed in the midbrain ectoderm (f) at HH stage 10 (d) and HH stage 11-12 (e). *Hes2* mRNA was not detected in the midbrain ectoderm at HH stage 10 (g), though low levels of expression was detected in the midbrain ectoderm (i) at HH stage 11-12 (h). *Hes5* mRNA is not expressed in the midbrain at HH stage 10 (j), but a few midbrain ectoderm cells (l) expressed low levels of *Hes5* mRNA at HH stage 11-12 (k-i).

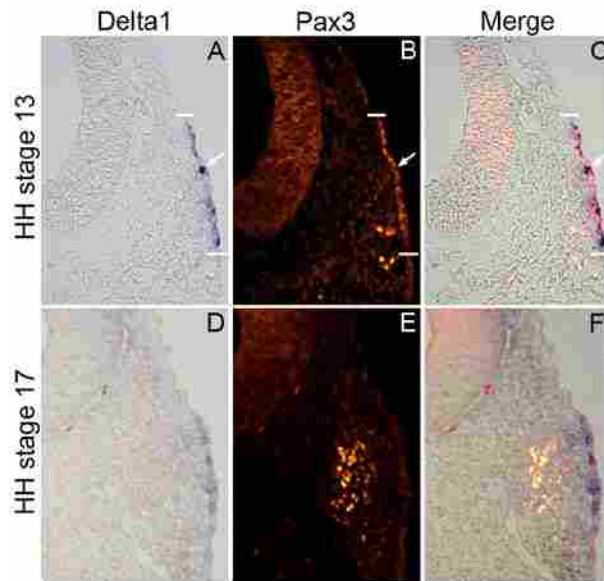


Figure 1.3 *Delta1* gene expression domain overlaps with Pax3 protein expression

At HH stage 13, *Delta1* is expressed in the ectoderm (A), and at HH stage 17, lower levels of *Delta1* expression is shown in the ectoderm with no obvious expression of *Delta1* in the formed ganglion, characterized by Pax3 protein expression (D). Pax3 protein is expressed in the ectoderm and migrating cells at HH stage 13 (B), and at HH stage 17, most Pax3+ cells have left the ectoderm aggregating in the formed ganglion (E). At HH stage 13, individual cells expressing higher levels of *Delta1* also express Pax3 (C, arrow).



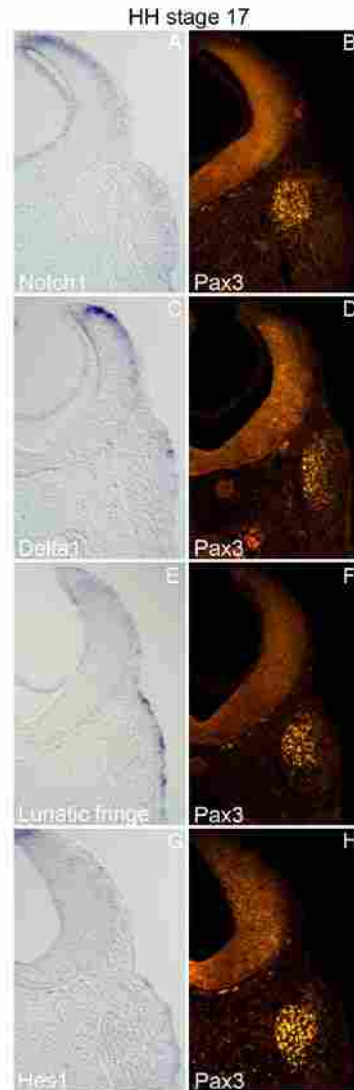


Figure 1.4 Notch pathway gene expression remains in the ectoderm at a later developmental stage. At HH stage 17, residual low-level expression of *Notch1*, *Delta1*, *Lunatic fringe*, and *Hes1* (A,C,E,G) is shown in the ectoderm. No obvious expression of Notch pathway genes is in the formed ganglion, characterized by Pax3 protein expression (A,C,E,G). At this stage, most Pax3+ cells have left the ectoderm and are aggregating in the formed ganglion (B,D,F,H).

Genes	Stage 9	Stage 10-11	Stage 12-13	Stage 17
<b>Notch1</b>	Neural plate/tube	Neural plate/tube, otic placode, <b>trigeminal placode</b> , spinal cord, somites, paraxial mesoderm	Neural plate/tube, otic placode, <b>trigeminal placode</b> , olfactory placode, hindbrain, spinal cord, somites, paraxial mesoderm	Neural plate/tube, otic placode, <b>trigeminal placode</b> , olfactory placode, epibranchial placode, midbrain/hindbrain, spinal cord, somites, paraxial mesoderm
<b>Notch2</b>		Olfactory placode, <b>trigeminal placode</b> , otic placode	Olfactory placode, <b>trigeminal placode</b> , otic placode, lens placode, hindbrain	Olfactory placode, <b>trigeminal placode</b> , otic placode, lens placode, hindbrain
<b>Delta1</b>	Neural plate/tube, somites, paraxial mesoderm	Neural plate/tube, somites, paraxial mesoderm, olfactory placode, <b>trigeminal placode</b> , otic placode, ventral torso, spinal cord	Neural plate/tube, somites, paraxial mesoderm, olfactory placode, <b>trigeminal placode</b> , otic placode, epibranchial placodes, midbrain/hindbrain, head ectoderm, spinal cord	Neural plate/tube, somites, paraxial mesoderm, olfactory placode, <b>trigeminal placode</b> , otic placode, epibranchial placodes, midbrain/hindbrain, head ectoderm, spinal cord
<b>Delta4</b>	Paraxial mesoderm	Paraxial mesoderm	Paraxial mesoderm, midbrain ectoderm	Paraxial mesoderm, midbrain ectoderm
<b>Jagged1</b>	Hindbrain ectoderm	Hindbrain ectoderm, forebrain ectoderm, otic placode	Forebrain ectoderm, otic placode, lens placode	Forebrain ectoderm, otic placode, lens placode, olfactory placode, epibranchial placodes
<b>Lunatic Fringe</b>	Neural plate/tube	Neural plate/tube, <b>trigeminal placode</b> , spinal cord, paraxial mesoderm	Neural plate/tube, <b>trigeminal placode</b> , olfactory placode, otic placode, epibranchial placodes, midbrain/hindbrain, spinal cord, paraxial mesoderm	Neural plate/tube, <b>trigeminal placode</b> , olfactory placode, otic placode, epibranchial placodes, midbrain/hindbrain, spinal cord, paraxial mesoderm, somites
<b>Hes1</b>	Neural plate/tube, paraxial mesoderm	Neural plate/tube, olfactory placode, <b>trigeminal placode</b> , spinal cord, paraxial mesoderm	Neural plate/tube, olfactory placode, <b>trigeminal placode</b> , lens placode, otic placode, brain, spinal cord, paraxial mesoderm, somites	Neural plate/tube, olfactory placode, <b>trigeminal placode</b> , lens placode, otic placode, epibranchial placode, brain, spinal cord, paraxial mesoderm, somites
<b>Hes2</b>	Neural plate/tube, paraxial mesoderm	Neural plate/tube, <b>trigeminal placode</b> , otic placode, spinal cord, paraxial mesoderm	Neural plate/tube, otic placode, olfactory placode, lens placode, <b>trigeminal placode</b> , epibranchial placode, brain, somite, spinal cord, paraxial mesoderm	Neural plate/tube, otic placode, olfactory placode, lens placode, <b>trigeminal placode</b> , epibranchial placode, brain, somite, spinal cord, paraxial mesoderm
<b>Hes5</b>	Neural plate/tube	Neural plate/tube, head ectoderm	Neural plate/tube, olfactory placode, otic placode, midbrain/hindbrain, spinal cord, paraxial mesoderm	Neural plate/tube, olfactory placode, otic placode, epibranchial placode, midbrain/hindbrain, spinal cord, paraxial mesoderm
<b>Neurogenin2</b>	Midbrain	Midbrain, <b>trigeminal placode</b>	Midbrain, <b>trigeminal placode</b> , olfactory placode	Midbrain, <b>trigeminal placode</b> , olfactory placode, neural plate/tube, spinal cord

Table 1.1 Spatiotemporal expression of Notch signaling genes

Spatiotemporal gene expression information was gathered from whole mount in situ hybridization staining on chick embryos at stages 9, 10-11, 12-13 and 17. Notch signaling genes are located in the left column and include Notch ligand, Notch receptor, and Notch effector genes. Also, included is expression information on the proneural marker Neurogenin2. Gene expression was seen in the anatomical structures listed on the right of the gene name and corresponds to the embryonic stage which is listed on the top row (Lassiter et al., 2010).

expression overlaps the mRNA *Delta1* domain in the ectoderm, at stages 13 and 17 of chick development (Figs 1.3A–1.3F), also individual cells expressing high levels of *Delta1* express Pax3 at stage 13 (Figs 1.3A–1.3C, arrow). It is important to note that expression of Notch pathway genes and effectors are confined primarily to the ectoderm, being downregulated upon epithelial to mesenchymal transition (EMT), with faint expression or no expression in mesenchyme cells. In addition, no Notch pathway gene mRNA expression tested was expressed in the opV ganglion (Fig 1.4). This indicates a distinct difference in the differentiation state between opV ectoderm and mesenchyme cells.

### *Discussion*

The fate of cells contributing to the opV placode is to become epidermal ectoderm or sensory neuron. The process of cellular differentiation in the placode is complex and requires a variety of signaling pathway molecules at specific times of development; these molecules include Wnt, FGF, and PDGF (Canning et al., 2008; Lassiter et al., 2007; Lassiter et al., 2009; McCabe and Bronner-Fraser, 2008). However, these molecules have not been shown to be sufficient in expanding the placodal domain, nor generating an increase in neurogenesis. To further investigate other pathway molecules that may be necessary for terminal differentiation of the opV placode, it was hypothesized to study the Notch pathway.

My part in this research was to characterize the spatiotemporal mRNA expression of Notch ligands, receptors and effectors. From this study, we learned that Notch signaling may begin as early as stage HH 10, which developmental stage is shortly after opV cell fate determination. We also learned that Notch pathway molecules are confined to the ectoderm and that their highest expression occurred during peak differentiation and migration. This research preceded experimentation of the Notch signaling pathway to understand its function in sensory

neurogenesis.

Experiments that were performed included blocking Notch signaling using the gamma-secretase inhibitor, DAPT, or activating Notch signaling by misexpression of the Notch intracellular domain (NICD). Notch activation resulted in a significant reduction in sensory neurogenesis. Cells remained in the ectoderm and did not differentiate. Expression of the opV specification marker Pax3 was also lost in NICD targeted cells. DAPT exposure resulted in a dramatic increase in neurogenesis without increasing proliferation, where many differentiated cells were found in the mesenchyme and, surprisingly, within the ectoderm (Lassiter et al., 2010). This is the first result clearly showing prolific neuronal differentiation in the ectoderm of the trigeminal placodes after experimental manipulation of a molecular signaling pathway, thus identifying Notch signaling as a primary regulator of the sensory neuron fate in the opV placode. These results also led to the study of other molecules expressed in the opV placode and how they are affected by Notch signaling through knocking down or activating Notch signaling.

## CHAPTER 2: Pax3 Splice Form Expression and Isoform Function in the Ophthalmic Trigeminal Placode

### *Introduction*

Ophthalmic trigeminal (opV) placodes are areas of bilaterally thickened ectoderm located dorsolateral to the midbrain and rostral hindbrain. Cells making up the opV placode delaminate and aggregate deep within the mesenchyme contributing neurons to the ophthalmic trigeminal (opV) ganglion (D'Amico-Martel and Noden, 1983). The opV placodes contribute only sensory neurons to the ganglion, making this a good model to study sensory neurogenesis and neuron differentiation.

Pax3 is the earliest marker expressed in the opV placode and Pax3<sup>+</sup> cells of the placode differentiate as sensory neurons or ectoderm (Baker and Bronner-Fraser et al., 2000; Baker et al., 2002; Dude et al., 2009). Pax3 mRNA expression in the placode begins at the 4 somite stage (ss) and protein expression is seen at 7ss (Baker et al., 1999). The placode cells are specified and committed to a neuron fate at 8ss (Baker et al., 1999) and later in development these cells proceed through an EMT between 10-13ss. At this stage, specifically 10ss, the pre-neuronal marker *Neurongenin2* (*Ngn2*) mRNA is expressed in the Pax3<sup>+</sup> opV placode cells. These Pax3<sup>+</sup> cells ultimately ingress into the mesenchyme, migrating to the site of the opV ganglion (Lassiter et al., 2007). At 17ss, differentiated neurons are marked by *Islet1* and ingression is enhanced (Lassiter et al., 2007). Pax3 expression continues to be expressed in opV placodal cells even after neuronal differentiation (Baker et al., 2002). Toward the end of neuronal differentiation at 35ss, the ganglion is morphologically distinct and Pax3 is no longer expressed in the ectoderm, but it continues to be expressed in sensory neurons of the trigeminal ganglion (Stark et al., 1997). Thus, Pax3 expression in the placode begins early at the time of cell specification and

commitment, and its expression continues throughout placode development and neuronal differentiation.

Pax3 is a transcription factor of the *Pax* family of genes. It consists of an N-terminal inhibitory domain, a conserved paired domain (PD), a conserved octapeptide motif (OM), a homeodomain (HD), and a C-terminal transactivation domain (Goulding et al., 1991; Chalepakis et al., 1994b; Barr et al., 1999). The N-terminal inhibitory domain is necessary for the transcriptional inhibitory activity of Pax3 and includes part of the paired domain (Chalepakis et al., 1994a; Barr et al., 1999). The paired domain is bipartite DNA binding domain made of a conserved N-terminus sub-region and a less conserved C-terminus region that are separated by a linker region. The paired domain is necessary and sufficient for Pax3 DNA-binding, while the homeodomain is necessary for binding only certain DNA regions (Czerny et al., 1993; Fortin et al., 1998; Phelan and Loeken, 1998; Apuzzo et al., 2004). The paired domain and the homeodomain are interdependent (Fortin et al., 1998; Apuzzo et al., 2004). They cooperate to recognize DNA-binding sites and both domains may be required for complete transcriptional activity (Baldwin et al., 1995). The octapeptide motif is involved in protein-protein interactions, it influences binding properties of the paired domain and homeodomain, and its phosphorylation is necessary for normal transcriptional activity (Fortin et al., 1998; Apuzzo et al., 2004; Amstutz et al., 2008). The C-terminal transactivation domain is required for gene expression, as it is known to activate transcription (Chalepakis et al., 1994a; Murakami et al., 2006). The activating mechanism may be through the domains involvement in protein-protein interactions to recruit transcription factors (Stuart et al., 1994; Mansouri, 1998; Apuzzo et al., 2004). The C-terminal transactivation domain may also promote gene expression through regulating the binding specificity and activity of the homeodomain. Researchers substituted the Pax3 transactivation

domain with a viral VP16 transactivation domain, which changed the specificity and activity of homeodomain-specific transactivation. This change led them to conclude that the transactivation domain may have an inhibitory action on the homeodomain (Cao and Wang, 2000).

Pax3 is expressed in different tissue types. In the early embryo it is expressed in the dorsal neural tube, dermomyotome, limb precursor muscle cells, neural crest cells, and placodes (Goulding et al., 1991; Bober et al., 1994; Stark et al., 1997). Pax3 functions in many different ways depending on the cell type which it is expressed. Pax3 is necessary for normal neurogenesis and myogenesis as seen in the abnormal tissue phenotypes within the *Splotch* mouse mutant and Waardenburg's syndrome in humans (Auerbach, 1954; Waardenburg, 1951; Epstein et al., 1991; Tassabehji et al., 1993). Specifically, Pax3 acts as a transcriptional activator or a repressor (Chalepakis et al., 1994a, Kioussi et al., 1995; Vogan et al., 1996, Mayanil et al., 2001; Kwang et al., 2002; Relaix et al., 2003; Blake et al., 2005; Hsieh et al., 2006) and Pax3 is associated with cell proliferation, cell differentiation, cell positional identity, and cell migration (Epstein et al., 1993; Evans and Lillycrop, 1996; Maroto et al., 1997, Mayanil et al., 2001; Baker and Bronner-Fraser, 2000; Streit, 2004; Wu et al., 2008; Collins et al., 2009). Recently, it has been shown that Pax3 is necessary for normal neuronal differentiation of opV placode cells (Dude et al., 2009).

Dude et al., (2009), misexpressed Pax3 in the otic region of chick embryos and stained for opV placode markers. They found that Pax3 is sufficient to induce the opV placode markers FGFR4 and Ngn2, but the neuronal differentiation marker *Islet1* was not induced. They concluded that Pax3 is sufficient for the upregulation of opV placode markers, but additional signals are needed for Pax3+ cells to differentiate as sensory neurons. This study also misexpressed a Pax3-Engrailed fusion protein in the opV placode, which represses Pax3 target

gene expression as the two Pax3 DNA-binding domains are fused with an Engrailed repressor domain (Bajard et al., 2006; Relaix et al., 2006). The results from this experiment showed a decrease of targeted cells that expressed FGFR4, Ngn2, or Islet1 when compared to targeted control cells. In addition, the Pax3-Engrailed targeted cells that delaminated from the opV placode were significantly lower than targeted control cells. It was concluded that Pax3 target gene expression is necessary for neuronal differentiation and delamination. With this data in mind and knowing that Pax3 expression in the opV placode coincides with specification and commitment of the sensory neuron fate, I began to investigate whether different isoforms of Pax3 are expressed at key developmental stages that may regulate neuron differentiation within the opV placode. Pax3 isoforms may negatively regulate the expression of the Pax3 or an inactive isoform may compete for Pax3 binding sites.

Pax3 directly or indirectly regulates the expression of many downstream targets (Mayanil et al., 2001). Alternative splicing of Pax3 produces the potential of multiple isoforms that can stabilize binding to suboptimal recognition sequences or recognize specific DNA sequences of different target genes (Vogan and Gros, 1997). Thus, Pax3 potentially regulates multiple target expression through different DNA-binding sites that can be optimized through alternative splicing. Alternative splicing of Pax3 has been shown in human cells and mouse embryos. For example, a Pax3 isoform was described with ten exons in the mouse embryo (Goulding et al., 1991) and later two similar Pax3 isoforms were discovered both with different intron splicing at the C-terminal end (Barber et al., 1999). In addition, the Pax3f isoform was discovered with deletion of exon 6, 7, and 8 (Barber et al., 1999). A Pax3 isoform missing exon 8 of the transactivation domain is transcriptionally inactive and can inhibit the activity of Pax3 in mice through competitive inhibition (Pritchard et al., 2003). Isoforms identified as Pax3a and Pax3b



are truncated after exon 4, lacking the homeodomain, (Tsukamoto et al., 1994) and a similar mutant Pax3 protein with truncation after the octapeptide domain has shown to bind promoter sequence and through reporter assays a corresponding Pax3 construct truncated after the octapeptide domain have shown to inhibit transcription (Chalepakis et al., 1994a). Other isoforms that have been found include Pax3g and Pax3h, which lack part of the transactivation domain (Parker et al., 2004). Alternative splicing of Pax3 may allow for different transcriptional activities produced by this transcription factor on its target genes.

In conclusion, Pax3 displays repressive and activating potential, functioning as a transcription factor expressed in many embryonic tissues, including the opV placode. A gain-of-function study showed that Pax3 activates transcription of *c-met* and *MyoD* during embryogenesis (Relaix et al., 2003), and Pax3 repressed myelin basic protein promoter activity in a cotransfection assay (Kioussi et al., 1995). It has been shown that Pax3 expression coincides with opV placode cell specification and commitment, which evidence provides a possible role of Pax3 in the specification and commitment of placodal cells (Baker et al., 1999). Another study has shown that functional Pax3 is necessary for neurogenesis in the opV ganglion, as the ophthalmic nerve is reduced or absent in *Splotch* mice (Tremblay et al., 1995). Finally, Pax3 misexpression is sufficient to activate expression of proneural markers, but is not sufficient for neuronal differentiation (Dude et al., 2009). Together these data lead to the hypothesis that Pax3 isoforms associated with different transcriptional activities are differentially expressed at stages of development to promote the normal neuronal fate in the opV placode. To test this hypothesis, I investigated whether various isoforms are present in chick head ectoderm and the opV ganglion at different developmental stages, what quantitative expression patterns are present, the transcriptional activity of various Pax3 isoforms in the opV placode, and whether Pax3 isoform

misexpression impacts normal placode development.

### *Materials and methods*

#### Chick

Fertilized chick (*Gallus gallus domesticus*, White Leghorn) eggs were incubated at 37°C in a humidified incubator until the appropriate stage was reached as specified by Hamburger and Hamilton, 1951.

#### RNA isolation

Whole chick embryos were collected at 6-8ss, 16-18ss, 35-36ss, and 43-44ss for RNA isolation. RNA isolation was also performed for whole-head tissue that was dissected from chick embryos at 8ss and 20ss. In addition, ectoderm was dissected from chick embryos at 6-8ss, 16-18ss, and 35ss as well as the trigeminal ganglion at 35ss. To facilitate separation of the ectoderm and ganglia from the mesenchyme at the two later embryonic stages, pre-warmed 1mg/ml dispase (Roche, Indianapolis, IN) diluted in DMEM (Gibco, Grand Island, NY) was added to the tissue and incubated at 38°C for five minutes. The enzyme was neutralized by adding 0.1% bovine serum albumin (Equitech Bio, Inc., Kerrville, TX) to this solution and placed on ice for ten minutes before rinsing with PBS. RNA isolation for all tissue samples was performed using the PureLink Micro-to-Midi Total RNA Purification System (Invitrogen, Carlsbad, CA) according to the manufacturer's instructions.

Ectoderm of the trigeminal placode was dissected from chick embryos at 10-15ss, 20-25ss, and 32-37ss. The trigeminal ganglia were collected at 32-37ss. To study the effect of Notch signaling on Pax3 expression, chick embryos were cultured with 200µM N-[N-(3,5-Difluorophenacetyl-L-alanyl)]-S-phenylglycine t-Butyl Ester (DAPT (EMD Chemicals Inc.,

Cincinnati, OH)) at 10-15ss and incubated at 37°C for 12 hours. The cultured ectoderm of the trigeminal placode was also collected for this study.

Dissection was performed by cutting the heads of the chick embryos caudal to the otic placode and through the optic vesicles or cups. Separation of the ectoderm and the ganglia from the mesenchyme was facilitated by incubating the dissected heads with ice-cold 3U/ml dispase I (Roche, Indianapolis, IN) in DMEM (Gibco, Grand Island, NY), 20mM Hepes, pH 8.0 for 15-20 minutes. The tissue was then transferred to ice-cold 0.05% Trypsin with EDTA (Hyclone, Logan, UT) for five minutes and then incubated at 37°C for at least 20 minutes. Trypsin was neutralized with 10% fetal bovine serum (Hyclone, Logan, UT) in DMEM for five minutes at room temperature and then washed in PBS. The desired tissue was dissected from the mesenchyme using fine surgical instruments and stored in PBS with rRNasin RNase inhibitor (Promega, Madison, WI) on ice. RNA lysis solution with 2-mercaptoethanol was added to lyse the cellular tissue. The collected RNA was then purified using the RNeasy Mini Kit (Qiagen, Valencia, CA) according to the manufacturer's instructions.

### RT-PCR

Reverse transcription of RNA was performed using a Superscript Double-Stranded cDNA Synthesis Kit (Invitrogen, Carlsbad, CA) with oligo primers according to the manufacturer's instructions.

Forward and reverse primer pairs used for PCR amplification of the Pax3 splice forms included the following: Pax3V1 forward 5'-CTGCGTCTCCAAGATCCTCT-3' and reverse 3'-AAAAGCCATCAGTTGGTTGG-5', and the primer pair for Pax3V2 forward 5'-AGCAACTGGAAGAGCTGGAA-3' and reverse 3'-TGACAGGGTCCATGCTGTAG-5'. PCR amplification was performed using Go Taq Green Master Mix (Promega, Madison, WI) on a

PCR Mastercycler Personal (Eppendorf, Hauppauge, NY). PCR cycling parameters began with an initial 95°C step for two minutes, then a cycle of 95°C for 30 seconds, 54°C for 30 seconds, and 72°C for 90 seconds, repeated for 35 times, and followed by a final extension at 72°C for five minutes. The Go Taq Master Mix was diluted to a 1x concentration, the dNTP mix was diluted to 0.2mM of each nucleotide, and the primers were diluted to 1.0µM.

### DNA sequencing

PCR products were run on a 1.5% agarose gel and multiple bands were excised. DNA within these bands was purified using the Wizard SV Gel and PCR Clean-up System (Promega, Madison, WI). Sequencing of all PCR products were performed at the DNA Sequencing Center (Brigham Young University, Provo, UT).

### Mapping splicing enhancers and splicing silencers in the exon

Putative exonic splicing enhancers and silencers were found using the software available at: [cubweb.biology.columbia.edu/pesx/](http://cubweb.biology.columbia.edu/pesx/). Pax3 sequence found in NCBI database was entered into the software and a search for exonic splicing enhancers was performed. Citation to use this software is Zhang and Chasin, 2004; Zhang et al., 2005.

### Quantitative PCR

Dilution series of all cDNA samples consisted of no dilution, 33% dilution, 10% dilution, 3% dilution and 1% dilution. Three replicates of each dilution were performed using iTaq Supermixes with ROX (BioRad, Hercules, CA) on a 7000 Sequence Detection System cyclor (Applied Biosystems, Carlsbad, CA). The following primers and probes were used: Pax3V1 primer pair: forward 5'-CTGCGTCTCCAAGATCCTCT-3' and reverse 3'-GCTCTTCCAGTTGCTCTGCT-5'; probe upstream of the exon 4 deletion

5'-CCGCTACCAGGAGACGGGATCCATC-3' and probe inside of the deletion 5'-AGCTCCATCAGCCGCATCCTGCG-3'. Pax3V2 primer pair: forward 5'-AGCAACTGGAAGAGCTGGAA-3' and reverse 3'-TGACAGGGTCCATGCTGTAG-5'; probe upstream of the exon 6 and 7 deletion 5'-GCTTTTGAGAGGACACACTACCCTGACA-3' and probe inside of the deletion 5'-TTTAGCAACCGCCGTGCTAGATG-3'. The PCR cycling parameters were 50°C for one second, 94°C for five minutes, and 40 cycles of 94°C for 15 seconds, 55°C for 30 seconds, and 72°C for 30 seconds. The iTaq Supermix was diluted to a 1x concentration and the primers were diluted to 1.0µM. Analysis of data and statistical inference was performed on the data.

cDNA samples were diluted to a concentration of 100ng/µl. Three to five replicates of each sample were performed using SsoFast EvaGreen Supermix (Bio-Rad, Hercules, CA) on a CFX Connect Real-Time System cycler (Bio-Rad, Hercules, CA). The following primers were used: Pax3 primer pair: forward 5'-CAGCAGAGCAACTGGAAGAG-3' and reverse 3'-GCTTCCTCCATCTAGCAC-5'. Pax3V2 primer pair: forward 5'-CAGCAGAGCAACTGGAAGAG-3' and reverse 3'-GTCCCATTACCTGAACTCG -5'. The PCR cycling parameters were 95°C for 30 seconds, and 40 cycles of 95°C for five seconds, 53°C for five seconds, and followed by a melting curve from 65°C to 95°C at five second increments. The SsoFast EvaGreen Supermix was diluted to a 1x concentration and the primers were diluted to 0.5µM. The upstream primer was the same in each set of primer pairs, however, to amplify Pax3 the downstream primer was located in exon 6 of Pax3. To distinguish the amplification of Pax3V2 a downstream primer that recognized the sequence of the 3' end of exon 5 and of the 5' end of exon 8 was used. Quantitative PCR assay was performed and SYBR green detected to show the cycle threshold (Ct) values of each sample performed in replicate of

three or five. Beta-actin mRNA expression was used to normalize the samples among the groups and used to calculate the delta Ct followed by the delta delta Ct, which allowed for the comparison of fold expression changes between all samples. One-way ANOVA was used to show whether all the means of the groups were equal or not. Tukey-Kramer test was performed to determine which of the means differed significantly in the analysis of variance.

### Plasmid constructs

The Pax3 gene was cut from the Bluescript vector and ligated into pGEM- T Easy (Promega, Madison, WI). Using the Pax3 construct, exon 4 was cut from the DNA and the construct was ligated to produce the Pax3V1 construct. Exons 6 and 7 were cut from the Pax3 construct and ligation was performed to produce the Pax3V2 construct. Next, the sequences for Pax3, Pax3V1, and Pax3V2 were cut from the pGEM- T Easy constructs and ligated individually into the pCIG (gift from McMahon lab) expression vector using the *EcoRI* restriction site. Cloning was performed using a T4 DNA ligase in the Ligafast Rapid DNA Ligation System (Promega, Madison, WI). These constructs were under the chick  $\beta$ -actin promoter and CMV-IE enhancer allowing for misexpression of the inserted gene sequence. A nuclear green fluorescent protein (GFP) sequence is downstream of the promoter allowing for the detection of the construct's expression activity in targeted cells. DNA sequencing was performed on the plasmid constructs to verify the correct insert of the Pax3, Pax3V1, and Pax3V2 constructs.

### Cellular transfections

Cells were grown for at least 24 hours in 10 ml of growth medium to the desired 80-90% confluence at 37°C, 5% CO<sub>2</sub>. Cells were transfected with the empty vector pCIG, the Pax3 construct, or the Pax3V2 construct using the Lentiphos HT kit (Clontech, Mountain View, CA)

according to the manufacturer's instructions. The cells were incubated at 37°C, 5% CO<sub>2</sub> for eight hours and the transfection medium was replaced with growth medium and the cells were incubated for 24 hours. The cells were then fixed for 10 minutes, rinsed and washed two times in PBS for five minutes in preparation for primary antibody staining.

### Immunocytochemistry

Fixed cells that were previously transfected with an empty vector or construct were incubated with a 1:300 dilution of Pax3 primary antibody (Developmental Studies Hybridoma Bank, Iowa City, IA) at room temperature for one hour. The cells were rinsed once and washed two times for five minutes with PBS and then incubated with 1:1000 dilution of Alexa 546-conjugated goat anti-mouse IgG2a (Invitrogen, Grand Island, NY) for 15 minutes at room temperature. The secondary antibody was rinsed off the cells and washed two times with PBS for five minutes. The cells were then imaged using fluorescent microscopy.

### *In ovo* electroporation

The empty vector pCIG, Pax3, Pax3V1, and Pax3V2 plasmid constructs were individually misexpressed at two different developmental stages, 8ss and 16ss via electroporation *in ovo*. Electroporation of the individual construct was performed with a BTX pulse electroporator (10V, 10msec, 7 pulses). After electroporation, the eggs were incubated for 30-36 hours and collected.

### Electroporation in whole-embryo explants

Embryos of 5-7ss were explanted from their egg and cultured similarly to the Easy Chick (EC) method as described by Chapman et al., (2001). Briefly, this method included cracking an egg into a petri dish and carefully removing the thick albumin away from the chick embryo using

a kimwipe. Rings made from filter paper the size of a quarter with a small circle punched out from the middle were placed on top of the yolk with the embryo being in the middle of the small circle. The filtered ring was cut out of the yolk and the embryo was staged. The excess yolk was removed using a saline wash or manually removed by blunt forceps and a second filtered ring was placed below the embryo, sandwiching the vitelline membrane between the two filtered rings. This was a variation of the EC culture allowing for subsequent removal of the cultured embryo onto a new media. The explanted embryos were immediately placed into a petri dish with simple saline and electroporation of the empty vector pCIG, Pax3, Pax3V1, or Pax3V2 construct was performed with a BTX pulse electroporator (10V, 10msec, 7 pulses). The electroporated embryos were placed on top of pre-warmed culture media (37°C) that had previously been poured into 35mm petri dishes. The cultured embryos were incubated at 37°C in a humidified chamber until the desired stage was reached.

### Tissue culture

After electroporation, embryos were cultured in a six-well plate on an agar-albumen substrate and incubated at 37°C for 12 hours. At this point, the embryos were transferred from the culture to another well within a six-well plate with the agar-albumen substrate that contained either 200µM N-[N-(3,5-Difluorophenacetyl-L-alanyl)]-S-phenylglycine t-Butyl Ester (DAPT (EMD Chemicals Inc., Cincinnati, OH)) or dimethylsulfoxide (DMSO (Sigma-Aldrich Corp., St. Louis, MO)). Embryos were incubated at 37°C for 24 hours before being collected in PBS and fixed.

### Immunohistochemistry

Embryos were embedded in gelatin and cryosectioned. Sections of 12µm were mounted



on Superfrost Plus Glass slides (Fisher Scientific, Pittsburgh, PA) and the gelatin removed in PBS at 37°C for ten minutes. Embryo sections were incubated overnight at 4°C with a dilution 1:300 Pax3 primary antibody (Developmental Studies Hybridoma Bank, Iowa City, IA) and a dilution of 1:200 Islet1 primary antibody (Developmental Studies Hybridoma Bank, Iowa City, IA) in BSA/PBS buffer (0.1% bovine serum albumen, 0.1% Tween-20 (Equitech Bio, Inc., Kerrville, TX, Fisher Scientific, Pittsburgh, PA)). The primary antibody was rinsed and washed twice for ten minutes in PBS at room temperature. The tissue was then covered with Alexa 633- and Alexa 546-conjugated goat anti-mouse IgG2a and IgG2b (Invitrogen, Grand Island, NY), respectively. IgG2a was diluted 1:200 and IgG2b 1:1000 in BSA/PBS buffer. The tissue was incubated with the secondary antibodies for one hour at room temperature, upon which it was rinsed and washed twice for ten minutes in PBS. Antibody staining was seen using a BX-61 fluorescent microscope (Olympus, Center Valley, PA).

### Statistical Analysis

Cell counts were performed on randomly selected opV placodes using the Olympus Microsuite software (Olympus, Center Valley, PA). Cell counts for the electroporation experiments included cells expressing GFP, Pax3 antibody, Pax3 antibody and GFP, Islet1 antibody, and Pax3 antibody, GFP, and Islet1 antibody in the ectoderm and in the mesenchyme. One-way ANOVA and Tukey-Kramer test was used to analyze data using SAS software, version 9.2 (SAS Institute Inc., Cary, NC). One-way ANOVA was used to show whether all the means of the groups were equal or not. Tukey-Kramer test was performed to determine which of the means differed significantly in the analysis of variance. P-values of  $\leq 0.05$  were considered statistically significant.

## *Results*

### Identification of Pax3 alternative splice forms

The coding sequence of the Pax3 gene in chick (*Gallus gallus*) is 1455 base pairs (bp) encoding 484 amino acids (NM\_204269, NP\_989600.1). We predict that full-length Pax3 contains nine exons in chick, similar to the different splice forms of Pax3 in human and mouse that contains nine exons (Fig 2.1) (Barber et al., 1999; Parker et al., 2004). The main protein domains of Pax3 include a 129 amino acid paired domain, a seven amino acid octapeptide domain, a homeodomain of 60 amino acids, and a C-terminal transactivation domain that is serine, threonine, and proline rich (Chalepakis et al., 1994a; Chalepakis et al., 1994b; Seo et al., 1998; Barr et al., 1999) (Fig 2.1). The genomic structure of human Pax3 has been characterized (Barr et al., 1993; Lalwani et al., 1995), and this was used in addition to the genomic data in the NCBI GenBank to produce a predicted genomic map of chick Pax3 (NC\_006096.3) (Fig 2.1). The full-length Pax3 in chick appears to be most similar to the Pax3d splice form described by Barber et al., (1999), as it contains nine exons and the chick amino acid C-terminus (AFHYLKPDIA) is identical to the mouse and human Pax3d (Blake and Ziman 2005; Barber et al., 1999; NP\_989600.1). The chick full-length splice form will be referred to as Pax3 through the rest of this study. In order to study the presence of possible Pax3 splice variants and their temporal expression patterns cDNA was obtained to perform RT-PCR.

Using cDNA from 6-8ss, 16-18ss, and 35-37ss, two primer pair sets were designed to amplify the N-terminal and C-terminal regions of the Pax3 gene. The N-terminal primers amplified two PCR products of different size which were gel extracted and sequenced (Fig 2.2). Sequencing confirmed that the longer product of 616bp was the same as the Pax3 sequence found in NCBI (NM\_204269). Sequencing also showed that 135 bp is absent in the shorter

product between positions 451 and 586 of the Pax3 sequence. This splice variant was named Pax3V1 that contains a deletion of exon 4 (Fig 2.3).

The genomic sequence for Pax3 intron 3 and a part of the N-terminal end of exon 4 is not available through the NCBI GenBank to verify a 5'-splice site, however, available sequence of intron 4 shows a 3'-splice site at position 38751 and a possible branch-point at position 38714. Fifteen putative exonic splice enhancers (PESE) are located in exon 4, but no putative exonic splice silencers (PESS) are present. (Zhang and Chasin, 2004; Zhang et al., 2005) (Fig 2.4). Though the absence of putative exonic splice silencers might suggest the retention of exon 4, it is possible that intronic splicing silencers are present allowing for the deletion of exon 4. The Pax3V1 splice form is most similar to a *plotch* allele (*Sp*) mutant in mouse that also includes a deletion of exon 4 (Epstein et al., 1993).

The second primer pair amplified four PCR products of different sizes of the Pax3 C-terminal region, which were gel extracted and sequenced (Fig 2.5). The longest product of 705bp was the same Pax3 sequence found in NCBI (NM\_204269) and the smallest product contained a 381bp deletion within the sequence. This deletion was found between positions 792 and 1173 of the Pax3 sequence. This splice variant was named Pax3V2 that contains a deletion of exons 6 and 7 (Fig 2.3). The middle two bands were sequenced and as they produced atypical products that were not a part of the Pax3 gene, the research on these bands was not continued.

Intron 5 of Pax3 includes a 5'-splice site at position 38958 and intron 7 includes a 3'-splice site at 60834 and a possible branch point at 60813. Exon 6 includes six PESEs and at least one PESS. There is a possible second PESS, but a discrepancy of the third base pair from the 5' starting site of exon 6 is present. The genomic reference sequence (NC\_006096.3) shows this nucleotide to be a cytosine, while the mRNA reference sequence (NM\_204269) shows this

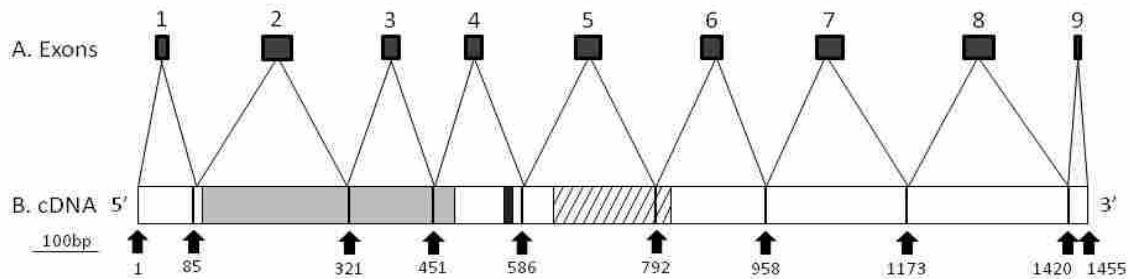


Figure 2.1 Predicted genomic structure of Pax3 in chick

(A) Pax3 has nine predicted exons in chick. The diagonal lines stemming from the boxes that represent the exons show the exon's base pair location along the cDNA. (B) The Pax3 cDNA is represented here showing the exon boundaries and protein domains. The exon boundaries are marked by the black slashes and arrows. Underneath each arrow is the base pair number that represents the beginning of the corresponding exon. The paired domain is represented by the solid grey region of cDNA, the octapeptide is represented by the solid black region of cDNA, and the homeodomain is represented by the diagonal lines within the cDNA. The transactivation domain has not been characterized in chick, but is considered to be in that region of cDNA immediately downstream of the homeodomain.

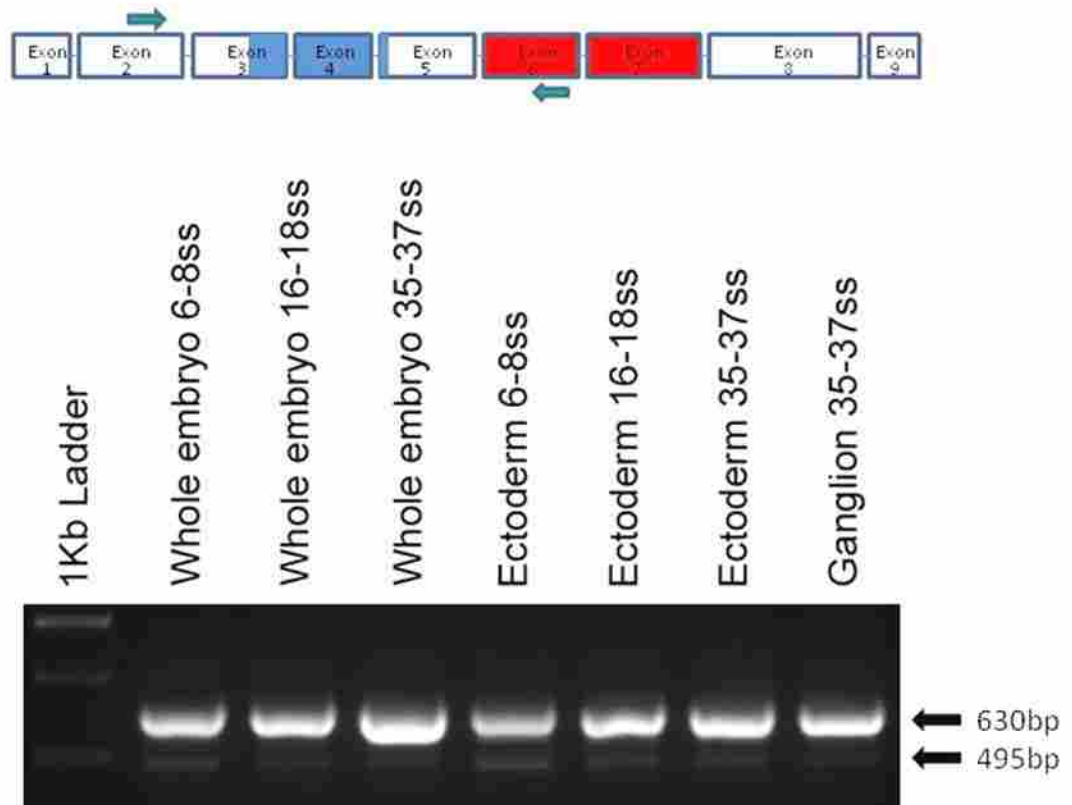


Figure 2.2 N-terminal amplification of Pax3 gene

Total RNA isolated from whole chick, chick ectoderm, and chick opV trigeminal ganglion at different developmental stages was reverse transcribed into cDNA and amplified using a primer pair for exon 1-5 cDNA. The PCR products were separated on 1.5% agarose gels. Predicted isoform sizes are as follows: Pax3, 630 base pairs (bp) and Pax3V1, 495bp.

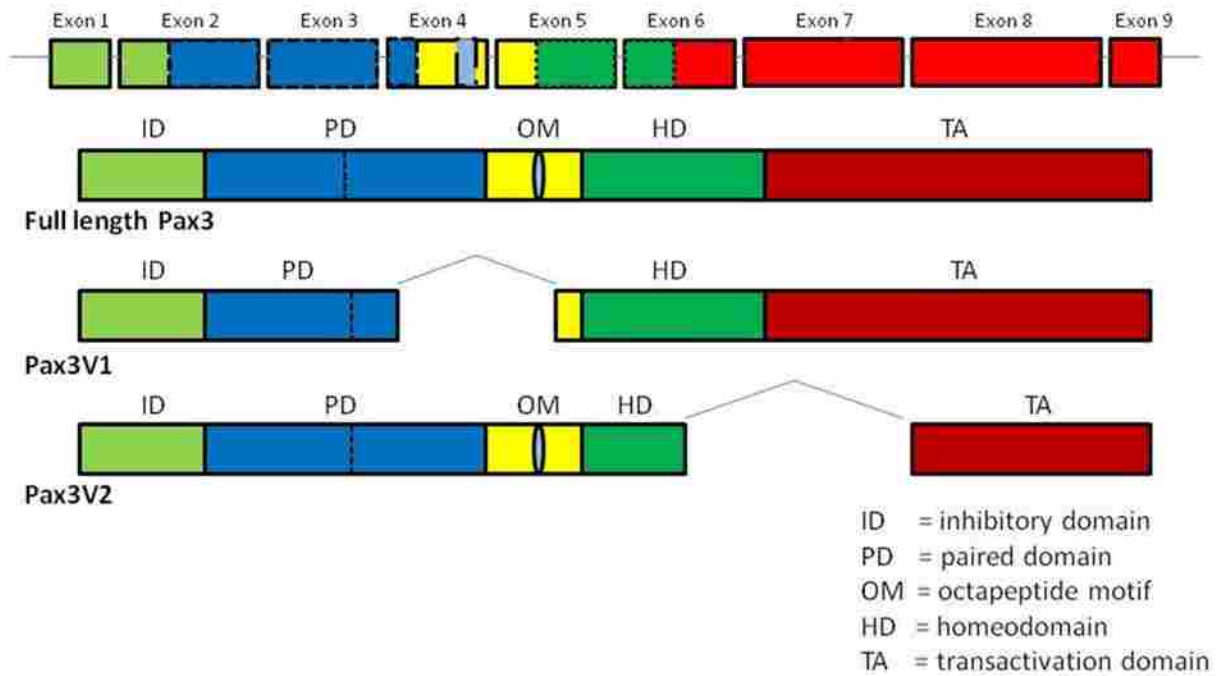


Figure 2.3 Predicted isoforms of Pax3 in chick

The nine exons of Pax3 in chick are shown in the top diagram corresponding with the full-length Pax3 isoform depicting the protein domains that is underneath the top diagram. The Pax3V1 isoform is shown to contain a deletion of exon 4 and the Pax3V2 isoform is shown to contain a deletion of exons 6 and 7.



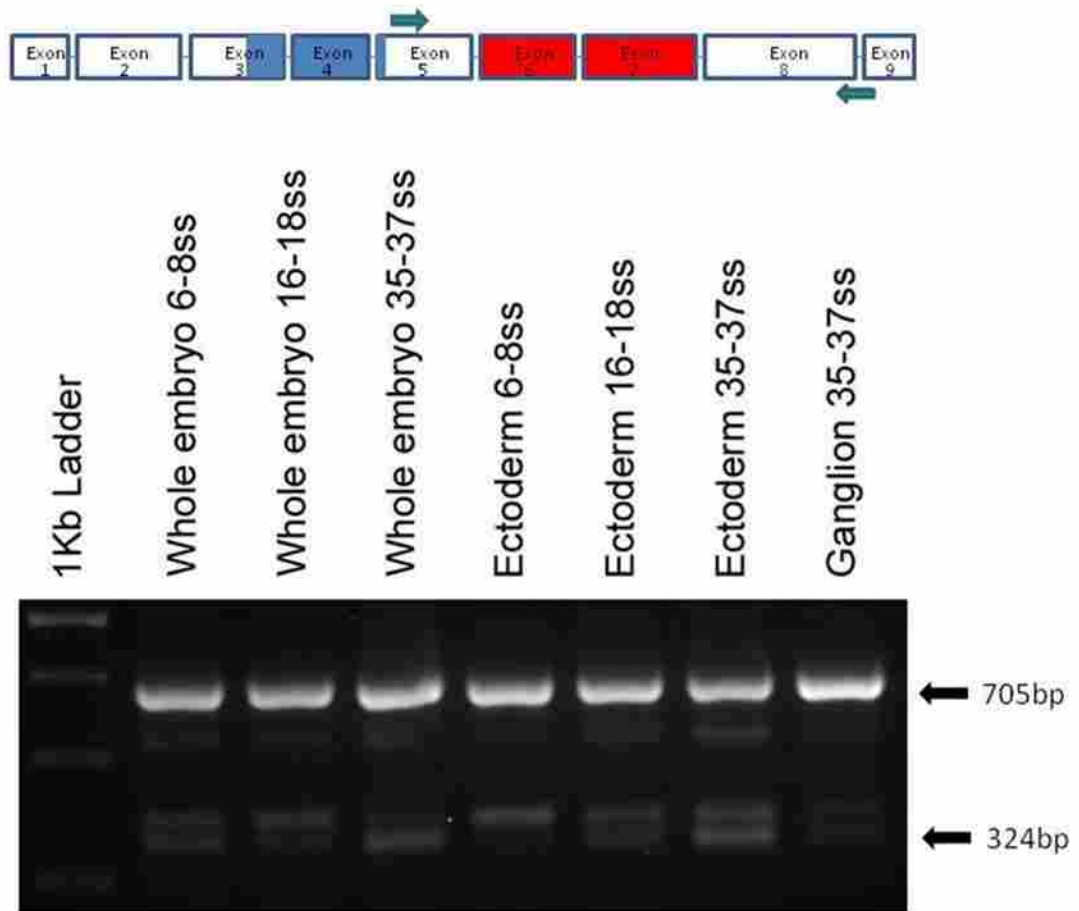


Figure 2.5 C-terminal amplification of Pax3 gene

Total RNA isolated from whole chick, chick ectoderm, and chick opV trigeminal ganglion at different developmental stages was reverse transcribed into cDNA and amplified using a primer pair for exon 5-8 cDNA. The PCR products were separated on 1.5% agarose gels. Predicted isoform sizes are as follows: Pax3, 705bp, and Pax3V2, 324bp.



nucleotide to be a thymine, which corresponded to the DNA sequencing obtained in this study. If this nucleotide is thymine, then exon 6 does include two PESSs (Zhang and Chasin, 2004; Zhang et al., 2005) (Fig 2.6). The possible PESSs are at position 47735 and 47737. Exon 7 includes four PESEs and two PESSs. The two exonic splice silencers are at position 49123 and 49139. The presence of these motifs suggests that exon skipping of both exon 6 and exon 7 is possible during alternative splicing. The presence of the PESSs and the low ratio of PESEs to PESSs give additional evidence of the likelihood that this form of alternative splicing occurs within this region of Pax3 (Zhang and Chasin, 2004; Zhang et al., 2005). The Pax3V2 splice form resembles the mouse Pax3g and Pax3h splice forms that have deletions of exon 8 resulting in a portion of the transactivation domain missing from the isoform (Pritchard et al., 2003; Parker et al., 2004).

The Pax3 protein sequence in chick contains 484 amino acids (NP\_989600.1) (Fig 2.7). The isoforms Pax3V1 and Pax3V2 contain exon deletions that may not introduce a premature stop codon. In Pax3V1, exon 4 is spliced as confirmed by DNA sequencing corresponding to amino acids 81 to 241, and translation proceeds from exon 3 to exon 5 (Fig 2.8). This deletion includes a part of the C-terminal region of the paired domain and the entire octapeptide domain of Pax3. The Pax3V2 isoform contains a deletion of exon 6 and exon 7 as confirmed by DNA sequencing corresponding to amino acids 230 to 336, causing translation of this isoform to proceed from exon 5 to exon 8 (Fig 2.9). This deletion includes a part of the C-terminal region of the homeodomain and a majority of the transactivation domain of Pax3.

	tttttttct	tcaactaaag	ctaagtgttt	atttttat	ttcattttga	gCATCAGCAG	38760
	CCCAGTCTGA	TGAAGGCTCT	GATATCGATT	CTGAACCAGA	CTTACCCTTA	AAAAGAAAGC	38820
Exon5	AGCGTCGCAG	CAGGACAACC	TTCACAGCAG	AGCAACTGGA	AGAGCTGGAA	AGAGCTTTTG	38880
	AGAGGACACA	CTACCCTGAC	ATTTATACTC	GGGAAGAACT	CGCACAAAGA	GCCAAACTCA	38940
	CGGAAGCTCG	AGTTCAgta	tgaatttaa	ggctgcctaa	caaaggggaag	ttcctattaa	39000
Intron5	tgcgacagtc	ctttagtatt	ctcacacgat	cctgctctag	gttagaagga	aaacgtgaag	39060
	gcactgattg	cattttaaat	atgatgccat	tatttctgat	gcaccttat	taaacgtaca	47700
	gaaatcaaat	atgcctaatt	aatcatttg	tagGTCTGGT	TTAGCAACCG	CCGTGCTAGA	47760
Exon6	TGGAGGAAGC	AGGCAGGAGC	CAACCAACTG	ATGGCTTTCA	ACCACCTGAT	CCCAGGAGGG	47820
	TTTCCACCCA	GGGCCATGCC	GACTCTGCCG	ACATACCAGC	TCTCTGAGCC	ATCCTATCAG	47880
	CCCACCTCCA	TACCGCAAGg	tacagtagca	aacaggtact	tggctagagg	gtgctactgg	47940
Intron6	gggcttcatg	tgctgatcca	ctgcagaaac	attttcttct	aaaaatgtag	aaaaaagaac	48000
	tgaacttatt	acgctagaaa	aagaggaggg	aaatgatcaa	cgtgtttctt	ttccttccag	49020
	CCGTGTCTGA	TCCAAGCAGT	ACAGTCCATA	GACCTCAGCC	TCTCCCTCCA	AGCACTGTAC	49080
Exon7	ACCAAAGCAG	CCTCCCTTCA	AACCCAGAGA	GCAGCTCTGC	CTATTGCCTA	CCCAGCACCA	49140
	GGCATGGATT	TTCCAGCTAT	ACAGACAGCT	TTGTGCCTCC	GTCCGGGCCC	TCAAATCCCA	49200
	TGAACCTGTC	CATTGGCAAT	GGCCTTTCAC	CTCAGgtcag	tcctgtgttt	tcagacagag	49260
Intron7	gatttgctgt	ataccagaac	caaagagtct	attccctcag	gccacagtat	aatgaattgc	49320
	atcctaagtc	tacctgtttc	aggaaatcaa	tgaaagactt	gaagactcct	acagctccta	60780
	caacaataca	gttttccatg	tgttttaact	caatcattct	accttttatt	ttagGTAATG	60840
	GGACTCTTGA	CTAACCATGG	TGGTGTGCCT	CACCAGCCCC	AAACTGATTA	TGCCCTGTCC	60900
Exon8	CCTTTGACTG	GAGGTCTGGA	GCCCACCACC	ACTGTCTCAG	CCAGCTGCAG	TCAGCGGCTA	60960
	GATCACATGA	AGAGTTTAGA	CAGCCTGCCT	ACATCACAGT	CCTACTGCCC	ACCGACCTAT	61020
	AGCACCACCG	GCTACAGCAT	GGACCCTGTC	ACAGGCTACC	AGTATGGACA	GTATGGACAA	61080
	Agtgagtgct	gtgacacaat	aatcatttat	caattgtatg	tttttttttt	tttttttttt	61140
	gtctgtaaca	aagaaaatta	caggaattag	accctaattg	ctgactgcta	ctactctcca	61200

Figure 2.6 Pax3 sequence of exons 5, 6, 7, and 8

The genomic sequence was obtained from the NCBI GenBank at the reference sequence: NC\_006096.3. The exons and introns are labeled on the left and the nucleotide number is on the right of the genomic sequence. Nucleotides of an exon are in upper case, and nucleotides of an intron are in lower case.

```

1  MTTLAGAVPRMMRPGAGQSYPRGGFPLEVSTPLGQGRVNQ
41  LGGVFINGRPLPNHIRHKIVEMAHHGIRPCVISRQLRVSH
81  GCVSKILCRYQETGSIRPGAIGGSKPKQVTTDPVEKKIEE
121 YKRENAGMFSWEIRDRLKDGVCDRNTVPSVSSISRILRS
161 KFGKGEAAAELERKEAEEGDKKAKHSIDGILSERASAAQ
201 SDEGSDIDSEPDLPKRRKRRSRTTFTAEQLEELERAFER
241 THYPDIYTRELAQRAKLTEARVQVWFSNRRARWRKQAGA
281 NQLMAFNHLIPGGFPPSAMPTLPTYQLSEPSYQPTSIPQA
321 VSDPSSTVHRPQPLPPSTVHQSSLPSNPESSAYCLPSTR
361 HGFSSYTDSFVPPSGPSNPMNPAIGNGLSPQVMGLLTNHG
401 GVPHQPQTDYALSPLTGGLEPTTTVSASCSQRLDHMKSLD
441 SLPTSQSYCPPTYSTTGYSMDPVTGYQYGGQSAFHLYK
481 PDIA*

```

Figure 2.7 Amino acid sequence of Pax3 isoform

The Pax3 protein sequence in chick is 484 amino acids long. The predicted paired domain is made up of amino acids 34 through 162 and the predicted homeodomain is located from amino acid 219 through 278. The predicted octapeptide domain is located between these two domains at amino acid 186 through 192. The transactivation domain has not been defined in chick though has been described as a proline, serine, and threonine rich domain located at the C-terminal end of the protein. The predicted transactivation domain may include amino acids 279 through 484.

```

1  MTTLAGAVPRMMRPGAGQSYPRGGFPLEVSTPLGQGRVNO
41  LGGVFINGRPLPNHIRHKIVEMAHHGIRPCVISRQLRVSH
81  GCVSKILCRYQETGSIRPGAIGGSKPKQVTPDVEKKIEE
121 YKRENAGMFSWEIRDRLKDGVCDRNTVPSASAAQSDEGS
161 DIDSEPDLPKQRRSRTTFTAEQLEELERAFERTHYPD
201 IYTREELAQRAKLTEARVQVWFNRRARWRKQAGANQLMA
241 FNHLIPGGFPPSAMPTLPTYQLSEPSYQPTSIPQAVSDPS
281 STVHRPQLPSTVHQSSLPSNPESSAYCLPSTRHGFSS
321 YTDSFVPPSGPSNPMNPAIGNGLSPQVMGLLTNHGGVPHQ
361 PQTDYALSPLTGGLEPTTTVSASCSQRDLMKSLDSLPTS
401 QSYCPPTYSTTGYSMDPVTGYQYGGQSAFHLYLKPDI*

```

Figure 2.8 Predicted amino acid sequence of Pax3V1 isoform

The Pax3V1 isoform in chick is 439 amino acids long and contains a deletion of 45 amino acids that occurs after amino acid 150. This deletion includes 12 amino acids of the C-terminus paired domain and the entire octapeptide domain. A premature stop codon is not introduced in the amino acid sequence in green as this was confirmed by DNA sequencing.

```

1  MTTLAGAVPRMMRPGAGQSYPRGGFPLEVSTPLGQGRVNQ
41  LGGVFINGRPLPNHIRHKIVEMAHHGIRPCVISRQLRVSH
81  GCVSKILCRYQETGSIRPGAIGGSKPKQVTTDPVEKKIEE
121 YKRENAGMFSWEIRDRLKDGVCDRNTVPSVSSISILRS
161 KFGKGEEEEEALERKEAEEGDKKAKHSIDGILSERASAAQ
201 SDEGSDIDSEPDLPKRRKQRRSRTTFTAEQLEELERAFER
241 THYPDIYTREELAQRAKLTARVQVMGLLNHGGVPHQPQ
281 TDYALSPLTGGLEPTTTVSASCSQRLDHMKSLDSLPTSQS
321 YCPPTYSTTGYSMDPVTGYQYGQYQGSFAHYLKPDI*

```

Figure 2.9 Predicted amino acid sequence of Pax3V2 isoform

The Pax3V2 isoform in chick is 357 amino acids long and contains a deletion of 127 amino acids that occurs after amino acid 265. This deletion includes 13 amino acids of the C-terminus homeodomain and the N-terminus of the C-terminal transactivation domain. A premature stop codon is not introduced in the amino acid sequence in green as this was confirmed by DNA sequencing.

### Quantitative analysis of the splice form Pax3 and the splice form Pax3V2

It was important for us to understand the quantitative expression of Pax3 and Pax3V2 during different developmental stages in the chick. This may allow us to see a change of expression that coincides with an important developmental process in the opV placode and show a possible change in the fold expression of Pax3 and Pax3V2. Samples that were used in this study included ectodermal tissue of the opV placode collected at 6-8ss, 10-15ss, 20-25ss, and 32-37ss. Tissue from opV ganglia was also collected at 32-37ss and analyzed.

The quantitative fold expression change between Pax3 and PaxV2 is similar during the different time points and tissue examined (Figs 2.10A and 2.10B). Both are present in the ectoderm at the time of opV placodal cell commitment, 6-8ss, and their ectodermal expression increases in concentration at 10-15ss. A slight increase of expression is present at 20-25ss in the ectoderm, when opV cellular delamination and neuronal differentiation is at its peak. Then at 32-37ss the concentration of Pax3 and Pax3V2 in the ectoderm decreases as most Pax3+ cells have delaminated and migrated to form the opV ganglion. At 32-37ss, the concentration of Pax3 and Pax3V2 is the highest in the ganglia compared to any of the other stages where ectoderm was collected (Fig 2.10A). There were significant differences between the quantitative expressions of the isoforms at different stages (Table 2.1). Expression of Pax3 increased significantly between stages 6-8ss and 20-25ss in the ectoderm, and then its expression decreased significantly from stage 20-25ss to 32-37ss in the ectoderm. Though the same pattern of quantitative expression was seen with the Pax3V2 isoform, its change was not as significant (Table 2.2). The quantitative expression of both Pax3 and Pax3V2 decrease significantly when comparing the ectoderm to the ganglia at 32-37ss (Table 2.2). This corresponds to past results showing a decline of Pax3 expression in the opV placode by 35ss, with expression of Pax3

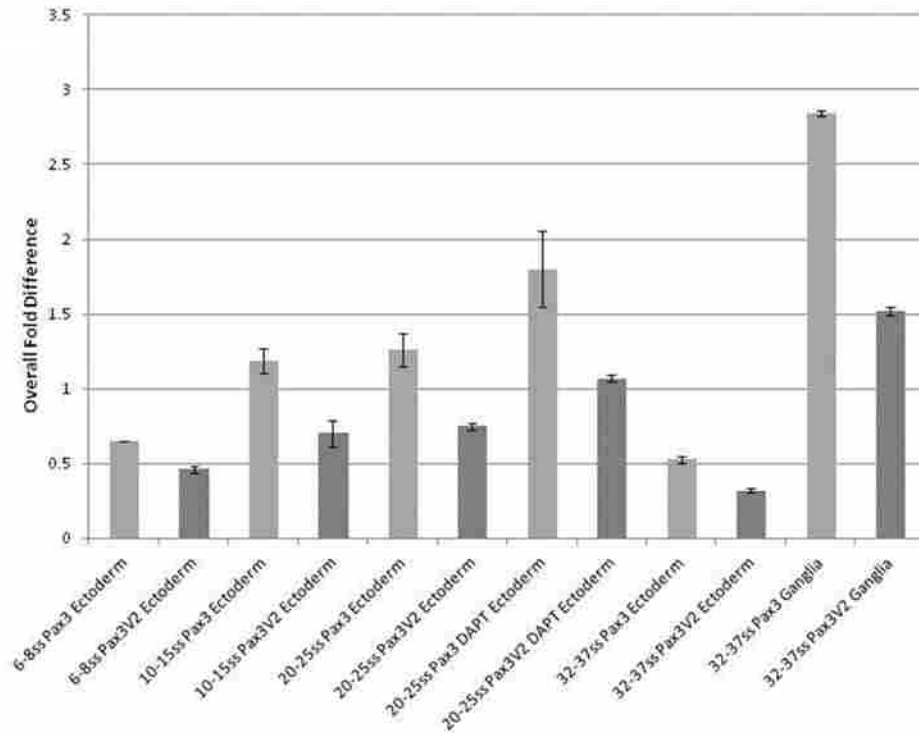
remaining in the ganglion (Stark et al., 1997).

The Lassiter et al., (2010) publication on Notch signaling in the opV placode showed that neurogenesis was enhanced when Notch signaling was blocked by the chemical, DAPT. We wanted to know if exposing developing chicks to DAPT would change the expression of Pax3 or Pax3V2. Therefore, chicks were collected at 10-14ss and transferred to culture media containing DAPT. The embryos were incubated at 37°C for 12 hours and collected at 20-25ss to compare this tissue to the ectoderm tissue collected from chick embryos of the same stage that were not cultured with DAPT.

Knocking down the Notch signaling pathway had an interesting effect on the quantity of Pax3 and Pax3V2 expression. Ectoderm of the opV region that was previously exposed to DAPT had a significant increase in the amount of Pax3 and Pax3V2 expression when compared to non-treated ectoderm of the same region (Table 2.2). This may imply that Notch signaling has an inhibitor effect on the transcription of Pax3 and Pax3V2.

Lastly, the quantitative fold difference between Pax3 and Pax3V2 was similar, independent of the developmental stage or of the DAPT treatment (Fig 2.10B). At the earlier stage of 6-8ss, Pax3 fold difference was not significantly different from Pax3V2 when compared to the later stages (Table 2.3). The fold difference between the two mRNA transcripts increased moderately by 10-15ss and leveled off through 32-37ss. There was a moderate increase in the expression of Pax3 when compared to Pax3V2 in the ganglia at 32-37ss, though no significant difference was shown (Table 2.4). This data shows that Pax3 is expressed approximately 1.4 to 1.9 times greater than its isoform Pax3V2 during different embryonic stages and in the different tissue types studied. Expression of both genes increases during neuronal differentiation in the ectoderm and then decreases with opV ganglion formation. Finally, this data shows that both Pax3 and Pax3V2 expression is significantly increased when Notch signaling is blocked.

A.



B.

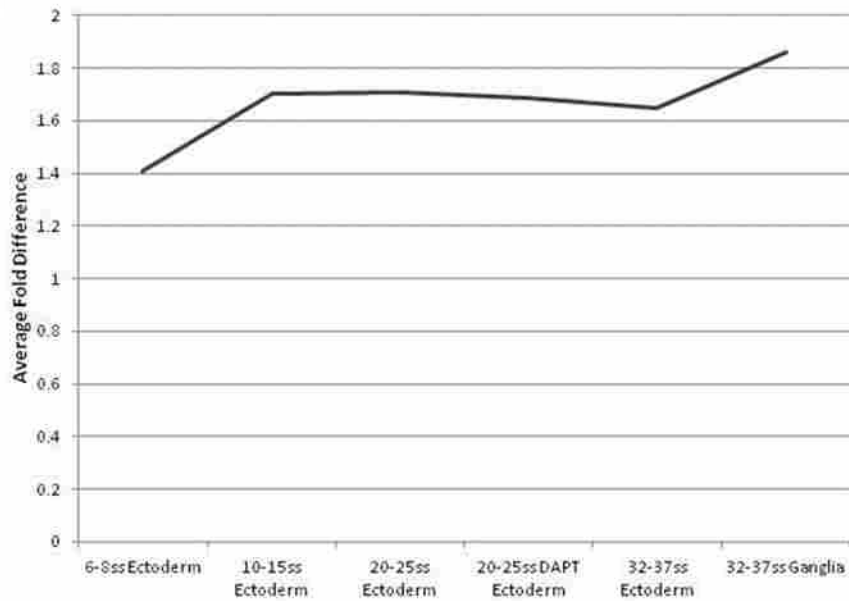


Figure 2.10 Fold expression change between the spatiotemporal expression of Pax3 and Pax3V2 (legend on page 43)



Figure 2.10 Fold expression change between the spatiotemporal expression of Pax3 and Pax3V2

Figure 2.10A shows the overall average fold expression change between Pax3 and Pax3V2 expression in opV development. A similar pattern of greater Pax3 expression than Pax3V2 is shown throughout all tissue samples. Beginning at 6-8ss in the ectoderm, we show that Pax3 and Pax3V2 expression is less than at 10-15ss and 20-25ss in the ectoderm, which two stages are similar in Pax3 and Pax3V2 expression. However, as DAPT is exposed to developing chick embryos and collected at 20-25ss a significant increase in both Pax3 and Pax3V2 expression in the ectoderm is shown. At 32-37ss, Pax3 and Pax3V2 expression decreases in the ectoderm, but increases in the ganglia. Figure 2.10B shows the average fold expression change between Pax3 and Pax3V2 in individual tissue groups. The average fold difference between Pax3 and Pax3V2 is the smallest at 6-8ss in the ectoderm, and increases at 10-15ss in the ectoderm. The average fold difference appears to be the same in the ectoderm at 10-15ss, 20-25ss not treated with DAPT, 20-25ss treated with DAPT, and 32-37ss. The average fold difference increases in ganglia tissue at 32-37ss.

Source	DF	SS	MS	F value	p-value
Model	11	26.53	2.41	50.41	<0.0001
Error	44	2.11	0.05		
Corrected Total	55	28.64			

Table 2.1 Analysis of variance between groups using the overall fold difference

This ANOVA table is showing whether there is a significant difference between any two groups when comparing the overall fold difference. The overall fold difference was used to make a quantitative comparison between all experiments. The table shows a large F value and a small p-value supporting that there is a significant difference between at least two experimental groups. Upon further analysis, the key differences that were significant included the difference between Pax3 expression in the ectoderm at 6-8ss and 10-15ss, and the individual differences between Pax3 expression and Pax3V2 expression in the ectoderm at 20-25ss with and without DAPT treatment. Degrees of freedom (DF), sum of squares (SS), mean squares (MS)

Experiment	Experimental number	Mean of the experimental fold difference	Number of replicates
<b>Pax3</b>			
6-8ss ecotoderm	1	0.6477	3
10-15ss ectoderm	2	1.1875	5
20-25ss ectoderm	3	1.2589	5
20-25ss ectoderm DAPT	4	1.8003	5
32-35ss ectoderm	5	0.529	5
32-35ss ganglia	6	2.8414	5
<b>Pax3V2</b>			
6-8ss ecotoderm	7	0.462	3
10-15ss ectoderm	8	0.7015	5
20-25ss ectoderm	9	0.7481	5
20-25ss ectoderm DAPT	10	1.0691	5
32-35ss ectoderm	11	0.319	5
32-35ss ganglia	12	1.5166	5

p-values	1	2	3	4	5	6
1		0.0595	0.0185	<.0001	0.9998	<.0001
2			1	0.0032	0.0012	<.0001
3				0.0145	0.0002	<.0001
4					<.0001	<.0001
5						<.0001

p-values	7	8	9	10	11	12
1	0.9957	1	1	0.2908	0.6537	0.0001
2	0.0024	0.0425	0.0965	0.9992	<.0001	0.4407
3	0.0006	0.0104	0.0265	0.9629	<.0001	0.7745
4	<.0001	<.0001	<.0001	0.0002	<.0001	0.6581
5	1	0.9815	0.9059	0.0149	0.9276	<.0001
6	<.0001	<.0001	<.0001	<.0001	<.0001	<.0001

p-values	7	8	9	10	11	12
7		0.9331	0.8143	0.0198	0.9988	<.0001
8			1	0.2811	0.2306	<.0001
9				0.4784	0.1146	<.0001
10					0.0001	0.0842
11						<.0001

Table 2.2 Tukey-Kramer analysis of individual fold differences (legend on page 46)

Table 2.2 Tukey-Kramer analysis of individual fold differences

Quantitative analysis was performed with primer pairs that amplified Pax3 or the Pax3V2 variant. The overall fold difference between the experimental groups was calculated from the Ct values. The upper part of the table defines the experiment analyzed, the number designated to the experiment, and the mean of the experimental fold difference. The lower part of the table shows the p-values calculated between individual experiments using the overall fold difference.

Source	DF	SS	MS	Fvalue	p-value
Model	5	0.39	0.08	1.64	0.1912
Error	22	1.06	0.05		
Corrected Total	27	1.45			

Table 2.3 Analysis of variance between groups using the sample's fold difference

This ANOVA table is showing whether there is a significant difference between any two groups when comparing the sample's fold difference. The fold difference was determined between the quantitative values of two different amplicons produced from the same sample. The table shows a small F value and a large p-value supporting that there is not a significant difference between any samples. Degrees of freedom (DF), sum of squares (SS), mean squares (MS)

Sample pairs	Sample number	Mean fold difference between the sample pairs	Number of replicates			
<b>Pax3</b>						
<b>Pax3V2</b>						
6-8ss ectoderm	6-8ss ectoderm	1	1.4069	3		
10-15ss ectoderm	10-15ss ectoderm	2	1.7007	5		
20-25ss ectoderm	20-25ss ectoderm	3	1.7068	5		
20-25ss ectoderm DAPT	20-25ss ectoderm DAPT	4	1.6835	5		
32-35ss ectoderm	32-35ss ectoderm	5	1.6455	5		
32-35ss ganglia	32-35ss ganglia	6	1.8591	5		
p-values	1	2	3	4	5	6
1		0.4667	0.4447	0.5304	0.6746	0.0911
2			1	1	0.9985	0.8586
3				1	0.9976	0.8771
4					0.9998	0.8
5						0.6444

Table 2.4 Tukey-Kramer analysis between sample pairs using the sample's fold difference

Quantitative analysis was performed with primer pairs that amplified Pax3 or the Pax3V2 variant. The fold difference between the two amplicons of the same sample was calculated from the Ct values. The upper part of the table defines the samples analyzed, the number designated to the sample pairs, and the mean of the fold difference between the sample pair. The lower part of the table shows the p-values calculated between individual experiments using the fold difference of the sample pairs.

Misexpression of Pax3 and Pax3V1 may contribute to the maintenance of placodal cells, as Pax3V2 may contribute to the neuronal differentiation of placodal cells

The previous information showed that transcriptional modifications of the chick Pax3 gene produces alternative splice variants. The information also showed that Pax3 and the isoform Pax3V2 have different quantitative expression over different stages and in different tissues. From this information we wanted to understand the function of the alternative splice variants in the opV trigeminal placode and used misexpression experiments for this purpose. Constitutively expressing constructs were designed to be misexpressed in the chick at different developmental stages (Fig 2.11).

There was a possibility that the Pax3 antibody used would not detect the Pax3 protein of isoform Pax3V2 as the deletion is at the C-terminal end of the protein. This region is recognized by the Pax3 antibody for chick. To verify this and to test our misexpression construct we transfected cells with the Pax3 and Pax3V2 construct and then stained for Pax3 protein (Fig 2.12). The results showed that the constructs did produce Pax3 protein and that the antibody was able to recognize and attach to the C-terminal region of the Pax3V2 isoform (Fig 2.12F). Upon confirming that our constructs were functional, *in ovo* electroporation of these constructs were performed at 6-8ss, 10-12ss (data not shown), and 14-16ss.

Misexpression experiments were performed to understand the function of both Pax3V1 and Pax3V2 isoforms and to verify if they were sufficient for sensory neurogenesis. Each construct was electroporated in the chick embryo at 6-8ss before ectodermal commitment of opV placodal cells or at 14-16ss, which marks the beginning of neuronal differentiation. The embryos were incubated for 24-32 hours and tissue sections were analyzed through antibody staining of Pax3 and Islet1. Pax3 is a cellular marker of the opV placode and staining for Pax3

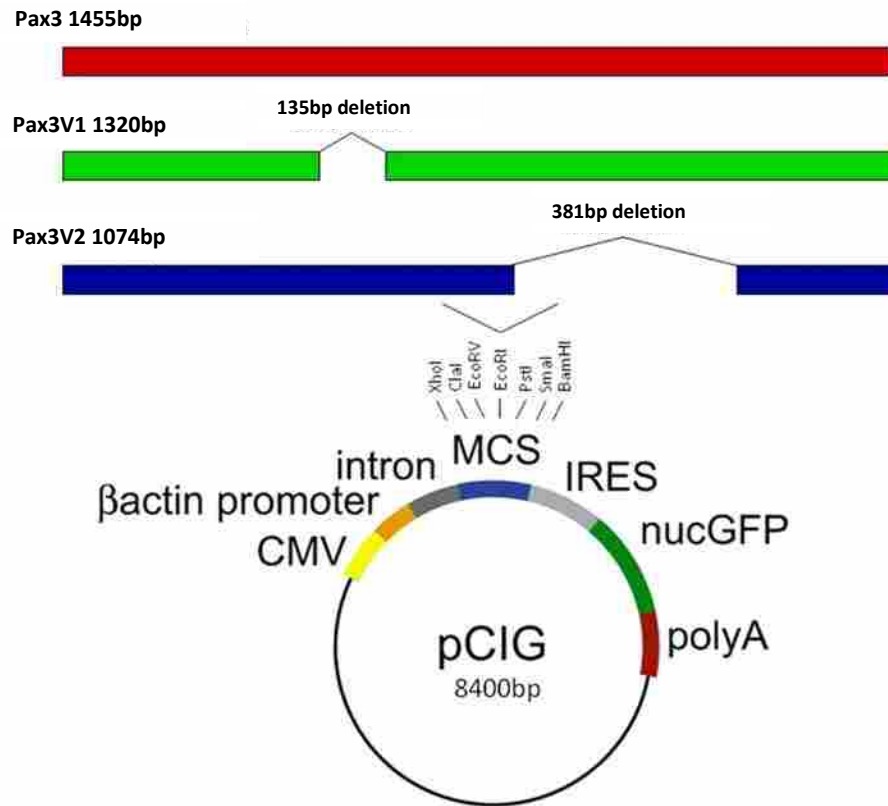


Figure 2.11 Plasmid constructs

Pax3 plasmid constructs produced by inserting Pax3 sequence into the pCIG vector (8400bp) at the EcoRI restriction site. The Pax3 insert (1455) contains the entire transcriptional coding region. The Pax3V1 insert (1320bp) contains an exon deletion between amino acids 451-586 and the Pax3V2 insert (1074bp) contains the deletion of two exons between amino acids 792-1173.

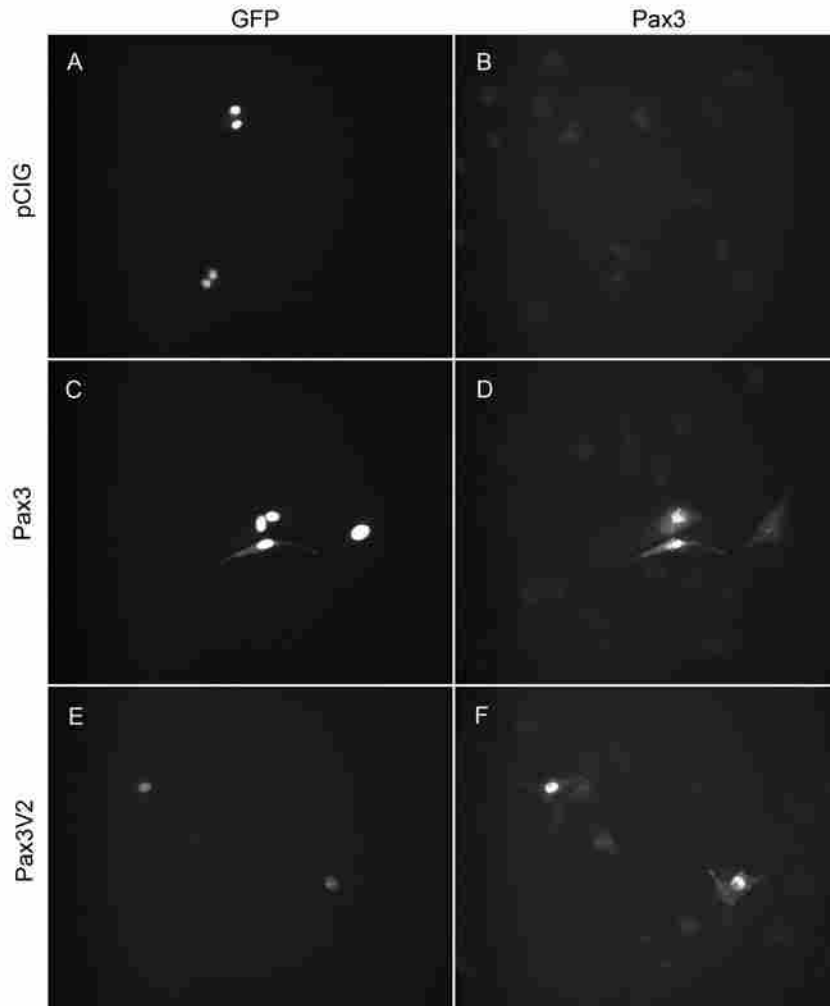


Figure 2.12 GFP expression and Pax3 antibody staining of cells transfected with plasmid constructs. GFP expression of the pCIG vector and Pax3 constructs transfected into cells (A, C, and E). The transfected cells were stained for Pax3 and though expression is absent from the empty pCIG vector (B), Pax3 expression is shown in cells transfected with the Pax3 construct (D) and the Pax3V2 construct (F).



allows us to determine if targeted cells are within the placode for further analysis (Stark et al., 1997). *Islet1* is expressed in all trigeminal neurons and is a marker for neuronal differentiation (Begbie et al., 2002; Fedtsova et al., 2003, Lassiter et al., 2007; Dude et al., 2009). These two markers allowed for specific analysis of neurogenesis within the opV region.

Most commonly, Pax3<sup>+</sup> opV cells are maintained in the ectoderm, and eventually become fated as neurons to delaminate from the ectoderm. Upon delamination they begin migrating through the mesenchyme and express *Islet1*. Even after these differentiating cells condense to form the opV ganglion, they continue to express *Islet1*. Using this pattern of differentiation, we can contrast the results of the controls with experimental embryos to analyze the following possibilities. A significant change in the amount of Pax3<sup>+</sup> cells remaining within the ectoderm may occur, and depending on the experiment these cells may or may not differentiate as neurons within the ectoderm which can be shown by aberrant *Islet1* expression in the ectoderm as this does not commonly occur. In addition, a significant change in the amount of Pax3<sup>+</sup> cells delaminating into the mesenchyme and migrating may occur. Corresponding to this change, we can analyze a change in the amount of *Islet1*<sup>+</sup> cells in the mesenchyme allowing us to understand the experiments effect on neurogenesis. Furthermore, as the electroporated construct are marked by GFP, cell-autonomous behavior on neurogenesis influenced by the constitutively active isoform can be analyzed using *Islet1*. With these scenarios in mind, the following experiments and analyses were performed.

The main interest of this study was focused in the opV placode, however, the area caudal to the otic region was also analyzed. Staining showing the results of the misexpression experiments are shown in figures 2.13 and 2.14. Targeted cells in the ectoderm were analyzed, and it was shown that a significant amount of targeted Pax3<sup>+</sup> cells for Pax3 and Pax3V1

constructs remained in the ectoderm compared to pCIG controls (Fig 2.15A). There were also significant amounts of Pax3V1 targeted Pax3+ cells remaining in the ectoderm when compared to the Pax3V2 construct (Fig 2.15A). Targeted cells in the mesenchyme were counted and analysis showed a significant reduction of targeted Pax3+ cells for Pax3, Pax3V1, and Pax3V2 when compared to pCIG controls (Fig 2.15C). In addition, Islet1+ cells were counted in the mesenchyme and compared to the pCIG controls, Pax3, Pax3V1, and Pax3V2 had a significant reduction of Islet1+ cells, though the reduction in the Pax3 and Pax3V1 embryos was significantly less than in those embryos electroporated with the Pax3V2 construct (Fig 2.16A). Targeted Pax3+ cells in the mesenchyme that also expressed Islet1 was reduced in embryos electroporated with the Pax3, Pax3V1, and Pax3V2 constructs when compared with pCIG controls, however, again a significant reduction was shown in the Pax3 and Pax3V1 embryos when compared to embryos electroporated with the Pax3V2 construct (Fig 2.16C). More conclusive results were desired at this point and a different time point of electroporation was studied to determine if a Pax3 isoform specifically contributes to neuronal differentiation.

Embryos were electroporated at 14-16ss, which marks the beginning of neuronal differentiation and migration, and incubated for 24 hours. The embryos were analyzed as previously described with antibody staining of Pax3 and Islet1. Compared to the pCIG controls, there was a significant amount of targeted Pax3+ cells remaining in the ectoderm of embryos electroporated with the Pax3 and Pax3V1 constructs, but no significant difference from the control was shown with the Pax3V2 construct (Fig 2.15B). A significant reduction of Islet1+ cells was seen in the mesenchyme of embryos electroporated with the Pax3V1 construct when compared to the pCIG controls and a significant reduction was seen in Pax3V1 electroporated embryos when compared to Pax3V2 (Fig 2.16B). Compared to the pCIG controls, a significant

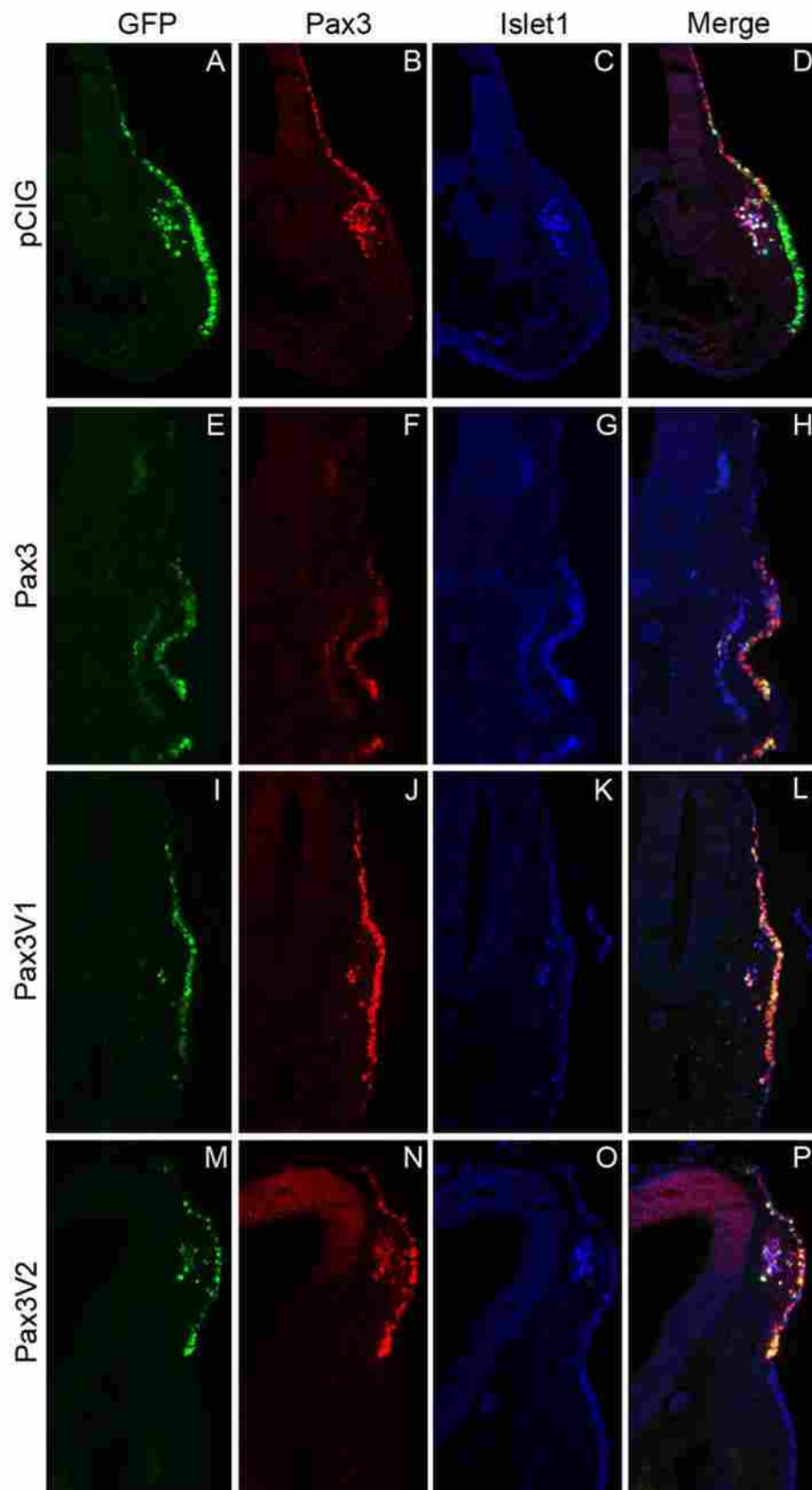


Figure 2.13 Pax3 isoform electroporation at 6-8ss may contribute to neuronal differentiation (legend on page 54)

Figure 2.13 Pax3 isoform electroporation at 6-8ss may contribute to neuronal differentiation

The sections are of the opV placode from embryos that were electroporated *in ovo* at 6-8ss and then incubated for 32 hours. The sections were then stained for Pax3 and Islet1. (A-D) pCIG misexpression; (E-H) Pax3 misexpression; (I-L) Pax3V1 misexpression; (M-P) Pax3V2 misexpression. Pax3 targeted cells remained in the ectoderm with electroporation of Pax3 and Pax3V1 when compared with the control (D, H, and L). A decrease number of Pax3 cells and Islet1 cells in the mesenchyme were seen in all electroporated isoforms when compared to the control (B, F, J, N, and C, G, K, O). A decrease number of targeted Islet1 cells in the mesenchyme were seen for all electroporated isoforms when compared to the control, though this was more pronounced with the Pax3 and Pax3V1 isoforms (D, H, L, and P).

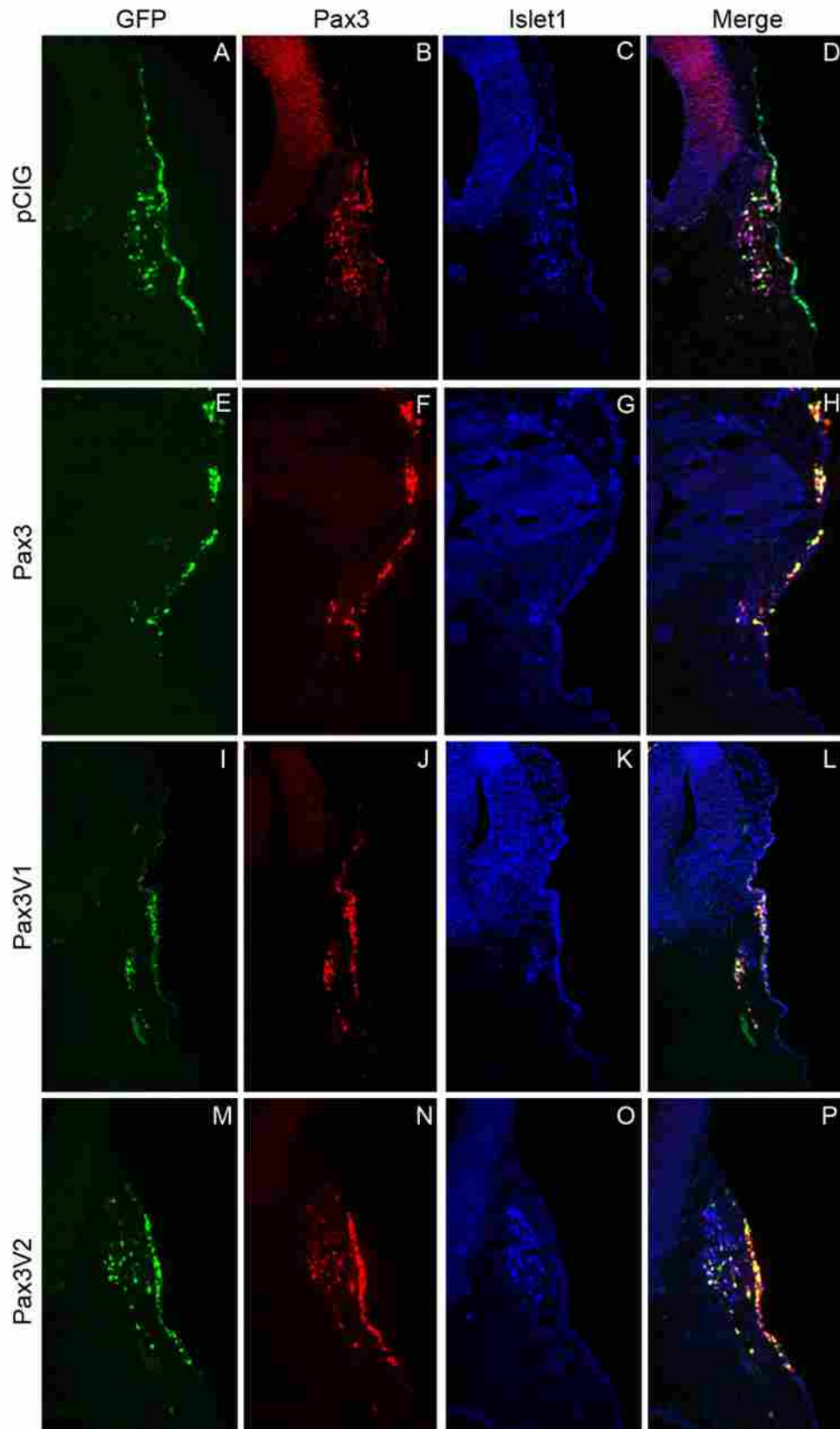


Figure 2.14 Pax3 isoform electroporation at 14-16ss may contribute to neuronal differentiation (legend on page 56)

Figure 2.14 Pax3 isoform electroporation at 14-16ss may contribute to neuronal differentiation  
These sections are of the opV placode from embryos that were electroporated at 14-16ss and then incubated for 24 hours. The sections were then stained for Pax3 and Islet1. (A-D) pCIG misexpression; (E-H) Pax3 misexpression; (I-L) Pax3V1 misexpression; (M-P) Pax3V2 misexpression. Pax3 targeted cells remained in the ectoderm with electroporation of Pax3 and Pax3V1 when compared with the control (D, H, and L). A decrease number of Islet1 cells in the mesenchyme were seen in embryos electroporated with the Pax3V1 isoform when compared to the control (C and K). A decrease number of targeted Islet1 cells in the mesenchyme were seen for all electroporated isoforms when compared to the control, though this was more pronounced with the Pax3 and Pax3V1 isoforms (D, H, L, and P).

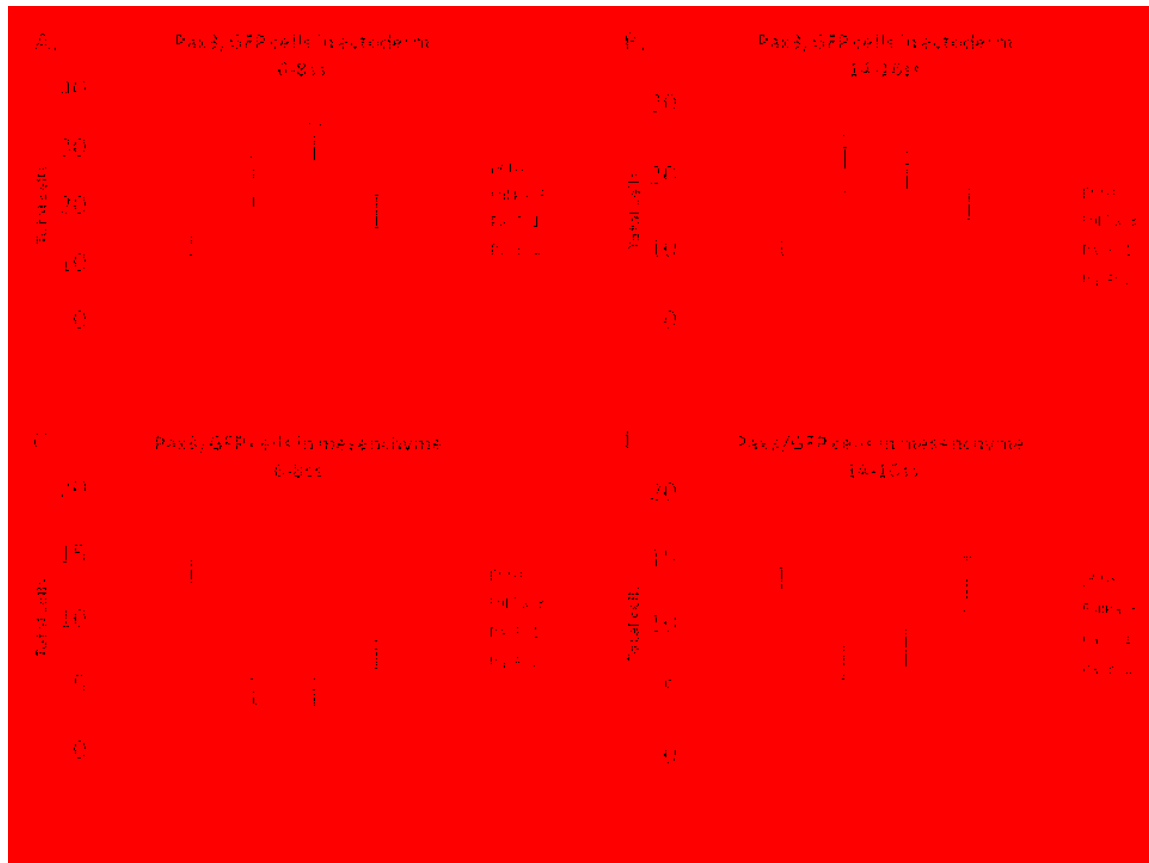


Figure 2.15 In ovo misexpression of Pax3 constructs at 6-8ss and 14-16ss

(A.) Colocalization of Pax3 and GFP expressing cells in the ectoderm at 6-8ss.

(B.) Colocalization of Pax3 and GFP expressing cells in the ectoderm at 14-16ss.

(C.) Colocalization of Pax3 and GFP expressing cells in the mesenchyme at 6-8ss.

(D.) Colocalization of Pax3 and GFP expressing cells in the mesenchyme at 14-16ss.

Error bars represent the standard error of the mean.

(\*) p-value <0.05 between the experimental groups and the control group, pCIG

(^) p-value <0.05 between two experimental groups

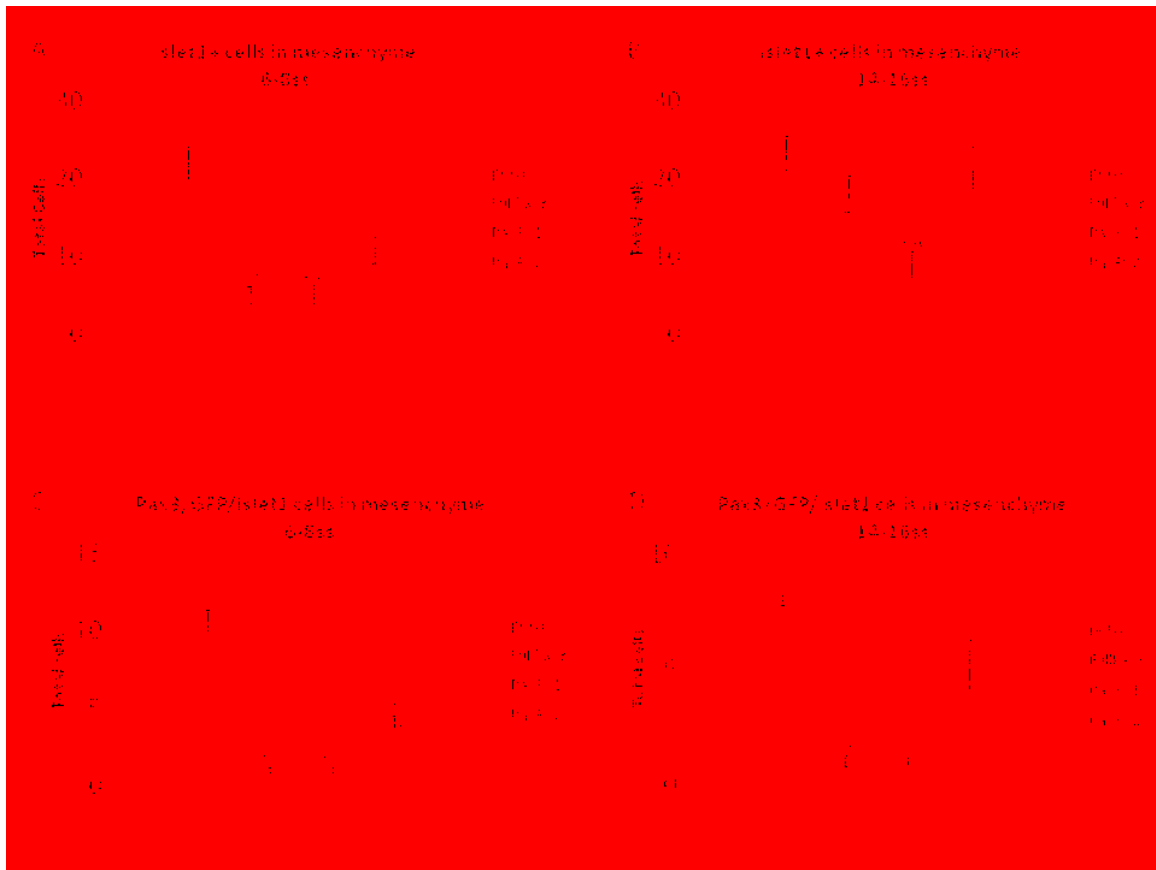


Figure 2.16 *In ovo* misexpression of Pax3 constructs at 6-8ss and 14-16ss, continued

(A.) Islet1 positive cells in the mesenchyme at 6-8ss.

(B.) Islet1 positive cells in the mesenchyme at 14-16ss.

(C.) Colocalization of Pax3, GFP, and Islet1 expressing cells in the mesenchyme at 6-8ss.

(D.) Colocalization of Pax3, GFP, and Islet1 expressing cells in the mesenchyme at 14-16ss.

Error bars represent the standard error of the mean.

(\*) p-value <0.05 between the experimental groups and the control group, pCIG

(^) p-value <0.05 between two experimental groups



reduction of targeted Pax3<sup>+</sup> cells expressing Islet1 were seen in the mesenchyme in embryos electroporated with the Pax3, Pax3V1, and Pax3V2 constructs (Fig 2.16D). In addition, there was a significant reduction of targeted Pax3<sup>+</sup> cells expressing Islet1 in the mesenchyme of Pax3 and Pax3V1 electroporated embryos when compared to Pax3V2 (Fig 2.16D).

Each Pax3 construct was electroporated in the otic region of the embryo at 6-8ss and 14-16ss. This region was analyzed with Pax3 and Islet1 antibody staining to see if the Pax3 isoforms were sufficient for neurogenesis. There was no noticeable neurogenesis produced by any of the Pax3 isoforms and it was concluded that none of the Pax3 isoforms were sufficient to produce neurogenesis (data not shown).

These data suggest that ectodermal cells targeted with Pax3 and Pax3V1 remain in the ectoderm. They also suggest that Pax3, Pax3V1, and Pax3V2 causes a reduction of neurogenesis as shown with a decrease of Islet1<sup>+</sup> cells in the mesenchyme and that these isoforms may not contribute to terminal differentiation of sensory neurons as the targeted Pax3<sup>+</sup> cells in the mesenchyme do not express Islet1. However, the data shows that Pax3V2 did differ from Pax3 and Pax3V1. Pax3V2 did not have as severe of a reduction in Islet1<sup>+</sup> cells in the mesenchyme as Pax3 or Pax3V1, nor as few targeted Pax3<sup>+</sup> cells in the mesenchyme expressing Islet1. Since this preliminary study showed a few significant differences between Pax3V2 and the other Pax3 isoforms, but did not appear to be similar to pCIG controls we thought by enhancing neurogenesis a more defined difference between the isoforms may result when analyzing neurogenesis. In addition to this idea, research has found that Pax3 directly binds to the promoter of the *Hes1* gene, regulating its transcription (Nakazaki et al., 2008). Hes1 is a transcription factor that is unregulated from Notch signaling (Jarriault et al., 1998). This information was exciting as it showed a direct relationship between Pax3 and the Notch signaling

pathway. This led us to investigate the function of Pax3 and its isoforms in a culture system that would block Notch signaling, enhancing neurogenesis and allowing for the understanding of how inhibiting Notch signaling affects Pax3 function.

DAPT is a gamma-secretase inhibitor that prevents Notch signaling leading to an increase in sensory neurogenesis shown through a significant increase of Islet1+ cells in the mesenchyme when compared to controls (Lassiter et al., 2010). A few modifications of the culture technique developed by Chapman et al., (2001) allowed for this study. These modifications included the addition of chemicals within the culture media. Modifications also included placing an additional ring underneath the yolk membrane allowing for the transfer of chick embryos during the incubation period without harming the embryo. This ability to safely transfer chick embryos between culture media allowed for the regulation of embryos being incubated in the presence or absence of experimental chemicals. Furthermore, using the double ring method allowed for the electroporation of explanted embryos with better results. To test the effectiveness of the EC culture with a chemical, DAPT was added to the culture media and embryos were incubated on the media resulting in an increase in neurogenesis similar to prior results produced in the Stark lab (data not shown). This approach was then used to combine electroporation with DAPT treatment. Embryos were electroporated with a different Pax3 construct at 5-7ss and incubated on the culture media for 12 hours. The embryos were transferred from this culture media onto another culture media containing either DAPT or DMSO and incubated for another 24 hours. The embryos were then analyzed with antibody staining of Pax3 and Islet1 (Figs 2.17 and 2.18). Compared to the pCIG control and Pax3V2, targeted Pax3+ cells expressing Islet1 in the mesenchyme were significantly reduced in embryos electroporated with Pax3 and Pax3V1 constructs when exposed to DAPT (Fig 2.19). These data are different from that seen in

experiments performed *in ovo*. Pax3V2 misexpression resulted in near-normal differentiation, while Pax3 and Pax3V1 misexpression prevented differentiation, even when blocking Notch signaling.

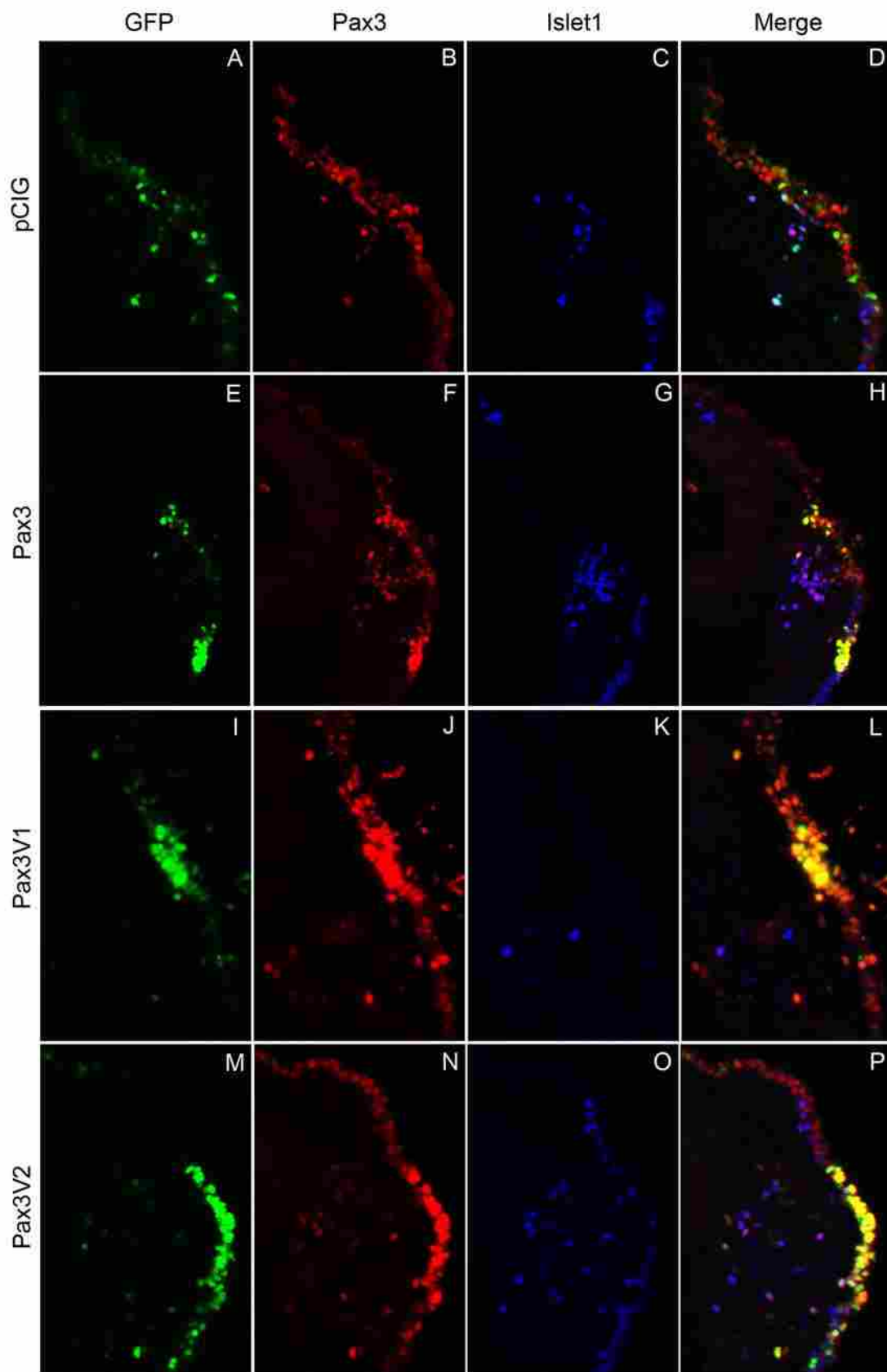


Figure 2.17 Pax3 isoform may contribute to neuronal differentiation (legend on page 63)

**Figure 2.17 Pax3 isoform may contribute to neuronal differentiation**

These sections are of the opV placode that were electroporated at 5-7ss and then cultured for 36 hours with DMSO. The sections were then stained for Pax3 and Islet1. (A-D) pCIG misexpression; (E-H) Pax3 misexpression; (I-L) Pax3V1 misexpression; (M-P) Pax3V2 misexpression. (B, N) Pax3 expression in the mesenchyme and Pax3 colocalization with Islet1 is similar in the misexpression of pCIG and Pax3V2 (D, P). (F, J) Pax3 expression is decreased in the mesenchyme and Pax3 colocalization with Islet1 in the mesenchyme is significantly decreased in misexpression studies of Pax3 and Pax3V1 (H, L).

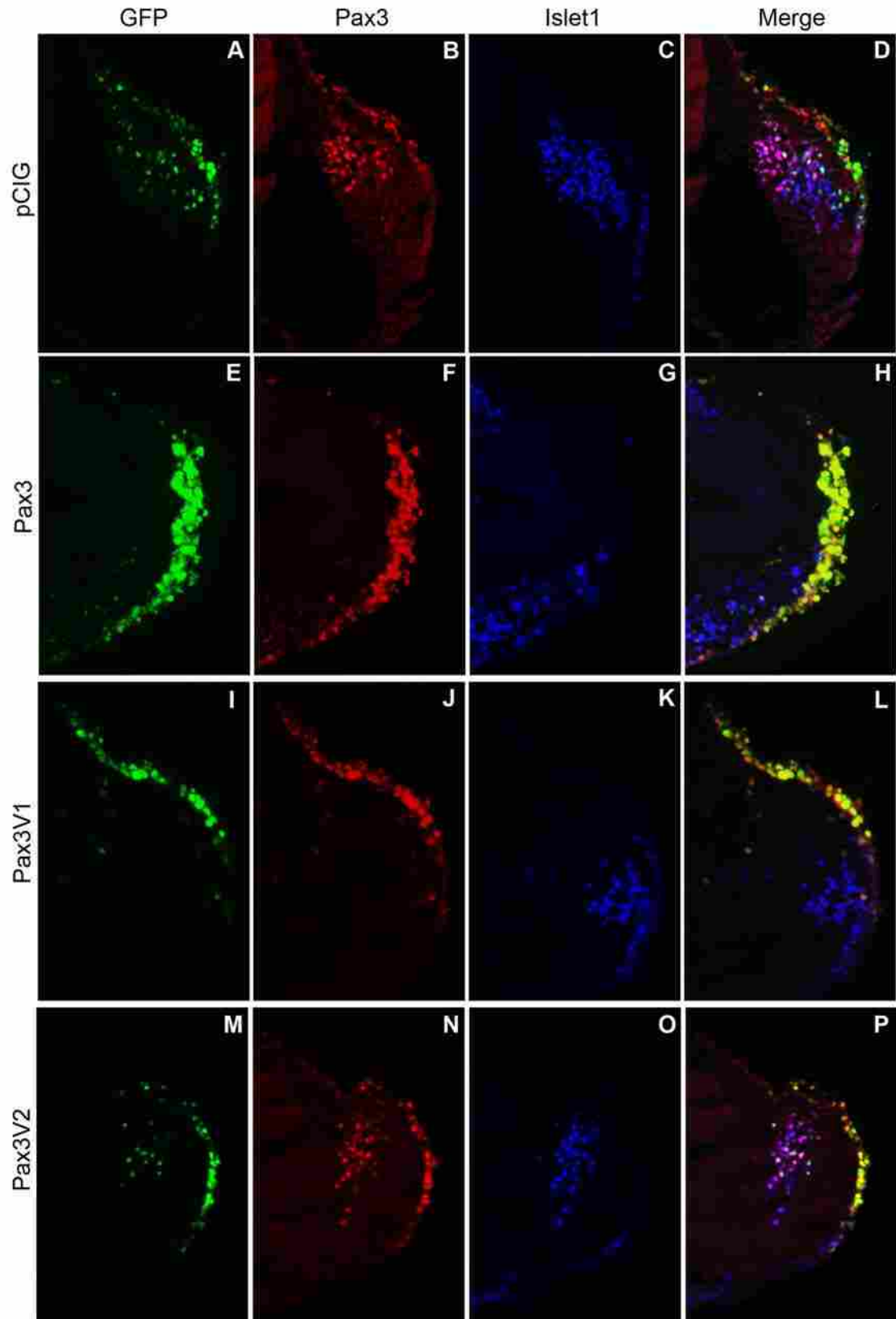


Figure 2.18 Pax3 isoform contributes to neuronal differentiation with inhibition of Notch signaling (legend on page 65)

Figure 2.18 Pax3 isoform contributes to neuronal differentiation with inhibition of Notch signaling  
These sections are of the opV placode that were electroporated at 5-7ss, cultured for 12 hours, and then cultured with DAPT for 24 hours. The sections were then stained for Pax3 and Islet1. (A-D) pCIG misexpression; (E-H) Pax3 misexpression; (I-L) Pax3V1 misexpression; (M-P) Pax3V2 misexpression. (B, N) Pax3 expression in the mesenchyme and Pax3 colocalization with Islet1 is similar in the misexpression of pCIG and Pax3V2 (D, P). (F, J) Pax3 expression is decreased in the mesenchyme and Pax3 colocalization with Islet1 in the mesenchyme is significantly decreased in misexpression studies of Pax3 and Pax3V1 (H, L).

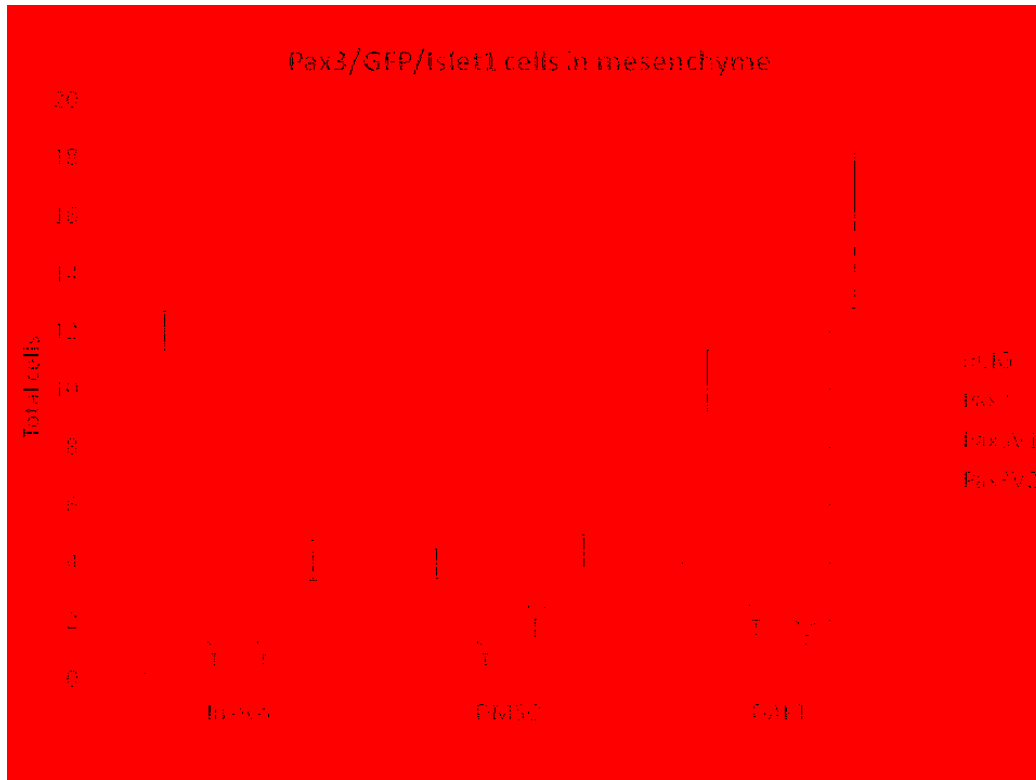


Figure 2.19 Misexpression of Pax3 constructs *in ovo* and *ex ovo* in culture

This figure shows the total number of Pax3, GFP, and Islet1 expressing cells seen in the mesenchyme. The first group of cell counts were from chick embryos electroporated at 6-8ss and incubated *in ovo* until embryos reached 24-28ss before being collected. The second and third group of cell counts were collected from chick embryos electroporated at 6-8ss and incubated on culture media with DMSO or DAPT, respectively, until embryos reached 24-28ss.

Error bars represent the standard error of the mean.

(\*) p-value <0.05 between the experimental groups and the control group, pCIG

(^ ) p-value <0.05 between two experimental groups



Table A

Source	DF	SS	MS	F value	p-value
Model	3	1551.20	517.07	7.81	0.0003
Error	39	2580.58	66.17		
Corrected Total	42	4131.78			

Table B

Source	DF	SS	MS	F value	p-value
Model	3	701.94	233.98	6.50	0.0015
Error	32	1152.30	36.01		
Corrected Total	35	1854.24			

Table 2.5A and 2.5B Analysis of variance of Pax3/GFP cells in the ectoderm

This ANOVA table is showing whether there is a significant difference between any two groups when comparing the Pax3/GFP expressing cells that remain in the ectoderm. Cell counts on randomly selected opV placodes were used to make a quantitative comparison between all experiments. The tables show a large F value and a small p-value supporting that there is a significant difference between at least two experimental groups. Table 5A shows data from misexpression occurring at 6-8ss and Table 5B shows data from misexpression occurring at 14-16ss. Degrees of freedom (DF), sum of squares (SS), mean squares (MS)

Table A

Misexpression construct	Construct number	Mean of the cell counts	Sample size
pCIG	1	13.44	10
Pax3	2	23.41	11
Pax3V1	3	29.73	12
Pax3V2	4	19.18	10

p-values	1	2	3	4
1		0.0374	0.0002	0.4027
2			0.2612	0.6360
3				0.0216

Table B

Misexpression construct	Construct number	Mean of the cell counts	Sample size
pCIG	1	9.62	9
Pax3	2	20.57	7
Pax3V1	3	20.27	11
Pax3V2	4	15.91	10

p-values	1	2	3	4
1		0.0052	0.0022	0.1381
2			0.9996	0.4258
3				0.3837

Table 2.6A and 2.6B Tukey-Kramer analysis of Pax3/GFP cells in the ectoderm  
Pax3/GFP expressing cells were counted in randomly selected opV placodes and a Tukey-Kramer analysis was done to show significant differences between experimental groups. The upper part of the table defines the experiments analyzed, the number designated to the experiment, and the mean of the cell counts for the respective experiment. The lower part of the table shows the p-values calculated between individual experiments. Table 6A shows data from misexpression occurring at 6-8ss and Table 6B shows data from misexpression occurring at 14-16ss.

Table A

Source	DF	SS	MS	F value	p-value
Model	3	529.40	176.47	21.66	<.0001
Error	39	317.81	8.15		
Corrected Total	42	847.21			

Table B

Source	DF	SS	MS	F value	p-value
Model	3	264.03	88.01	3.53	0.0258
Error	32	798.15	24.94		
Corrected Total	35	1062.18			

Table 2.7A and 2.7B Analysis of variance of Pax3/GFP cells in the mesenchyme

This ANOVA table is showing whether there is a significant difference between any two groups when comparing the Pax3/GFP expressing cells that are in the mesenchyme. Cell counts on randomly selected regions of the opV placodes were used to make a quantitative comparison between all experiments. Table A shows a large F value and a small p-value supporting that there is a significant difference between at least two experimental groups. Table B shows a moderately small F value and a small p-value that may indicate a significant difference between any two experimental groups, though there is a possibility that a significance difference is not present. Table 7A shows data from misexpression occurring at 6-8ss and Table 7B shows data from misexpression occurring at 14-16ss. Degrees of freedom (DF), sum of squares (SS), mean squares (MS)

Table A

Misexpression construct	Construct number	Mean of the cell counts	Sample size
pCIG	1	12.58	10
Pax3	2	3.50	11
Pax3V1	3	4.25	12
Pax3V2	4	6.56	10

p-values	1	2	3	4
1		<.0001	<.0001	.0002
2			.9220	.0837
3				.2489

Table B

Misexpression construct	Construct number	Mean of the cell counts	Sample size
pCIG	1	12.68	9
Pax3	2	6.71	7
Pax3V1	3	8.13	11
Pax3V2	4	13.11	10

p-values	1	2	3	4
1		0.1033	0.1985	0.9978
2			0.9358	0.0723
3				0.1394

Table 2.8A and 2.8B Tukey-Kramer analysis of Pax3/GFP cells in the mesenchyme  
Pax3/GFP expressing cells were counted in the mesenchyme of randomly selected regions of the opV placodes and a Tukey-Kramer analysis was done to show significant differences between experimental groups. The upper part of the table defines the experiments analyzed, the number designated to the experiment, and the mean of the cell counts for the respective experiment. The lower part of the table shows the p-values calculated between individual experiments. Table 8A shows data from misexpression occurring at 6-8ss and Table 8B shows data from misexpression occurring at 14-16ss.

Table A

Source	DF	SS	MS	F value	p-value
Model	3	2112.26	704.09	35.30	<.0001
Error	39	777.93	19.95		
Corrected Total	42	2890.18			

Table B

Source	DF	SS	MS	F value	p-value
Model	3	1073.38	357.79	6.25	0.0018
Error	32	1830.93	57.22		
Corrected Total	35	2904.31			

Table 2.9A and 2.9B Analysis of variance of Islet1 cells in the mesenchyme

This ANOVA table is showing whether there is a significant difference between any two groups when comparing the Islet1 expressing cells that are in the mesenchyme. Cell counts on randomly selected regions of the opV placodes were used to make a quantitative comparison between all experiments. The tables show a large F value and a small p-value supporting that there is a significant difference between at least two experimental groups. Table 9A shows data from misexpression occurring at 6-8ss and Table 9B shows data from misexpression occurring at 14-16ss. Degrees of freedom (DF), sum of squares (SS), mean squares (MS)

Table A

Misexpression construct	Construct number	Mean of the cell counts	Sample size	
pCIG	1	22.36	10	
Pax3	2	4.86	11	
Pax3V1	3	5.03	12	
Pax3V2	4	10.15	10	
p-values	1	2	3	4
1		<.0001	<.0001	<.0001
2			0.9997	0.0471
3				0.0509

Table B

Misexpression construct	Construct number	Mean of the cell counts	Sample size	
pCIG	1	22.74	9	
Pax3	2	17.89	7	
Pax3V1	3	9.45	11	
Pax3V2	4	21.07	10	
p-values	1	2	3	4
1		0.5862	0.0024	0.9653
2			0.1180	0.8377
3				0.0090

Table 2.10A and 2.10B Tukey-Kramer analysis of Islet1 cells in the mesenchyme

Islet1 expressing cells were counted in the mesenchyme of randomly selected regions of the opV placodes and a Tukey-Kramer analysis was done to show significant differences between experimental groups.

The upper part of the table defines the experiments analyzed, the number designated to the experiment, and the mean of the cell counts for the respective experiment. The lower part of the table shows the p-values calculated between individual experiments. Table 10A shows data from misexpression occurring at 6-8ss and Table 10B shows data from misexpression occurring at 14-16ss.

Table A

Source	DF	SS	MS	F value	p-value
Model	3	653.26	217.75	45.91	<.0001
Error	39	185.00	4.74		
Corrected Total	42	838.25			

Table B

Source	DF	SS	MS	F value	p-value
Model	3	341.62	113.87	38.50	<.0001
Error	32	94.64	2.98		
Corrected Total	35	436.26			

Table 2.11A and 2.11B Analysis of variance of Pax3/GFP/Islet1 cells in the mesenchyme

This ANOVA table is showing whether there is a significant difference between any two groups when comparing the Pax3/GFP/Islet1 expressing cells that are in the mesenchyme. Cell counts on randomly selected regions of the opV placodes were used to make a quantitative comparison between all experiments. The tables show a large F value and a small p-value supporting that there is a significant difference between at least two experimental groups. Table 11A shows data from misexpression occurring at 6-8ss and Table 11B shows data from misexpression occurring at 14-16ss. Degrees of freedom (DF), sum of squares (SS), mean squares (MS)

Table A

Misexpression construct	Construct number	Mean of the cell counts	Sample size
pCIG	1	10.34	10
Pax3	2	0.67	11
Pax3V1	3	0.65	12
Pax3V2	4	3.60	10

p-values	1	2	3	4
1		<.0001	<.0001	<.0001
2			1.0000	0.0190
3				0.0153

Table B

Misexpression construct	Construct number	Mean of the cell counts	Sample size
pCIG	1	8.03	9
Pax3	2	0.71	7
Pax3V1	3	0.58	11
Pax3V2	4	4.51	10

p-values	1	2	3	4
1		<.0001	<.0001	0.0007
2			0.9985	0.0007
3				<.0001

Table 2.12A and 2.12B Tukey-Kramer analysis of Pax3/GFP/Islet1 cells in the mesenchyme Pax3/GFP/Islet1 expressing cells were counted in the mesenchyme of randomly selected regions of the opV placodes and a Tukey-Kramer analysis was done to show significant differences between experimental groups. The upper part of the table defines the experiments analyzed, the number designated to the experiment, and the mean of the cell counts for the respective experiment. The lower part of the table shows the p-values calculated between individual experiments. Table 12A shows data from misexpression occurring at 6-8ss and Table 12B shows data from misexpression occurring at 14-16ss.



Table A

Source	DF	SS	MS	F value	p-value
Model	3	644.83	214.94	52.38	<.0001
Error	32	131.32	4.10		
Corrected Total	35	776.15			

Table B

Source	DF	SS	MS	F value	p-value
Model	3	81.34	27.11	18.10	<.0001
Error	27	40.45	1.50		
Corrected Total	30	121.79			

Table C

Source	DF	SS	MS	F value	p-value
Model	3	1061.45	353.82	17.38	<.0001
Error	25	508.81	20.35		
Corrected Total	28	1570.26			

Table 2.13A, 2.13B, and 2.13C Analysis of variance of Pax3/GFP/Islet1 cells in the mesenchyme  
 This ANOVA table is showing whether there is a significant difference between any two groups when comparing the Pax3/GFP/Islet1 expressing cells that are in the mesenchyme. Cell counts on randomly selected regions of the opV placodes were used to make a quantitative comparison between all experiments. The tables show a large F value and a small p-value supporting that there is a significant difference between at least two experimental groups. Table 13A shows data from misexpression occurring at 6-8ss in ovo, Table 13B shows data from misexpression occurring at 6-8ss and then cultured in DMSO, and Table 13C shows data from misexpression occurring at 6-8ss and then cultured in DAPT. Degrees of freedom (DF), sum of squares (SS), mean squares (MS)

Table A

Misexpression construct	Construct number	Mean of the cell counts	Sample size
pCIG	1	11.34	10
Pax3	2	0.67	11
Pax3V1	3	0.68	12
Pax3V2	4	3.91	10

p-values	1	2	3	4
1		<.0001	<.0001	<.0001
2			1.0000	0.0062
3				0.0125

Table B

Misexpression construct	Construct number	Mean of the cell counts	Sample size
pCIG	1	4.02	9
Pax3	2	0.71	11
Pax3V1	3	1.71	7
Pax3V2	4	4.35	14

p-values	1	2	3	4
1		<.0001	0.0160	0.9506
2			0.4591	<.0001
3				0.0033

Table C

Misexpression construct	Construct number	Mean of the cell counts	Sample size
pCIG	1	9.49	10
Pax3	2	1.84	14
Pax3V1	3	1.17	11
Pax3V2	4	15.47	13

p-values	1	2	3	4
1		0.0210	0.0140	0.0924
2			0.9917	<.0001
3				<.0001

Table 2.14A, 2.14B, and 2.14C Tukey-Kramer analysis of Pax3/GFP/Islet1 cells in the mesenchyme Pax3/GFP/Islet1 expressing cells were counted in the mesenchyme of randomly selected regions of the opV placodes and a Tukey-Kramer analysis was done to show significant differences between experimental groups. The upper part of the table defines the experiments analyzed, the number designated to the experiment, and the mean of the cell counts for the respective experiment. The lower part of the table shows the p-values calculated between individual experiments. Table 14A shows data from misexpression occurring at 6-8ss in ovo, Table 14B shows data from misexpression occurring at 6-8ss and then cultured with DMSO, and Table 14C shows data from misexpression occurring at 6-8ss and then cultured with DAPT.

## *Discussion*

The Pax3 transcription factor is essential in the process of neuronal differentiation. The Splotch mutation in mice results in a non-functional Pax3 protein and its phenotype includes a reduced or absent opV ganglion and premature neurogenesis in neural crest cells (Tremblay et al., 1995; Nakazaki et al., 2008). This mutation shows that Pax3 is necessary for normal neurogenesis. Another study used the Pax3-Engrailed fusion protein to repress Pax3 target gene expression in the opV placode. Results of knockdown Pax3 with the Pax3-Engrailed fusion construct showed reduction in FGFR4, Ngn2, and Islet1 expression (Dude et al., 2009), all of which are opV placode markers that are involved in sensory neuronal differentiation (Marcelle et al., 1994; Stark et al., 1997; Begbie et al., 2002; Fedtsova et al., 2003; Lassiter et al., 2007). FGFR4 is necessary for the delamination of opV placode cells from the ectoderm and the latter transcription factors are necessary for terminal neuronal differentiation and survival (Lassiter et al., 2009; Fode et al., 1998; Sun et al., 2008). These experiments describe the necessity of Pax3 in sensory neurogenesis using knockdown approaches.

Misexpression studies of Pax3 have also been conducted to understand if Pax3 is sufficient for neurogenesis. Pax3 was misexpressed in the opV region which caused Pax3 positive cells to remain in the ectoderm and not to delaminate. It also reduced the neuronal markers Islet1 and Brn-3a, showing that Pax3 inhibits terminal neuronal differentiation. However, when misexpressed outside of the opV region, Pax3 was sufficient to upregulate FGFR4 and Ngn2 (Dude et al., 2009). This study shows that Pax3 is sufficient to upregulate expression of proneuronal genes, but was not sufficient for terminal sensory neurogenesis.

FGFR4 is necessary for opV placode cell delamination from the ectoderm and Ngn2 is a post-mitotic neuron marker that is expressed early in delaminating placode cells, but expression of both these molecules are lost as placodal cells migrate into the developing opV ganglia to form sensory neurons (Lassiter et al., 2009). These studies show the current understanding of the roles of Pax3 in sensory neurogenesis, but do not elucidate how Pax3 is both necessary for sensory neurogenesis and also inhibits neurogenesis in the opV placode. We have described two isoforms of Pax3 in the chick that may explain these previous findings.

One isoform, Pax3V1 contains a deletion that encompasses part of the paired domain and the entire octapeptide domain. The paired domain is necessary and sufficient to bind DNA (Treisman et al., 1991), though the C-terminal end of this domain does not appear to be as essential to DNA binding as mutations of this region did not affect DNA binding by the paired domain (Apuzzo et al., 2004). The octapeptide domain of Pax5 was shown to bind a co-repressor, providing evidence that the octapeptide domain is involved in protein to protein interactions (Eberhard et al., 2000). The octapeptide domain is located within a linker region between the paired domain and homeodomain of Pax3. Chimeric proteins of this region were produced to understand the linker region's role of the interaction between the paired domain and homeodomain. By substituting a Pax3 non-specific domain in place of the Pax3 linker region it was shown that the linker region provides for the functional interaction between the paired domain and homeodomain (Fortin et al., 1998). Misexpression experiments of Pax3V1 showed similar results as were seen after misexpressing Pax3. Pax3V1<sup>+</sup> cells remained in the ectoderm and did not express the differentiation marker Islet1. We had expected a functional difference between the Pax3V1 and Pax3V2 isoforms due to the partial deletion in the binding domain and complete deletion of the octapeptide in Pax3V1; however, as this was not seen in the results, our

focus became concentrated on the function of the other Pax3 isoform.

The second isoform, Pax3V2, contains partial deletion of the C-terminal region of the homeodomain and a large deletion of the transactivation domain. The homeodomain is recognizes DNA and contains residues that interacts with DNA (Biarrane et al., 2009). The transactivation domain is essential, but not sufficient for transcriptional activity (Lechner and Dressler, 1996), and it participates in protein to protein interactions of different transcriptional cofactors (Eberhard et al., 2000; Murakami et al., 2006). Misexpression experiments of the Pax3V2 isoform showed that even though many Pax3V2+ cells remained in the ectoderm, more delaminated from the ectoderm than Pax3 or Pax3V1 cells, and the migrating cells were typically Islet1+. The cellular behavior appeared similar to those in the pCIG controls. However, when the Pax3V2 isoform was misexpressed in competent ectoderm in the otic region, Islet1 expression was not enhanced showing that the Pax3V2 isoform is not sufficient for sensory neurogenesis. These results show that the Pax3V2 isoform is a permissive molecule for sensory neurogenesis specific to the opV placode and contributes to normal terminal differentiation of sensory neurons.

Quantitative analysis of mRNA expression showed a sustained increase of Pax3 and Pax3V2 in the ectoderm at 10-15ss and 20-25ss from 6-8ss, and then a significant decrease at 32-37ss. The fold difference between Pax3 and Pax3V2 was similar during these stages, as Pax3 was 1.7 to 1.8 times more abundant. When enhancing neurogenesis by blocking Notch signaling with DAPT, the fold difference was similar, with the concentrations of both variants increasing. The quantitative cDNA studies showed that Pax3 and Pax3V2 are expressed at the similar fold differences throughout the stages of opV placode differentiation.

This study shows that three splice forms of Pax3 are expressed in the chick opV placode

during neuronal differentiation. We show that the Pax3 splice form is expressed approximately 1.4 to 1.9 fold more than the Pax3V2 splice form, and that the expression of both Pax3 and Pax3V2 are significantly increased by inhibiting Notch signaling. Cells that have migrated into the mesenchyme and are targeted with either the Pax3 or Pax3V1 construct do not co-localize with the neuronal marker Islet1, even as Notch signaling is inhibited. In contrast, cells that have migrated in the mesenchyme and are targeted with the Pax3V2 construct co-localize with Islet1 as Notch signaling is inhibited. However, when the Pax3V2 construct is misexpressed in the otic region there is not a robust upregulation of Islet1 expression in targeted cells. These data lead to the conclusion that the Pax3 and Pax3V1 isoforms inhibit terminal neuronal differentiation, and the Pax3V2 isoform is permissive to terminal neuronal differentiation as the Pax3V2 isoform is not sufficient to upregulate Islet1 expression outside the opV placode.

An explanation for this conclusion is proposed in the following model of opV placode differentiation. Efficient transcription activation by Pax3 is dependent on two binding domains, the paired domain and the homeodomain that function interdependently (Chalepakis et al., 1994b; Underhill et al., 1995; Underhill and Gros, 1997; Apuzzo et al., 2004). A portion of the homeodomain including residues that interacts with DNA is deleted (Birrane et al., 2009), as well as the majority of the transactivation domain. The Pax3 transactivation domain has an influence on homeodomain by preventing its ability to bind DNA (Cao and Wang 2000). This was shown as the transactivation domain of Pax3 was replaced by an unrelated viral transactivation domain allowing the homeodomain to transactivate specific DNA sequences independent of the paired domain (Cao and Wang 2000). It is plausible that with a portion of the homeodomain and the majority of the transactivation domain missing there may be a change in transcriptional activity of the Pax3V2 isoform (Chalepakis et al., 1994a, Phelan et al., 1998,

Wang et al. 2007). As opV placode cells have progressed through the proneuronal stage, the Pax3V2 isoform may be able to bind more efficiently than the Pax3 isoform to promoter regions necessary for terminal differentiation. The Pax3 isoform may be an inhibitor factor to these promoters due to its amino-terminal inhibitor domain, which may inhibit transcription more effectively at higher Pax3 concentrations (Chalepakis et al., 1994a; Barr et al., 1999) produced by an increase of Pax3 expression at the time of peak differentiation in the opV placode shown in this study. Pax3V2 may be a competitive inhibitor of Pax3 as shown in mouse myoblasts where a significant reduction of transcriptional activity was reported of Pax3 in the presence of a Pax3 isoform. The isoform was missing exon 8 of Pax3, which contains part of the transactivation domain (Pritchard et al., 2003). Additional studies to determine the transcriptional activity of Pax3V2 is needed to confirm this model and to conclude that Pax3V2 is a permissive isoform, allowing Islet1 expression by blocking Pax3.



## CHAPTER 3: The Role of Wnt1 and Wnt3a in the Induction and Maintenance of Pax3 Expression in the Ophthalmic Trigeminal Placode

### *Introduction*

OpV placode development in mice is known to begin at embryonic day 8.5 (E8.5) as the early marker Pax3 expression is detected at this time (Goulding et al., 1991; Stark et al., 1997). This transcription factor is necessary for normal sensory neurogenesis of the opV cells (Dude et al., 2009). Pax3<sup>+</sup> cells delaminate and migrate to form the ganglion at E9.0 and ganglion formation is apparent by E9.5 with robust expression of the proneural marker, Islet1 (Nichols, 1986; Sun et al., 2008). Its induction in the opV placode is dependent on signaling molecules emanating from the neural tube (Stark et al., 1997). This signal or signals have not been discovered although Wnt ligands are a potential source as they are present during the time of Pax3 expression, and many of the Wnt ligands are expressed in the midbrain and hindbrain region adjacent to the developing placode (Hollyday et al., 1995; Ladher et al., 2000; Jin et al., 2001; Sanders et al., 2002; Quinlan et al., 2009). In addition, the Wnt receptor, frizzled-7, is expressed in the ectoderm of the trigeminal placode during early Pax3 expression (Stark et al., 2000).

Canonical Wnt signaling is activated when Wnt ligand binds to the transmembrane receptor, frizzled. This event inhibits the phosphorylation by GSK3 and subsequent degradation of  $\beta$ -catenin, allowing it to complex with Tcf/Lef in the nucleus, which can activate or repress gene expression (Blauwkamp et al., 2008). Experimentation with Wnt ligand or frizzled receptor has shown that the canonical Wnt signaling pathway is important in neurogenesis. In the central nervous system, a knockdown experiment of  $\beta$ -catenin resulted in less neuronal precursors differentiating to mature neurons in early mouse development (Slawny and O'Shea, 2011).

Misexpression of frizzled-10, which binds Wnt1, was found to increase sensory neurons and knockdown experiments of the receptor showed a decrease in sensory neurons during late neurogenesis in *Xenopus* (Garcia-Morales et al., 2009). These results were verified in the embryonic carcinoma cell line, P19, which was transfected with the frizzled-10 construct inducing an increase of neurons and siRNA knockdown of frizzled-10 inhibited neurogenesis (Garcia-Morales et al., 2009). A similar study overexpressed Wnt1 in the midbrain neuroepithelium and showed an increase of cells that were expressing the opV marker, Pax3, in the adjacent ectoderm. Following this experiment, a dominant negative construct of Wnt1 was used, which reduced the number of Pax3 cells in the opV placode of chick (Canning et al., 2008). Also, in opV placode cells a Wnt reporter showed that the canonical signaling pathway is active at the time of Pax3 expression. When the activity of  $\beta$ -catenin was blocked in the opV placode cells their fate was impeded or not maintained as seen through a decrease of Pax3<sup>+</sup> cells in the ectoderm. However, a dominant-active form of  $\beta$ -catenin was not sufficient to increase the number of cells expressing Pax3 in the placode (Lassiter et al., 2007). These results show that Wnt signaling is necessary in the process of neuronal differentiation and that it may function to induce Pax3 expression.

It is likely that Wnt1 and Wnt3a induce Pax3 expression as they are both expressed in the dorsal neural tube at the midbrain level comparable to the timing of Pax3 expression in the opV placode (Hollyday et al., 1995; Ladher et al., 2000; Jin et al., 2001; Quinlan et al., 2009). Previous knockout experiments of Wnt1 showed midbrain and hindbrain deficiencies in mouse embryos (Thomas and Capecchi, 1990; McMahon and Bradley, 1990). Mouse knockouts of Wnt3a have truncated anterior to posterior axes and notochords, CNS malformations, and a reduction or loss of the hippocampus (Takada et al., 1994; Lee et al., 2000). Wnt1;Wnt3a double

knockout experiments have shown a reduction in neural crest derivatives originating from the neural tube and a reduction in dorsolateral neural precursors in the neural tube. A reduction in the proximal axons of the trigeminal nerve was also shown in this analysis (Ikeya et al., 1997). In another study, Wnt1;Wnt3a double knockouts showed malformations of the dermomyotomes and reduction in gene expression involved in myogenesis (Ikeya and Takada, 1998). Though analysis of developmental systems has been done on Wnt1;Wnt3a double knockout mice, the study of the opV placode at early developmental stages has not been published. This study shows the requirement of Wnt1 and Wnt3a gene expression in the induction of Pax3 in the opV placode.

### *Material and methods*

#### Mice

Wnt1 mutant mice and Wnt3a mutant mice were obtained by Dr. Jeff Barrow. Both lines were kept as heterozygotes (+/-) and crossed to produce homozygous, double knockouts (Wnt1 -/-; Wnt3a -/-) and double wild-type (Wnt1 +/+; Wnt3a +/+) littermates for experimentation. Sox1-Cre, ROSA26, and *Porcn* mice were also obtained by Dr. Jeff Barrow. Sox1-Cre mice were produced by inserting Cre recombinase cDNA into the codon start site of Sox1 (Takashima et al., 2007). ROSA26 is a ubiquitously active promoter that is upstream of a loxP flanked transcriptional and translational stop cassette and lacZ reporter gene in ROSA26 mice. During Cre recombinase expression, the stop cassette is excised and the ROSA26 promoter drives expression of the lacZ reporter gene (Soriano, 1999). The *Porcn* targeting vector was created by recombineering, and has loxP sites around exons 2 and 3 causing the deletion of the protein start codon and the first three transmembrane domains in the presence of

Cre expression (Barrott et al., 2011). The mice were kept in a 12 hours lights on and 12 hours lights off cycle with water and food, ad libitum.

### Genotyping

Yolk sacs were collected and incubated with proteinase K (Roche, Indianapolis, IN) at 50°C overnight. Genomic DNA from the yolk sac was boiled in water for three minutes to degrade the proteinase K and PCR was run on the samples. The Wnt1 primers used were: 5'-GCCTCCTCCACGAACCTGTTGACG-3', 5'-GTCAGTGCAGCCCCCCCAGTG-3', 5'-CGCTCACTCACCGGCCTCGCCG-3', and 5'-GCTTTACGGTATCGCCGCTCCCG-3'. PCR amplification was performed using DreamTaq (Fremontas, Glen Burnie, MD) on a PCR Mastercycler Personal (Eppendorf, Hauppauge, NY). For Wnt1, the cycling parameters were an initial 95°C step for two minutes, then a cycle of 95°C for 30 seconds, 61°C for 30 seconds, and 72°C for 60 seconds, repeated 29 times, and followed by a final extension at 72°C for three minutes. The DreamTaq buffer was diluted to a 1x concentration, the dNTP mix was diluted to 0.6mM of each nucleotide, and the primers were diluted to 1.0µM. The Wnt3a primers used were 5'-TTTTGGATTCCTGCCTTTTG-3', 5'-TGGCTACCCGTGATATTGCT-3', and 5'-ACTCCCGAGAGACCATTCCT-3'. PCR amplification was performed using FlexiTaq (Promega, Madison, WI) on a PCR Mastercycler Personal (Eppendorf, Hauppauge, NY). For Wnt3a, the cycling parameters were an initial 95°C step for two minutes, then a cycle of 95°C for 30 seconds, 59°C for 20 seconds, and 72°C for 30 seconds, repeated for 34 times, and followed by a final extension at 72°C for five minutes. The FlexiTaq buffer was diluted to a 1x concentration, the dNTP mix was diluted to 0.4mM of each nucleotide, and the primers were diluted to 1.0µM.

### Immunohistochemistry

Embryos were embedded in gelatin and cryosectioned. Sections of 12 $\mu$ m were mounted on Superfrost Plus Glass slides (Fisher Scientific, Pittsburgh, PA) and the gelatin removed in PBS at 37°C for ten minutes. Embryo sections were incubated overnight at 4°C with a dilution 1:300 Pax3 primary antibody (Developmental Studies Hybridoma Bank, Iowa City, IA) and a dilution of 1:200 Islet1 primary antibody (Developmental Studies Hybridoma Bank, Iowa City, IA) in BSA/PBS buffer (0.1% bovine serum albumen, 0.1% Tween-20 (Equitech Bio, Inc., Kerrville, TX, Fisher Scientific, Pittsburgh, PA)). The primary antibody was rinsed and washed twice for ten minutes in PBS at room temperature. The tissue was then covered with Alexa 488- and Alexa 546-conjugated goat anti-mouse IgG2a and IgG2b (Invitrogen, Grand Island, NY), respectively. IgG2a was diluted 1:200 and IgG2b 1:1000 in BSA/PBS buffer. The tissue was incubated with the secondary antibodies for one hour at room temperature, and then rinsed and washed twice for ten minutes in PBS. Antibody staining was visualized using a BX-61 fluorescent microscope (Olympus, Center Valley, PA).

### $\beta$ -galactosidase staining

$\beta$ -galactosidase staining was performed immediately after the collecting of mouse embryos at E7.5, E8.5, and E9.5. After washing embryos in PBS, the embryos were fixed in a formaldehyde and glutaraldehyde mixture. E7.5 and E8.5 embryos were fixed for 20 minutes and E9.5 embryos were fixed for 30 minutes. Embryos were washed three times in 0.02% NP-40/PBS for five minutes and then stained with X-gal, overnight at 37°C. The embryos were washed three times in PBS for five minutes and then fixed in 4% paraformaldehyde. Embryos were prepared for sectioning by washing in PBS three times for five minutes and then stepped up into a 15% sucrose solution, upon which they were embedded in gelatin. Frozen embryos were

sectioned in a cryostat at 12 $\mu$ m. Gelatin was removed from the sections with PBS at 37°C and imaged using bright field microscopy.

#### Whole-mount *in situ* hybridization

Digoxigenin (Dig)-labeled RNA antisense probe was synthesized in the Barrow lab specific for Axin2. Axin2 is a scaffolding protein that complexes with other cellular proteins which binds  $\beta$ -catenin in the absence of Wnt signaling, leading to the degradation of  $\beta$ -catenin (Behrens et al., 1998; von Kries et al., 2000). Axin2 mRNA expression is elevated as the Wnt pathway is activated (Jho et al., 2002; Leung et al., 2002). Embryos were fixed in 4% paraformaldehyde and prepared for hybridization. Embryos were hybridized with the Axin2 probe, washed appropriately, and then incubated with anti-DIG alkaline-phosphatase (AP) antibody. This was followed by chromogenic staining with BM purple (Roche, Indianapolis, IN). Embryos were post-fixed in 4% formaldehyde and prepared for cryosectioning. Sections were imaged using a bright field microscope.

#### *Results*

##### The effect of Wnt1;Wnt3a double knockout on Pax3 expression in the opV placode

The Wnt1 and Wnt3a are likely signaling factors to induce Pax3 expression in the opV placode as they are expressed in the neural tube adjacent to the presumptive placode prior to Pax3 expression, and a Wnt receptor is expressed in the opV placode (Hollyday et al., 1995; Ladher et al., 2000; Jin et al., 2001; Quinlan et al., 2009; Stark et al., 2000). To determine if Wnt1 and Wnt3a are redundantly necessary for Pax3 expression in the placode, mutant mouse embryos were collected and studied at E8.5 and E9.5. Wild-type, Wnt1, and Wnt3a heterozygous mice have a well-developed midbrain and full-length tail (Figs 3.1A-3.1D). In contrast, Wnt1 mutant mice lack the midbrain region (Figs 3.1E, 3.1F), and Wnt3a mutant mice

have a truncated tail (Figs 3.1G, 3.1H). *Wnt1;Wnt3a* double mutant mice have an absent midbrain and truncated tail seen in the corresponding mutant, and the double mutant mice are moderately smaller than their littermates (Figs 3.1I, 3.1J).

Sections were performed on the mouse embryos and stained for Pax3 expression at E8.5 and for Pax3 and *Islet1* expression, the neuronal differentiation marker, at E9.5. At E8.5, Pax3 expression is found in the opV placode and in a few delaminated cells of the mesenchyme in wild-type and heterozygous mice (Figs 3.2A, 3.2D, respectively). Comparing the expression of these mice to the *Wnt1* mutant and to the *Wnt3a* mutant there appears to be no difference in the amount or spatial expression of Pax3 in the opV placode (Figs 3.2G, 3.2J, respectively). However, compared with the wild-type mice there is a marked reduction in the amount of Pax3 expression in the opV placode of double mutant mice. In addition, Pax3 expression is seen along the entire dorsolateral ectoderm of the wild-type mice in contrast to the Pax3 expression seen only in the most dorsolateral region of the double mutant mice (Fig 3.2M). At E9.5, Pax3 expression is mainly expressed in the opV ganglion with few cells expressing Pax3 in the placode of wild-type and heterozygous mice (Figs 3.2B, 3.2E, respectively). Pax3 expression does not appear to differ from *Wnt1* mutants or *Wnt3a* mutants in the opV ganglion or dorsal neural tube (Figs 3.2H, 3.2K, respectively). Comparing the expression of wild-type mice to the double mutant mice there may be a slight reduction of opV placodal cells expressing Pax3 in the opV ganglion, though there is a marked decrease of Pax3 expression in the dorsal region of the neural tube (Fig 3.2N). This later result was also seen in previous *Wnt1;Wnt3a* double knockout mice (Ikeya et al., 1997). There appears to be no reduction of *Islet1* expressing cells in the opV ganglion at this stage (Figs 3.2C, 3.2F, 3.2I, 3.2L, 3.2O). Sustained *Islet1* expression may be due to neural crest cells that contribute to the opV ganglion.

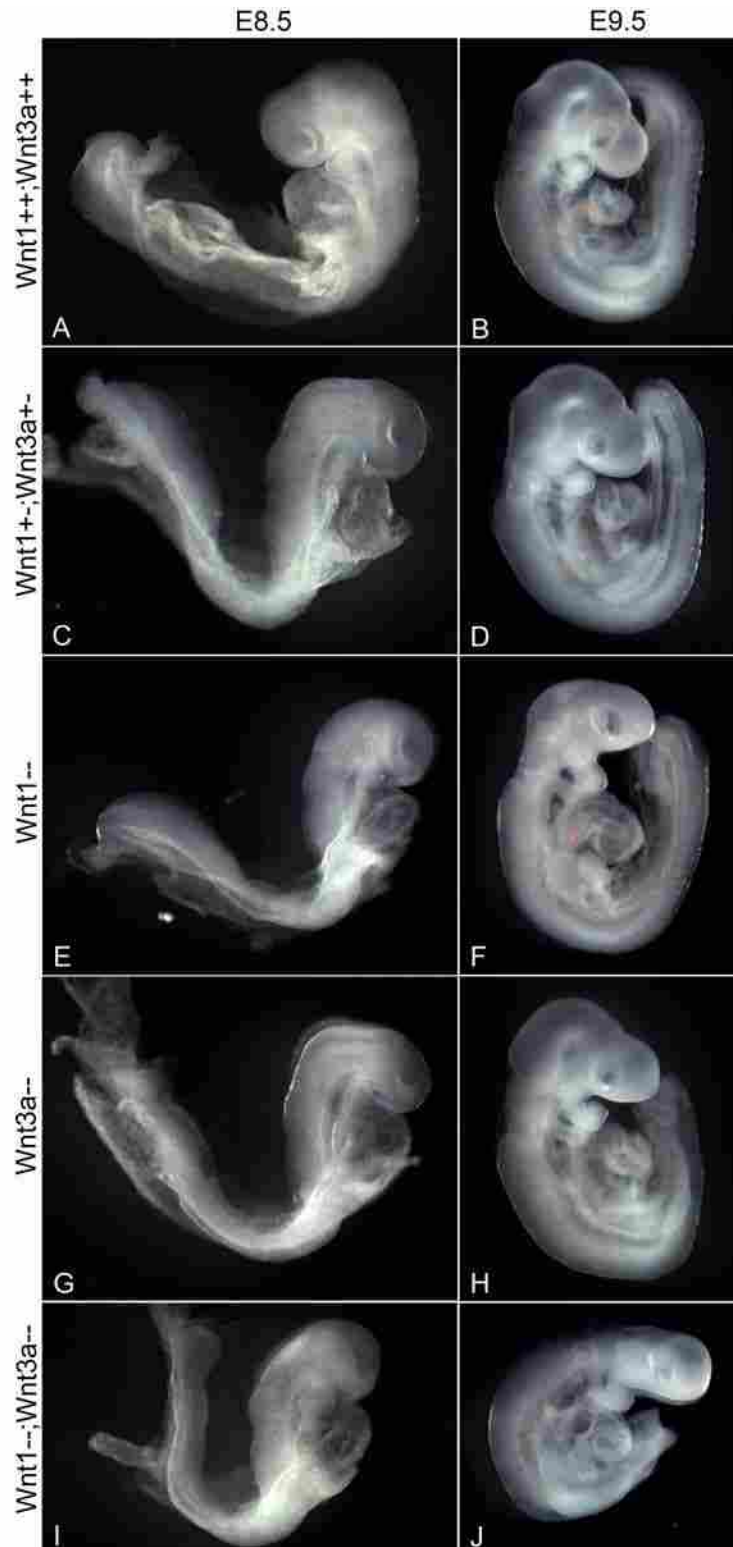


Figure 3.1 Whole-mount embryos of Wnt1 and Wnt3a double mutant mice at E8.5 and E9.5. These pictures show the phenotype of mouse embryos at different developmental stages and with different genotypes. The top of each column depicts the embryonic stage and at the side of each row the genotype is given.



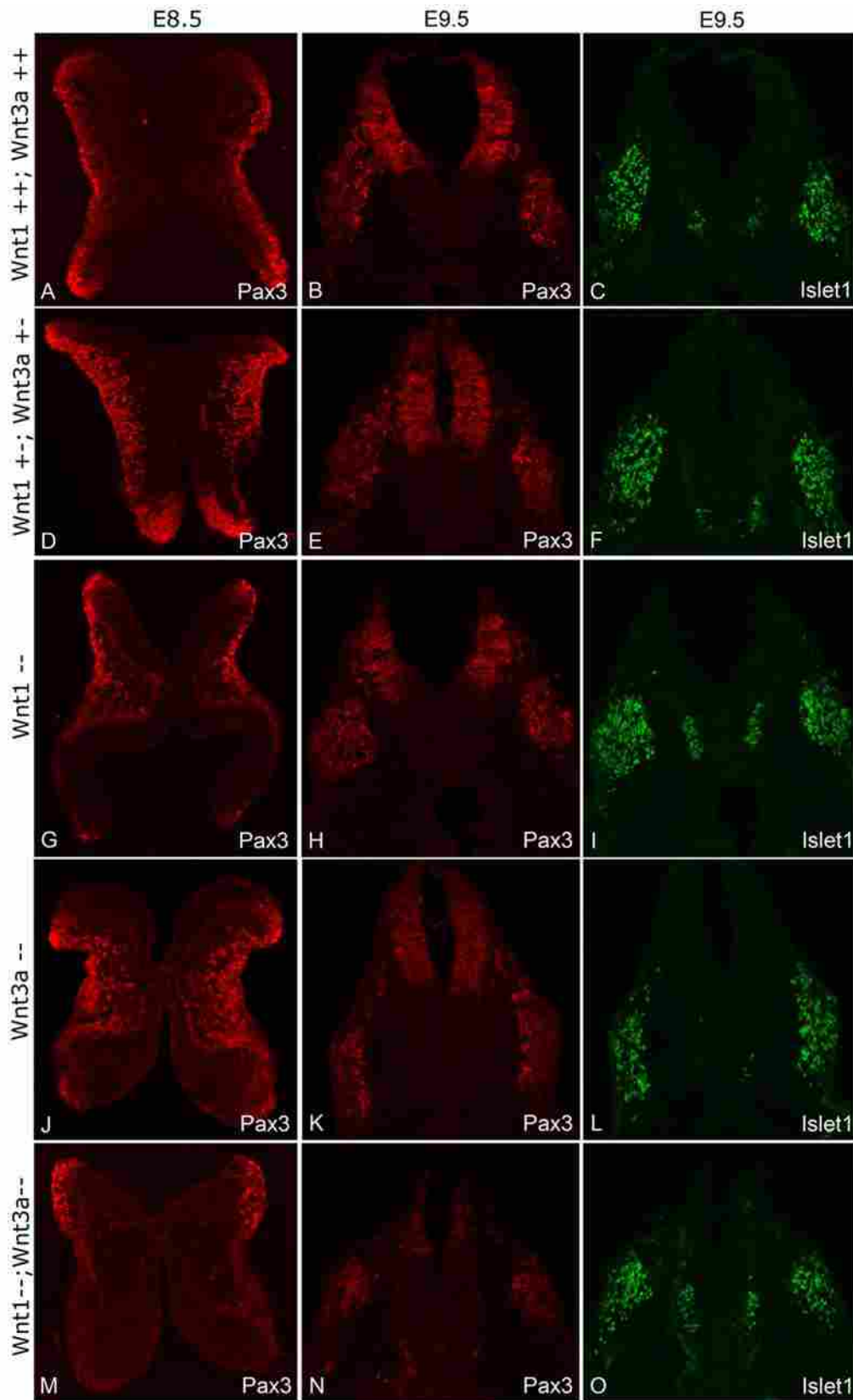


Figure 3.2 Expression of Pax3 and Islet1 in Wnt1 and Wnt3a double mutant mice during early opV placodal development (legend on page 92)

Figure 3.2 Expression of Pax3 and Islet1 in Wnt1 and Wnt3a double mutant mice during early opV placodal development

Pax3 and Islet1 expression is shown in mouse embryos at different developmental stages and with different genotypes in the opV placode and ganglion. The top of each column depicts the embryonic stage and at the side of each row the genotype is given. OpV placodal Pax3 expression is detected in mice at stage E8.5, as opV placodal and ganglion Pax3 expression and Islet1 expression is detected in mice at stage E9.5.

### Conditional knockout of Wnt signaling using Cre recombinase

A different approach was used to understand if Wnt signaling from the neural tube is necessary for Pax3 expression in the opV placode. In addition, we wanted to include Pax2 in this study as Wnt signaling may be necessary for its expression in the otic placode. Pax2 is a molecular marker for the otic placode and otic vesicle (Herbrand et al., 1998; Groves and Bronner-Fraser 2000). Sox1 is a transcription factor that is expressed in the neural fold ectoderm during the headfold stage in mouse (Pevny et al., 1998). This expression occurs approximately 24 hours before Pax3 expression in the opV placode and just before Pax2 expression in the otic placode. It is also known that *Porcupine* encodes an acyltransferase enzyme in mammals that is necessary for the post-translational modification of functional Wnt ligands (van den Heuvel et al., 1993; Kadowaki et al., 1996; Tanaka et al., 2000; Caricasole et al., 2002). *Porcupine* has one mammalian ortholog, *Porcn* (Tanaka et al., 2000). We obtained mice with a conditional allele of the X-linked mouse *Porcn* gene (Barrott et al., 2011) and crossed these mice with a mouse line that would drive Cre expression from a Sox1 promoter, producing a conditional knockout of Wnt ligand from the neural tube where Sox1-Cre was active. This knockout would occur before Pax3 expression, and if the Wnt ligand from the neural tube was responsible for Pax3 expression in the opV placode we would expect to see a reduction or absence of Pax3 expression.

Preliminary studies were performed at stages, E8.5 and E9.5. Whole-mount embryos at these stages showed no remarkable differences in the phenotype when comparing the control mice to the Sox1-Cre;Sry littermates (Figs 3.3A-3.3D). Sections of these embryos were performed and stained for Pax3 and Pax2 expression at E8.5, and Pax3, Pax2, and Islet1 expression at E9.5. Pax3 in the opV placode and Pax2 in the otic placode showed no difference in the amount of expression when comparing the Sox1-Cre mice to the control mice at E8.5 (Figs 3.4A, 3.4D, 3.5A, 3.5C). At E9.5, there was no difference in the amount of Pax3 or Islet1

expression in the opV placode, or in the amount of Pax2 expression in the otic placode (Figs 3.4B, 3.4E, 3.4C, 3.4F, 3.5B, 3.5D). A couple of theories may account for these results. One theory is that the Sox1 promoter is not turned on early enough in order to show a reduction in protein expression of Pax3, Pax2, or Islet1. This would allow Wnt ligands to be expressed from the neural tube, migrate to the ectoderm, and remain in the placode long enough to induce Pax3 expression before degradation occurs of the Wnt ligands. A second theory is that the Sox1-Cre is not effectively knocking down Wnt signaling in the neural tube allowing for enough Wnt ligands to induce Pax3 in the placode. In order to test this second theory the following control was performed.

To determine if the Cre recombinase was active in the neural tube a ROSA26 Cre reporter strain of mice were crossed with Sox1-Cre males. The ROSA26 strain has a knockin lacZ gene downstream of a ubiquitous promoter allowing for the identification of Cre expression with X-Gal staining (Soriano, 1999). Embryos at E7.5, E8.5, and E9.5 were collected and stained with X-Gal. Whole-mount embryos show few cells with Cre expression at E7.5 in the presumptive neural plate and this was verified in sections (Figs 3.6A and 3.6B). At E8.5, Cre expression had increased, though many cells did not have Cre expression (Figs 3.6C-3.6F). It was apparent at this embryonic stage that differences between Cre expressions occurred between littermates. Embryos at an earlier somite stage had less robust Cre expression within the neural plate and folds, while embryos at later somite stages presented with more cells expressing Cre within the neural plate and folds (Figs 3.6C-3.6F). At E9.5, there was no difference present between littermates in Cre expression within the neural tube. The majority of cells within the neural tube expressed Cre at this stage, though a few cells had no Cre expression as seen in sections (Figs 3.6G and 3.6H). This shows that Cre expression does occur in the presumptive

neural plate at E7.5 and the number of cells expressing Cre increases at E8.5 and at E9.5. This study also shows that although most cells within the neural tube express Cre, there are a few cells that do not express Cre allowing for the production of functional Wnt ligands (Figs 3.6B, 3.6D, 3.6F, and 3.6H). Next, it was necessary to find if Wnt signaling was knocked down or if it was still active in the Sox1-Cre;Porcn mutants.

Porcn female mice were crossed with Sox1-Cre males and embryos were collected at E8.5 and E9.5. Mouse embryos were prepared for *in situ* hybridization, which was performed using a probe specific for Axin2. Axin2 is a scaffolding protein involved in the regulation of the Wnt  $\beta$ -catenin signaling pathway and Axin2 expression is upregulated in cells after Wnt ligands have bound to their receptor (Behrens et al., 1998; von Kries et al., 2000; Jho et al., 2002; Leung et al., 2002). Sox1-Cre;Porcn embryos were stained using this probe to determine if Wnt signaling was reduced or inhibited. Whole-mount staining and sections of the Sox1-Cre;Porcn embryos showed that Axin2 expression was not reduced in embryos at E8.5 nor E9.5 when compared to control embryos (Fig 3.7). These data demonstrate that Wnt signaling was not affected and remained active in the mutant embryos. This study allows the consideration of another Cre driving gene that may be expressed earlier in development and that may have a more robust cellular location for the knockdown of Wnt expression.

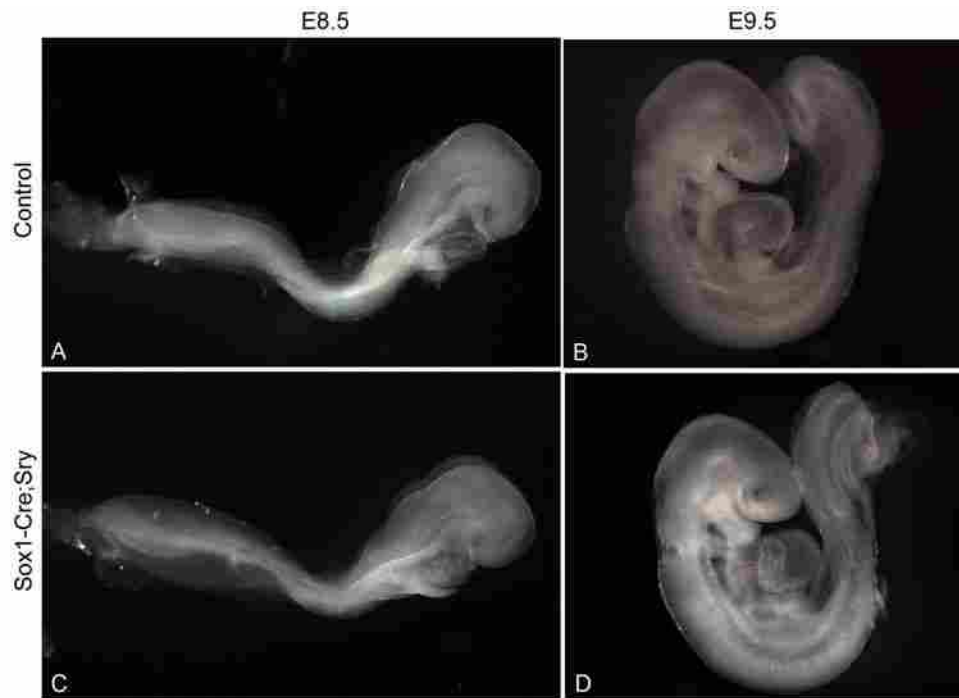


Figure 3.3 Whole-mount embryos of Sox1-Cre;Sry mice at E8.5 and E9.5

These pictures show the phenotype of mouse embryos at different developmental stages and with different genotypes. The top of each column depicts the embryonic stage and at the side of each row the genotype is given.

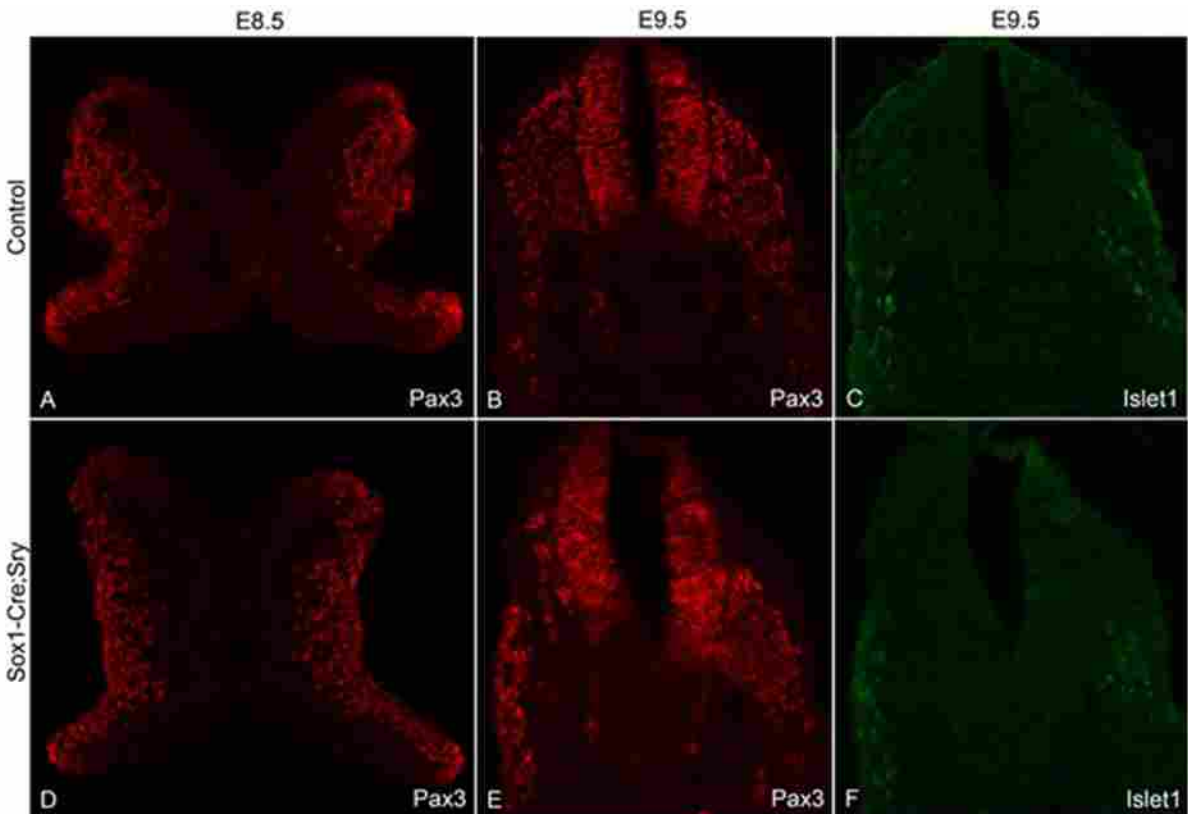


Figure 3.4 Expression of Pax3 and Islet1 in Sox1-Cre;Sry mice during early opV placodal development. Pax3 and Islet1 expression is shown in mouse embryos at different developmental stages and with different genotypes in the opV placode and ganglion. The top of each column depicts the embryonic stage and at the side of each row the genotype is given. OpV placodal Pax3 expression is detected in mice at stage E8.5, as opV placodal and ganglion Pax3 expression and Islet1 expression is detected in mice at stage E9.5.

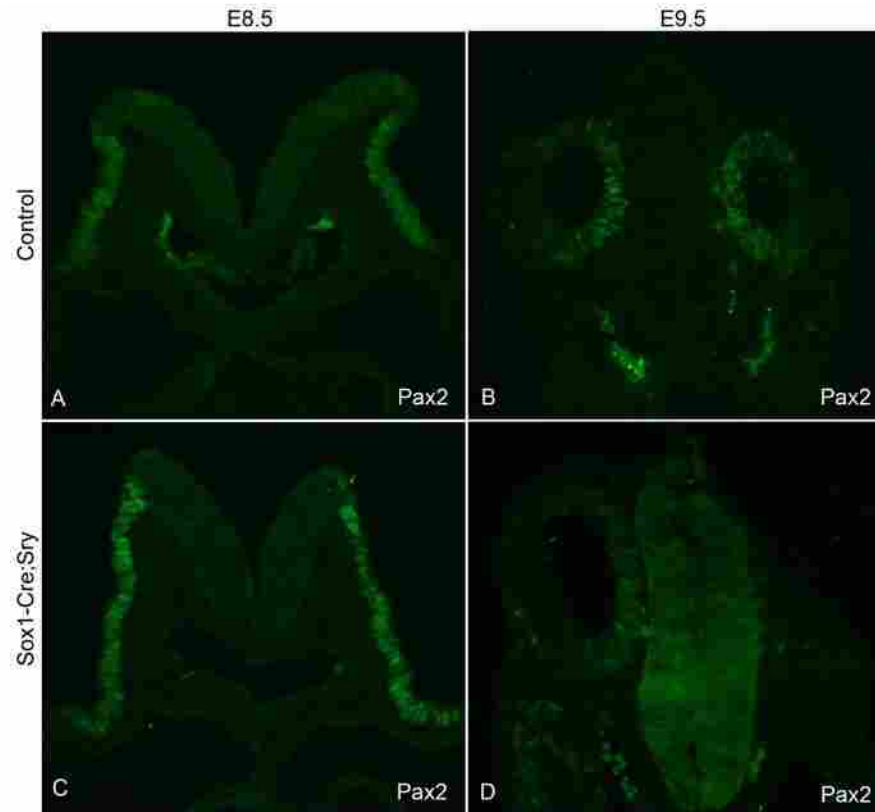


Figure 3.5 Expression of Pax2 in Sox1-Cre;Sry mice during early otic placodal development  
Pax2 expression is shown in mouse embryos at different developmental stages and with different genotypes in the otic placode. The top of each column depicts the embryonic stage and at the side of each row the genotype is given. Otic placode Pax2 expression is detected in both control and Cre;Sry mice at stages E8.5 and E9.5.



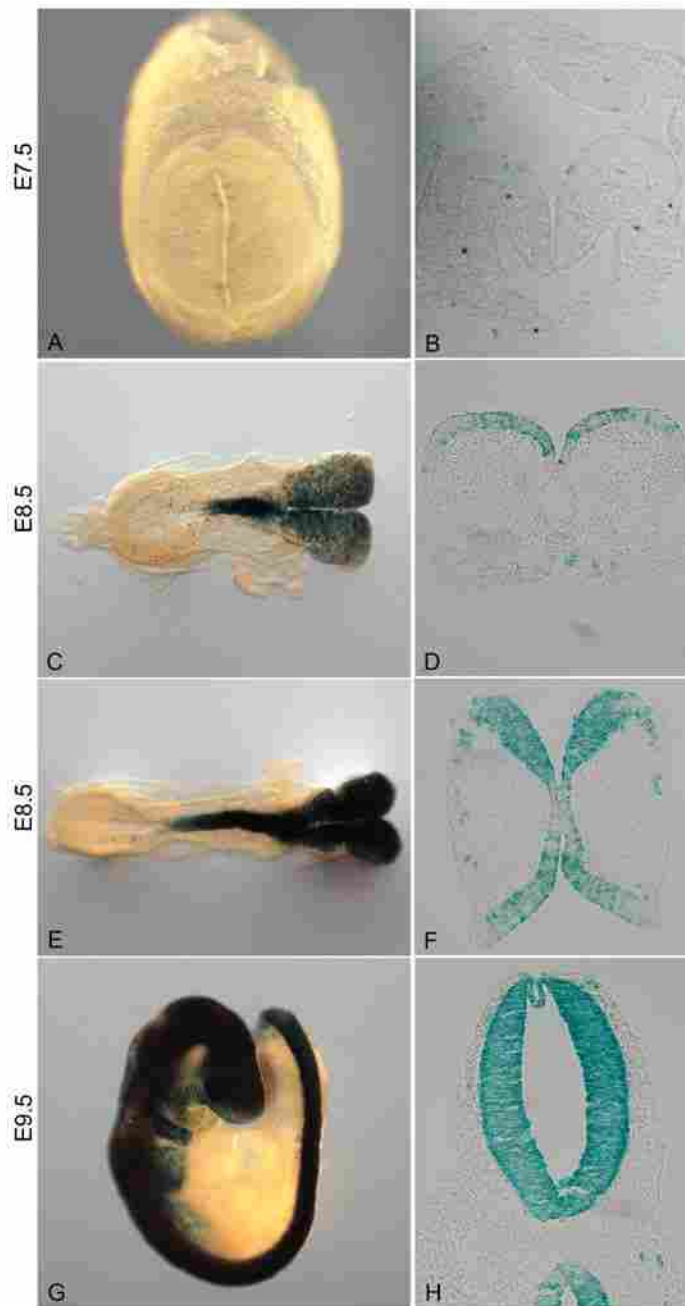


Figure 3.6 X-gal staining showing spatiotemporal Sox1-Cre expression in early mouse development. These pictures show the X-gal staining that detects beta-galactosidase expression in Sox1-Cre;Rosa embryos at different developmental stages indicated at the side of each row. The first column shows the expression in whole-mount embryos at the respective stage. Two different embryos are shown at the E8.5 stage as the variation of expression was significant. The second column shows sections through the opV placode.

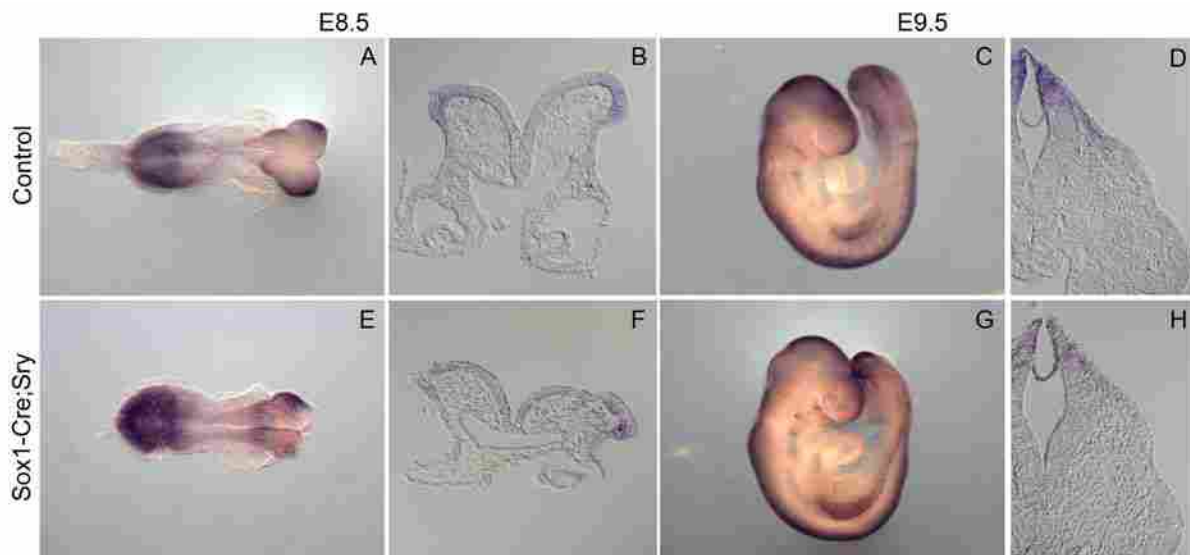


Figure 3.7 Staining of Axin2 expression showing spatiotemporal activity of Wnt signaling in Sox1-Cre;Sry mice

*In situ* hybridization staining for the scaffold protein, Axin2, which is involved in Wnt signaling appears the same in Sox1-Cre;Sry mice when compared to the controls. At E8.5, whole-mount embryos show staining in the developing midbrain and hindbrain as well as the tailbud (A and E). Sections through the opV placode show staining throughout the neural plate and in the placode (B and F). At E9.5, staining appears in the brain, spinal cord, somites, limb buds, tail bud, and branchial arches of whole-mount embryos (C and G). Sections through the opV placode shows staining in the dorsal neural tube, dorsolateral ectoderm, and dorsolateral mesenchyme (D and H).

## *Discussion*

Wnt signaling is involved in neurogenesis and is mainly thought to be involved in the differentiation of neurons or their maintenance. However, there is data showing that Wnt signaling may induce expression of molecules necessary for neurogenesis. Misexpression of Wnt in the neuroepithelium produced an increase in the number of cells expressing Pax3 in adjacent ectoderm (Canning et al., 2008) and knockdown Wnt activity produces a decrease in the number of cells expressing Pax3 in the opV placode (Lassiter et al., 2007). A double knockout model for Wnt1 and Wnt3a in mice was used to elucidate the possible inductive activity of Wnt signaling in the opV placode.

Wnt1 and Wnt3a ligands are expressed in the dorsal midbrain prior to the time of Pax3 expression in the opV placode.  $\beta$ -catenin is active in Pax3<sup>+</sup> cells of the placode (Lassiter et al., 2007) and it is possible that this activity is from Wnt ligands migrating from the neural tube and binding to the frizzled-7 receptor present in the opV placode. We propose that this activity is necessary for the induction of Pax3 expression in the opV placode. In order to verify this we used a double knockout approach of the Wnt1 and Wnt3a gene, and stained for Pax3 in the opV placode. Our results showed that Pax3 protein expression was markedly reduced in the opV placode of mouse embryos, but not absent. From this data, we conclude that Wnt1 and Wnt3a are necessary for the induction of Pax3 expression in the opV placode, and that other signals must be involved in Pax3 induction of the opV placode.

As there was not a complete absence of Pax3 expression in the opV placode from the double knockout experiment, it was possible that other Wnt signals have a redundant role in inducing Pax3. To verify this, a conditional knockout approach was used to delete Wnt activity in the neural tube prior to Pax3 expression. Sox1 gene expression occurs in the neural plate at

E7.5 during mice development. A Sox-Cre male mouse was obtained and crossed with a Porcn female mouse. The Porcn gene encodes a protein involved in post-translational modifications of Wnt ligand producing a functionally active protein. This cross deletes the Porcn gene prior to Pax3 expression, producing nonfunctional Wnt ligands from the neural tube. If functional Wnt ligand from the neural tube was necessary for Pax3 expression, then its expression would be absent from the opV placode. However, analyzing mouse embryos at E8.5 and E9.5 with Pax3 antibody it was concluded that Pax3 expression was not affected. Additional experiments were performed to verify the presence of Sox1-Cre and Wnt activity. From these results, it was concluded that activity of Sox1-Cre and Wnt was present in the tissue analyzed. However, when examining the Sox1-Cre activity in the neural tube at E7.5 there are few cells in the neural tube expressing Cre. There is a marked increase of Cre activity at E8.5 and the activity is shown to increase more at E9.5 though there are still cells in the neural tube that are not Sox1-Cre active. This data may explain why Wnt activity and Pax3 expression is still present when it should be reduced or absent. The Cre recombinase may be active too late in development to have an effect on Pax3 expression, or its activity may not be robust enough in the neural tube to decrease Wnt activity and Pax3 expression. It is possible that both of these considerations play a role in the results obtained. The use of a different Cre mouse line could be used to verify this theory.

## REFERENCES

- Abelló, G., Khatri, S., Giráldez, F., and Alsina, B. 2007. Early regionalization of the otic placode and its regulation by the Notch signaling pathway. *Mechanisms of Development* 124, (7-8): 631-45.
- Amstutz, R., Wachtel, M., Troxler, H., Kleinert, P., Ebauer, M., Haneke, T., Oehler-Janne, C., Fabbro, D., Niggli, F. K., and Schafer, B.W. 2008. Phosphorylation regulates transcriptional activity of PAX3/FKHR and reveals novel therapeutic possibilities. *Cancer Research* 68, (10) (May 15): 3767-76.
- Apuzzo, S., Abdelhakim, A., Fortin, A. S., and Gros, P. 2004. Cross-talk between the paired domain and the homeodomain of Pax3: DNA binding by each domain causes a structural change in the other domain, supporting interdependence for DNA binding. *The Journal of Biological Chemistry* 279, (32) (Aug 6): 33601-12.
- Auerbach, R. 1954. Analysis of the developmental effects of a lethal mutation in the house mouse. *Journal of Experimental Zoology* 127, 305-29.
- Bailey, A. M. and Posakony, J. W. 1995. Suppressor of hairless directly activates transcription of enhancer of split complex genes in response to notch receptor activity. *Genes Dev.* 9, 2609-2622.
- Bajard, L., Relaix, F., Lagha, M., Rocancourt, D., Daubas, P., and Buckingham, M. E. 2006. A novel genetic heirarchy functions during hypaxial myogenesis: Pax3 directly activates Myf5 in muscle progenitor cells in the limb. *Genes and Development* 20, (17): 2450-64.
- Baker, C. V., and Bronner-Fraser, M. 2000. Establishing neuronal identity in vertebrate neurogenic placodes. *Development (Cambridge, England)* 127, (14) (Jul): 3045-56.
- Baker, C. V., Stark, M. R., and Bronner-Fraser, M. 2002. Pax3-expressing trigeminal placode cells can localize to trunk neural crest sites but are committed to a cutaneous sensory neuron fate. *Developmental Biology* 249, (2) (Sep 15): 219-36.
- Baker, C. V., Stark, M. R., Marcelle, C., and Bronner-Fraser, M. 1999. Competence, specification and induction of pax-3 in the trigeminal placode. *Development (Cambridge, England)* 126, (1) (Jan): 147-56.
- Baldwin, C. T., Hoth, C. F., Macina, R. A., and Milunsky, A. 1995. Mutations in PAX3 that cause waardenburg syndrome type I: Ten new mutations and review of the literature. *American Journal of Medical Genetics* 58, (2) (Aug 28): 115-22.
- Barber, T. D., Barber, M. C., Cloutier, T. E., and Friedman, T. B. 1999. PAX3 gene structure, alternative splicing and evolution. *Gene* 237, (2): 311-9.

- Barr, F. G., Fitzgerald, J. C., Ginsberg, J. P., Vanella, M. L., Davis, R. J., and Bennicelli, J. L. 1999. Predominant expression of alternative PAX3 and PAX7 forms in myogenic and neural tumor cell lines. *Cancer Research* 59, (21) (Nov 1): 5443-8.
- Barr, F. G., Galili, N., Holick, J., Biegel, J. A., Rovera, G., and Emanuel, B. S. 1993. Rearrangement of the Pax3 paired box gene in the paediatric solid tumour alveolar rhabdomyosarcoma. *Nature Genetics* 3, (2): 113-7.
- Barrott, J. J., Cash, G. M., Smith, A. P., Barrow, J. R., and Murtaugh L. C. 2011. Deletion of mouse Poren blocks Wnt ligand secretion and reveals an ectodermal etiology of human focal dermal hypoplasia/Goltz syndrome. *Proc Natl Acad Sci USA* 108, (31): 12752-57.
- Begbie, J., Ballivet, M., and Graham, A. 2002. Early steps in the production of sensory neurons by the neurogenic placodes. *Mol. Cell. Neurosci.* 21, 502-511.
- Behrens, J., Jerchow, B. A., Würtele, M., Grimm, J., Asbrand, C., Wirtz, R., Kühl, M., Wedlich, D., and Birchmeier, W. 1998. Functional interaction of an axin homolog, conductin, with beta-catenin, APC, and GSK3beta. *Science* 280, (5363)L 596-9.
- Blake, J. A. and Ziman, M. R. 2005. Pax3 transcripts in melanoblast development. *Development, Growth & Differentiation* 47, (9) (Dec): 627-35.
- Blauwkamp, T. A., Chang, M. V., and Cadigan, K. M. 2008. Novel TCF-binding sites specify transcriptional repression by Wnt signalling. *EMBO Journal* 27, (10): 1436-46.
- Birrane, G., Soni, A., and Ladas, J. A. 2009. Structural basis for DNA recognition by the human PAX3 homeodomain. *Biochemistry* 48, (6): 1148-55.
- Bober, E., Franz, T., Arnold, H. H., Gruss, P., and Tremblay, P. 1994. Pax-3 is required for the development of limb muscles: A possible role for the migration of dermomyotomal muscle progenitor cells. *Development (Cambridge, England)* 120, (3) (Mar): 603-12.
- Canning, C. A., Lee, L., Luo, S. X., Graham, A., and Jones, C. M. 2008. Neural tube derived Wnt signals cooperate with FGF signaling in the formation and differentiation of the trigeminal placodes. *Neural Development* 3, (35): 1-16.
- Cao, Y. and Wang, C. 2000. The COOH-terminal transactivation domain plays a key role in regulating the in vitro and in vivo function of Pax3 homeodomain. *Journal of Biological Chemistry* 275, (13): 9854-62.
- Caricasole, A., Ferraro, T., Rimland, J. M., and Terstappen, G. C. 2002. Molecular cloning and initial characterization of the MG61/PORC gene, the human homologue of the Drosophila segment polarity gene Porcupine. *Gene* 288, (1-2): 147-57.

- Castro, D. S., Skowronska-Krawczyk, D., Armant, O., Donaldson, I. J., Parras, C., Hunt, C., Critchley, J. A., Nguyen, L., Gossler, A., Gottgens, B. et al. 2006. Proneural bHLH and Brn proteins coregulate a neurogenic program through cooperative binding to a conserved DNA motif. *Dev. Cell.* 11, 831-844.
- Chalepakis, G., Jones, F. S., Edelman, G. M., and Gruss, P. 1994a. Pax-3 contains domains for transcription activation and transcription inhibition. *Proceedings of the National Academy of Sciences of the United States of America* 91, (26) (Dec 20): 12745-9.
- Chalepakis, G., Wijnholds, J., and Gruss, P. 1994b. Pax-3-DNA interaction: flexibility in the DNA binding and induction of DNA conformational changes by paired domains. *Nucleic Acids Research.* 22, (15): 3131-7.
- Chapman, S. C., Collignon, J., Schoenwolf, G. C., and Lumsden, A. 2001. Improved method for chick whole-embryo culture using a filter paper carrier. *Developmental Dynamics* 220, (3): 284-9.
- Collins, C. A., Gnocchi, V. F., White, R. B., Boldrin, L., Perez-Ruiz, A., Relaix, F., Morgan, J. E., and Zammit, P.S. 2009. Integrated functions of Pax3 and Pax7 in the regulation of proliferation, cell size and myogenic differentiation. *PloS One* 4, (2): e4475.
- Czerny, T., Schaffner, G., and Busslinger, M. 1993. DNA sequence recognition by pax proteins: Bipartite structure of the paired domain and its binding site. *Genes & Development* 7, (10) (Oct): 2048-61.
- D'Amico-Martel, A. and Noden, D. M. 1983. Contributions of placodal and neural crest cells to avian cranial peripheral ganglia. *The American Journal of Anatomy* 166, (4) (Apr): 445-68.
- Daudet, N., Ariza-McNaughton, L. and Lewis, J. 2007. Notch signaling is needed to maintain, but not to initiate, the formation of prosensory patches in the chick inner ear. *Development* 134, 2369-2378.
- Dude, C. M., Kuan, C. Y., Bradshaw, J. R., Greene, N. D., Relaix, F., Stark, M. R., and Baker, C.V. 2009. Activation of Pax3 target genes is necessary but not sufficient for neurogenesis in the ophthalmic trigeminal placode. *Developmental Biology* 326, (2) (Feb 15): 314-26.
- Eberhard, D., Jiménez, G., Heavey, B., and Busslinger, M. 2000. Transcriptional repression by Pax5 (BSAP) through interaction with corepressors of the Groucho family. *EMBO Journal* 19, (10): 2292-303.
- Epstein, D. J., Vekemans, M., and Gros, P. 1991. Splotch (Sp2H), a mutation affecting development of the mouse neural tube, shows a deletion within the paired homeodomain of pax-3. *Cell* 67, (4) (Nov 15): 767-74.

- Epstein, D. J., Vogan, K. J., Trasler, D. G., and Gros, P. 1993. A mutation within intron 3 of the pax-3 gene produces aberrantly spliced mRNA transcripts in the splotch (sp) mouse mutant. *Proceedings of the National Academy of Sciences of the United States of America* 90, (2) (Jan 15): 532-6.
- Evans, J. and Lillycrop, K. A. 1996. Serum growth factor regulation of the paired-box transcription factor pax-3 in neuronal cells. *Neuroscience Letters* 220, (2) (Dec 13): 125-8.
- Fedtsova, N., Perris, R., and Turner, E. E. Sonic hedgehog regulates the position of the trigeminal ganglia. *Developmental Biology* 261, (2): 456-69.
- Fode, C., Gradwohl, G., Morin, X., Dierich, A., Lemeur, M., Gioridis, C. and Guillemot, F. 1998. The bHLH protein Neurogenin 2 is a determination factor for epibranchial placode-derived sensory neurons. *Neuron* 20, 483-494.
- Fortin, A. S., Underhill, D. A., and Gros, P. 1998. Helix 2 of the paired domain plays a key role in the regulation of DNA-binding by the pax-3 homeodomain. *Nucleic Acids Research* 26, (20) (Oct 15): 4574-81.
- Garcia-Morales, C., Liu, C. H., Abu-Elmagd, M., Hajihosseini, M. K., and Wheeler, G. N. 2009. Frizzled-10 promotes sensory neuron development in *Xenopus* embryos. *Developmental Biology* 335, (1): 143-55.
- Goulding, M. D., Chalepakis, G., Deutsch, G., Erselius, J.R., and Gruss, P. 1991. Pax-3, a novel murine DNA binding protein expressed during early neurogenesis. *The EMBO Journal* 10, (5) (May): 1135-47.
- Groves, A. K. and Bronner-Fraser, M. Competence, specification and commitment in otic placode induction. *Development* 127, (16): 3489-99.
- Hamburger, V. and Hamilton, H. L. 1951. A series of normal stages in the development of the chick embryo. *Journal of Morphology* 88:49-92.
- Henrique, D., Adam, J., Myat, A., Chitnis, A., Lewis, J., Ish-Horowicz, D. 1995. Expression of a delta homologue in prospective neurons in the chick. *Nature* 375, 787-790.
- Herbrand, H., Guthrie, S., Hadrys, T., Hoffman, S., Arnold, H. H., Rinkwitz-Brandt, S., and Bober, E. 1998. Two regulatory genes, cNkx5-1 and cPax2, show different responses to local signals during otic placode and vesicle formation in the chick embryo. *Development* 125, (4): 645-54.
- Hollyday, M., McMahon, J. A., and McMahon, A. P. 1995. Wnt expression patterns in chick embryo nervous system. *Mechanisms of Development* 52, (1): 9-25.



- Hsieh, M. J., Yao, Y. L., Lai, I. L., and Yang, W. M. 2006. Transcriptional repression activity of PAX3 is modulated by competition between corepressor KAP1 and heterochromatin protein 1. *Biochemical and Biophysical Research Communications* 349, (2) (Oct 20): 573-81.
- Ikeya, M. and Takada, S. 1998. Wnt signaling from the dorsal neural tube is required for the formation of the medial dermomyotome. *Development* 125, (24): 4969-76.
- Ikeya, M., Lee, S. M., Johnson, J. E., McMahon, A. P., and Takada, S. 1997. Wnt signalling required for expansion of neural crest and CNS progenitors. *Nature* 389, (6654): 966-70.
- Jarriault, S., Brou, C., Logeat, F., Schroeter, E. H., Kopan, R. and Israel, A. 1995. Signaling downstream of activate mammalian notch. *Nature* 377, 355-358.
- Jarriault, S., Le Bail, O., Hirsinger, E., Pourquié, O., Logeat, F., Strong, C. F., Brou, C., Seida, N.G. and Isra, I. A. 1998. Delta-1 activation of notch-1 signaling results in HES-1 transactivation. *Mol. Cell. Biol.* 18, 7423-7431.
- Jho, E. H., Zhang, T., Domon, C., Joo, C. K., Freund, J. N., and Costantini, F. 2002. Wnt/beta-catenin/Tcf signaling induces the transcription of Axin2, a negative regulator of the signaling pathway. *Molecular and Cellular Biology* 22, (4): 1172-83.
- Jin, E. J., Erickson, C. A., Takada, S., and Burrus, L. W. 2001. Wnt and BMP signaling govern lineage segregation of melanocytes in the avian embryo. *Developmental Biology* 233, (1): 22-37.
- Kadowaki, T., Wilder, E., Klingensmith, J., Zachary, K., and Perrimon, N. 1996. The segment polarity gene porcupine encodes a putative multitransmembrane protein involved in Wingless processing. *Genes and Development* 10, (24): 3116-28.
- Kageyama, R., Ohtsuka, T., Shimojo, H., and Imayoshi, I., 2008. Dynamic Notch signaling in neural progenitor cells and a revised view of lateral inhibition. *Nature Neuroscience* 11, (11): 1247-51.
- Kioussi, C., Gross, M. K., and Gruss, P. 1995. Pax3: A paired domain gene as a regulator in PNS myelination. *Neuron* 15, (3) (Sep): 553-62.
- Kwang, S. J., Brugger, S. M., Lazik, A., Merrill, A. E., Wu, L. Y., Liu, Y. H., Ishii, M., et al. 2002. Msx2 is an immediate downstream effector of Pax3 in the development of the murine cardiac neural crest. *Development (Cambridge, England)* 129, (2) (Jan): 527-38.
- Ladher, R. K., Church, V. L., Allen, S., Robson, L., Abdelfattah, A., Brown, N. A., Hattersley, G., Rosen, V., Luyten, F. P., Dale, L., and Francis-West, P. H. 2000. Cloning and expression of the Wnt antagonists Sfrp-2 and Frzb during chick development. *Developmental Biology* 218, (2): 183-98.

- Lalwani, A. K., Brister, J. R., Fex, J., Grundfast, K. M., Ploplis, B., San Agustin, T. B., and Wilcox, E. R. 1995. Further elucidation of the genomic structure of PAX3, and identification of two different point mutations within the PAX3 homeobox that cause Waardenburg syndrome type 1 in two families. *Am J Hum Genet.* 56, (1): 75-83.
- Lasky, J. L. and Wu, H. 2005. Notch signaling, brain development, and human disease. *Pediatric Research* 57, (5 Pt 2): 104R-109R.
- Lassiter, R. N., Ball, M. K., Adams, J. S., Wright, B. T., and Stark, M. R. 2010. Sensory neuron differentiation is regulated by notch signaling in the trigeminal placode. *Developmental Biology* 344, (2): 836-48.
- Lassiter, R. N., Dude, C. M., Reynolds, S. B., Winters, N. I., Baker, C. V., and Stark, M. R. 2007. Canonical Wnt signaling is required for ophthalmic trigeminal placode cell fate determination and maintenance. *Developmental Biology* 308, (2) (Aug 15): 392-406.
- Lassiter, R. N., Reynolds, S. B., Marin, K. D., Mayo, T. F. and Stark, M. R., 2009. FGF signaling is essential for ophthalmic trigeminal placode cell delamination and differentiation. *Dev. Dyn.* 238, 1073-1082.
- Lechner, M. S. and Dressler, G. R. 1996. Mapping of Pax-2 transcription activation domains. *J Biol Chem.* 271, (35): 21088-93.
- Lee, S. M., Tole, S., Grove, E., and McMahon, A. P. 2000. A local Wnt-3a signal is required for development of the mammalian hippocampus. *Development* 127, (3): 457-67.
- Leung, J. Y., Kolligs, F. T., Wu, R., Zhai, Y., Kuick, R., Hanash, S., Cho, K. R., and Fearon, E. R. 2002. Activation of AXIN2 expression by beta-catenin-T cell factor. A feedback repressor pathway regulating Wnt signaling. *J Biol Chem.* 277, (24): 21657-65.
- Mansouri, A. 1998. The role of Pax3 and Pax7 in development and cancer. *Critical Review of Oncology* 9, (2): 141-9.
- Marcelle, C., Eichmann, A., Halevy, O., Bréant, C., and Le Douarin, N. M. 1994. Distinct development expression of a new avian fibroblast growth factor receptor. *Development* 120, (3): 683-94.
- Maroto, M., Reshef, R., Munsterberg, A. E., Koester, S., Goulding, M., and Lassar, A. B. 1997. Ectopic pax-3 activates MyoD and myf-5 expression in embryonic mesoderm and neural tissue. *Cell* 89, (1) (Apr 4): 139-48.
- Mayanil, C. S., George, D., Freilich, L., Miljan, E. J., Mania-Farnell, B., McLone, D. G., and Bremer, E. G. 2001. Microarray analysis detects novel Pax3 downstream target genes. *The Journal of Biological Chemistry* 276, (52) (Dec 28): 49299-309.

- McCabe, K. L. and Bronner-Fraser, M. 2008. Essential role for PDGF signaling in ophthalmic trigeminal placode induction. *Development* 135, (10): 1863-74.
- McMahon, A. P. and Bradley, A. 1990. The Wnt-1 (int-1) proto-oncogene is required for development of a large region of the mouse brain. *Cell* 62, (6): 1073-85.
- Murakami, M., Tominaga, J., Makita, R., Uchijima, Y., Kurihara, Y., Nakagawa, O., Asano, T., and Kurihara, H. 2006. Transcriptional activity of Pax3 is co-activated by TAZ. *Biochemical and Biophysical Research Communications* 339, (2) (Jan 13): 533-9.
- Nakazaki, H., Reddy, A. C., Mania-Farnell, B. L., Shen, Y. W., Ichi, S., McCabe, C., George, D., McLone, D. G., Tomita, T., and Mayanil, C. S. 2008. Key basic helix-loop-helix transcription factor genes Hes1 and Ngn2 are regulated by Pax3 during mouse embryonic development. *Developmental Biology* 316, (2) (Apr 15): 510-23.
- Nelson, B. R., Hartman, B. H., Georgi, S. A., Lans, M. S., and Reh, T. A. 2007. Transient inactivation of Notch signaling synchronizes differentiation of neural progenitor cells. *Developmental Biology* 304, (2): 479-98.
- Nichols, D. H. 1986. Mesenchyme formation from the trigeminal placodes of the mouse embryo. *American Journal of Anatomy* 176, (1): 19-31.
- Ohtsuka, T., Ishibashi, M., Gradwohl, G., Nakanishi, S., Guillemot, F., and Kageyama, R. 1999. Hes1 and Hes5 as notch effectors in mammalian neuronal differentiation. *EMBO J.* 18, 2196-2201.
- Okamura, Y. and Saga, Y. 2008. Notch signaling is required for the maintenance of enteric neural crest progenitors. *Development* 135, (21): 3555-65.
- Parker, C. J., Shawcross, S. G., Li, H., Wang, Q. Y., Herrington, C. S., Kumar, S., MacKie, R. M. et al. 2004. Expression of PAX 3 alternatively spliced transcripts and identification of two new isoforms in human tumors of neural crest origin. *International Journal of Cancer. Journal International Du Cancer* 108, (2) (Jan 10): 314-20.
- Pevny, L. H., Sockanathan, S., Placzek, M., and Lovell-Badge, R. 1998. A role for SOX1 in neural determination. *Development* 125, (10): 1967-78.
- Phelan, S. A. and Loeken, M. R. 1998. Identification of a new binding motif for the paired domain of pax-3 and unusual characteristics of spacing of bipartite recognition elements on binding and transcription activation. *The Journal of Biological Chemistry* 273, (30) (Jul 24): 19153-9.
- Pritchard, C., Grosveld, G., and Hollenbach, A. D. 2003. Alternative splicing of Pax3 produces a transcriptionally inactive protein. *Gene* 305, (1) (Feb 13): 61-9.

- Quinlan, R., Graf, M., Mason, I., Lumsden, A., and Kiecker, C. 2009. Complex and dynamic patterns of Wnt pathway gene expression in the developing chick forebrain. *Neural Development* 4, (45): 1-27.
- Reeves, F. C., Fredericks, W. J., Rauscher 3<sup>rd</sup>, F. J., and Lillycrop, K. A. 1998. The DNA binding activity of the paired box transcription factor pax-3 is rapidly downregulated during neuronal cell differentiation. *FEBS Letters* 422, (1) (Jan 23): 118-22.
- Relaix, F., Montarras, D., Zaffran, S., Gauraud-Morel, B., Rocancourt, D., Tajbakhsh, S., Mansouri, A., Cumano, A., and Buckingham, M. 2006. Pax3 and Pax7 have distinct and overlapping functions in adult muscle progenitor cells. *Journal of Cellular Biology* 172, (1): 91-102.
- Relaix, F., Polimeni, M., Rocancourt, D., Ponzetto, C., Schafer, B. W., and Buckingham, M. 2003. The transcriptional activator PAX3-FKHR rescues the defects of Pax3 mutant mice but induces a myogenic gain-of-function phenotype with ligand-independent activation of met signaling in vivo. *Genes & Development* 17, (23) (Dec 1): 2950-65.
- Sanders, T. A., Lumsden, A., and Ragsdale, C. W. 2002. Arcuate plan of chick midbrain development. *Journal of Neuroscience* 22, (24): 10742-50.
- Schlosser, G. 2006. Induction and specification of cranial placodes. *Developmental Biology* 294, (2): 303-51.
- Seo, H. C., Saetre, B. O., Havik, B., Ellingsen, S., and Fjose, A. 1998. The zebrafish Pax3 and Pax7 homologues are highly conserved, encode multiple isoforms and show dynamic segment-like expression in the developing brain. *Mechanisms of Development* 70, (1-2) (Jan): 49-63.
- Shimojo, H., Ohtsuka, T. and Kageyama, R. 2008. Oscillations in notch signaling regulate maintenance of neural progenitors. *Neuron* 58, 52-64.
- Slawny, N. A. and O'Shea, K. S. 2011. Dynamic changes in Wnt signaling are required for neuronal differentiation of mouse embryonic stem cells. *Molecular and Cellular Neuroscience* 48, (3): 205-16.
- Soriano, P. 1999. Generalized lacZ expression with the ROSA26 Cre reporter strain. *Nature Genetics*. 21, (1): 70-1.
- Stark, M. R., Biggs, J. J., Schoenwolf, G. C., and Rao, M. S. 2000. Characterization of avian frizzled genes in cranial placode development. *Mechanisms of Development* 93, (1-2): 195-200.
- Stark, M. R., Sechrist, J., Bronner-Fraser, M., and Marcelle, C. 1997. Neural tube-ectoderm interactions are required for trigeminal placode formation. *Development (Cambridge, England)* 124, (21) (Nov): 4287-95.

- Streit, A. 2004. Early development of the cranial sensory nervous system: From a common field to individual placodes. *Developmental Biology* 276, (1) (Dec 1): 1-15.
- Stuart, E. T., Kioussi, C., and Gruss, P. 1994. Mammalian Pax genes. *Annual Review of Genetics* 28: 219-38.
- Sun, Y., Dykes, I. M., Liang, X., Eng, S. R., Evans, S. M., and Turner, E. E. 2008. A central role for Islet1 in sensory neuron development linking sensory and spinal gene regulatory programs. *Nature Neuroscience* 11, (11): 1283-93.
- Takada, S., Stark, K. L., Shea, M. J., Vassileva, G., McMahon, J. A., and McMahon, A. P. 1994. Wnt-3a regulates somite and tailbud formation in the mouse embryo. *Genes and Development* 8, (2): 174-89.
- Takashima, Y., Era, T., Nakao, K., Kondo, S., Kasuga, M., Smith, A. G., and Nishikawa, S. 2007. Neuroepithelial cells supply an initial transient wave of MSC differentiation. *Cell* 129, (7): 1377-88.
- Tanaka, K., Okabayashi, K., Asashima, M., Perrimon, N., and Kadowaki, T. 2000. The evolutionarily conserved porcupine gene family is involved in the processing of the Wnt family. *European Journal of Biochemistry* 267, (13): 4300-11.
- Tassabehji, M., Read, A. P., Newton, V. E., Patton, M., Gruss, P., Harris, R., and Strachan, T. 1993. Mutations in the PAX3 gene causing waardenburg syndrome type 1 and type 2. *Nature Genetics* 3, (1) (Jan): 26-30.
- Thomas, K. R. and Capecchi, M. R. 1990. Targeted disruption of the murine int-1 proto-oncogene resulting in severe abnormalities in midbrain and cerebellar development. *Nature* 346, (6287): 847-50.
- Treisman, J., Harris, E., and Desplan, C. 1991. The paired box encodes a second DNA-binding domain in the paired homeo domain protein. *Genes Dev.* 5, (4): 594-604.
- Tremblay, P., Kessel, M., and Gruss, P. 1995. A transgenic neuroanatomical marker identifies cranial neural crest deficiencies associated with the Pax3 mutant Splotch. *Developmental Biology* 171, (2): 317-29.
- Tsukamoto, K., Nakamura, Y., and Niikawa, N. 1994. Isolation of two isoforms of the PAX3 gene transcripts and their tissue-specific alternative expression in human adult tissues. *Hum Genet.* 93, (3): 270-4.
- van den Heuvel, M., Harryman-Samos, C., Klingensmith, J., Perrimon, N., and Nusse, R. 1993. Mutations in the segment polarity genes wingless and procupine impair secretion of the wingless protein. *EMBO Journal* 12, (13): 5293-302.

- Vogan, K. J. and Gros, P. 1997. The C-terminal subdomain makes an important contribution to the DNA binding activity of the pax-3 paired domain. *The Journal of Biological Chemistry* 272, (45) (Nov 7): 28289-95.
- Vogan, K. J., Underhill, D. A., and Gros, P. 1996. An alternative splicing event in the pax-3 paired domain identifies the linker region as a key determinant of paired domain DNA-binding activity. *Molecular and Cellular Biology* 16, (12) (Dec): 6677-86.
- von Kries, J. P., Winbeck, G., Asbrand, C., Schwarz-Romond, T., Sochnikova, N., Dell'Oro, A., Behrens, J., and Birchmeier, W. 2000. Hot spots in beta-catenin for interactions with LEF-1, conductin and APC. *Nature Structural Biology* 7, (9): 800-7.
- Underhill, D. A. and Gros, P. 1997. The paired-domain regulates DNA binding by the homeodomain within the intact Pax-3 protein. *Journal of Biological Chemistry* 272, (22): 14175-82.
- Underhill, D. A., Vogan, K. J., and Gros, P. 1995. Analysis of the mouse Splotch-delayed mutation indicates that the Pax-3 paired domain can influence homeodomain DNA-binding activity. *Proc Natl Acad Sci USA* 92, (9): 3692-6.
- Waardenburg, P. J. 1951. A new syndrome combining developmental anomalies of the eyelids, eyebrows and nose root with pigmentary defects of the iris and head hair and with congenital deafness. *American Journal of Human Genetics* 3, (3) (Sep): 195-253.
- Wang, Q., Kumar, S., Mitsios, N., Slevin, M., and Kumar, P. 2007. Investigation of downstream target genes PAX3c, PAX3e and PAX3g isoforms in melanocytes by microarray analysis. *Int J Cancer* 120, (6): 1223-31.
- Wu, M., Li, J., Engleka, K. A., Zhou, B., Lu, M. M., Plotkin, J. B., and Epstein, J. A. 2008. Persistent expression of Pax3 in the neural crest causes cleft palate and defective osteogenesis in mice. *The Journal of Clinical Investigation* 118, (6) (Jun): 2076-87.
- Zhang, X. H. and Chasin, L. A. 2004. Computational definition of sequence motifs governing constitutive exon splicing. *Genes and Development* 18, (11): 1242-50.
- Zhang, X. H., Kangsamaksin, T., Chao, M. S., Banerjee, J. K., and Chasin, L. A. 2005. Exon inclusion is dependent on predictable exonic splicing enhancers. *Molecular and Cellular Biology* 25, (16): 7323-32.

## APPENDIX

<u>Predicted splice form size</u>	<u>Predicted deletion size</u>	
Pax3	1455bp	N/A
Pax3V1	1320bp	135bp
Pax3V2	1074bp	381bp

Table 1 Predicted size of the Pax3 splice forms in chick  
The first column of the table shows the predicted size of each Pax3 splice form. The second column shows the applicable deletion size contained within the respective splice form.

	<u>PESE</u>	<u>PESS</u>
Exon 1	1	0
Exon 2	7	0
Exon 3	7	0
Exon 4	15	0
Exon 5	10	1
Exon 6	6	2
Exon 7	4	2
Exon 8	3	1
Exon 9	1	1

Table 2 Number of PESEs and PESSs per exon found in the Pax3 gene of chick  
The number of putative exonic splice enhancers (PESE) and putative exonic splice silencers (PESS) are listed next to each exon within the Pax3 gene of chick.



Table 3 Cell counts of *in ovo* misexpression embryos at 6-8ss

pCIG

5 Embryos		10 Placodes	Ectoderm					Mesenchyme						
			Pax3	GFP	Pax3/ GFP	Untargeted GFP	Islet1	Pax3/ GFP/ Islet1	Pax3	GFP	Pax3/ GFP	Untargeted GFP	Islet1	Pax3/ GFP/ Islet1
Embryo A	Section													
	1	3	54	41	21	20	0	0	50	17	15	2	31	12
	2	1	25	32	15	17	0	0	34	15	13	2	24	10
	3	6	27	29	12	17	0	0	16	13	11	2	12	9
	4	2	39	31	12	19	0	0	36	16	14	2	28	11
	5	8	20	27	5	22	0	0	14	4	4	0	9	3
Total cells			165	160	65	95	0	0	150	65	57	8	104	45
Embryo A														
	1	3	17	17	10	7	0	0	22	13	10	3	16	11
	2	1	9	18	7	11	0	0	14	8	8	0	12	7
	3	6	10	11	3	8	0	0	8	4	4	0	6	3
	4	2	9	15	6	9	0	0	14	10	8	2	15	6
	5	8	24	16	12	4	0	0	19	12	10	2	15	6
Total cells			69	77	38	39	0	0	77	47	40	7	64	33
Embryo B														
	1	5	23	35	17	18	0	0	23	9	9	0	31	8
	2	2	26	20	7	13	0	0	19	7	7	0	28	7
	3	1	24	31	11	20	0	0	23	12	10	2	28	10
	4	6	19	28	14	14	0	0	26	14	13	1	25	9
	5	3	19	34	14	20	0	0	20	10	10	0	29	8
Total cells			111	148	63	85	0	0	111	52	49	3	141	42
Embryo B														
	1	5	19	32	10	22	0	0	24	11	9	2	32	7
	2	2	24	19	6	13	0	0	26	9	6	3	39	6
	3	1	23	29	7	22	0	0	26	8	7	1	27	7
	4	6	23	31	13	18	0	0	35	15	12	3	43	10
	5	3	26	27	9	18	0	0	35	17	17	0	32	11
Total cells			115	138	45	93	0	0	146	60	51	9	173	41
Embryo C														
	1	9	16	22	10	12	0	0	25	12	12	0	25	12
	2	2	28	19	9	10	0	0	26	19	13	6	28	11
	3	4	33	23	18	5	0	0	34	16	13	3	24	4
	4	3	23	20	11	9	0	0	22	15	15	0	26	10

	5	8	27	23	12	11	0	0	23	12	12	0	24	8
Total cells			127	107	60	47	0	0	130	74	65	9	127	45
Embryo C														
	1	9	8	19	7	12	0	0	20	15	8	7	17	8
	2	2	24	24	12	12	0	0	7	6	4	2	8	3
	3	4	30	33	14	19	0	0	13	11	7	4	11	6
	4	3	25	27	13	14	0	0	15	10	9	1	12	8
	5	8	10	18	7	11	0	0	19	15	13	2	19	4
Total cells			97	121	53	68	0	0	74	57	41	16	67	29
Embryo D														
	1	3	33	24	22	2	0	0	55	33	30	3	36	30
	2	6	27	44	19	25	0	0	35	29	18	11	15	15
	3	5	38	29	17	12	0	0	59	38	23	15	20	20
	4	9	30	31	16	15	0	0	26	26	19	7	15	15
	5	4	42	24	16	8	0	0	65	38	29	9	21	19
Total cells			170	152	90	62	0	0	240	164	119	45	107	99
Embryo D														
	1	3	23	9	7	2	0	0	21	8	6	2	19	4
	2	6	25	15	12	3	0	0	55	30	27	3	51	26
	3	5	23	11	10	1	0	0	22	18	14	4	11	8
	4	9	34	15	13	2	1	0	24	13	12	1	28	12
	5	4	19	16	7	9	0	0	14	11	7	4	7	5
Total cells			124	66	49	17	1	0	136	80	66	14	116	55
Embryo F														
	1	5	27	44	27	17	0	0	37	26	22	4	46	22
	2	6	35	43	26	17	0	0	21	16	14	2	16	11
	3	1	28	28	23	5	0	0	26	19	16	3	23	14
	4	3	23	35	21	14	0	0	27	22	19	3	20	19
	5	8	19	23	15	8	0	0	12	12	10	2	10	8
Total cells			132	173	112	61	0	0	123	95	81	14	115	74
Embryo F														
	1	5	37	37	28	9	1	0	23	16	16	0	38	14
	2	6	36	25	20	5	0	0	32	18	17	1	24	17
	3	1	27	26	19	7	0	0	15	8	8	0	11	5
	4	3	29	20	19	1	0	0	22	18	10	8	20	11
	5	8	16	23	11	12	0	0	15	10	9	1	11	7
Total cells			145	131	97	34	1	0	107	70	60	10	104	54

# Pax3

7 Embryos		11 Placodes		Ectoderm					Mesenchyme					
		Pax3	GFP	Pax3/ GFP	Untargeted GFP	Islet1	Pax3/ GFP/ Islet1	Pax3	GFP	Pax3/ GFP	Untargeted GFP	Islet1	Pax3/ GFP/ Islet1	
Embryo A	Section													
	1	3	16	3	3	0	0	0	5	3	3	0	0	0
	2	4	31	12	11	1	0	0	8	4	3	0	0	0
	3	5	18	8	8	0	0	0	10	9	8	1	0	0
	4	7	26	13	13	0	0	0	11	5	4	1	2	0
	5	6	20	10	10	0	0	0	15	7	7	0	5	0
	Total cells		111	46	45	1	0	0	49	28	25	2	7	0
Embryo A														
	1	3	23	13	13	0	0	0	5	2	2	0	0	0
	2	4	29	8	8	0	0	0	9	4	4	0	6	0
	3	5	19	11	8	3	0	0	4	3	2	1	9	0
	4	7	20	16	9	7	0	0	13	7	5	2	11	2
	5	9	20	11	11	0	0	0	7	3	3	0	7	1
	Total cells		111	59	49	10	0	0	38	19	16	3	33	3
Embryo B														
	1	3	12	9	8	1	0	0	5	3	2	1	1	1
	2	1	12	9	6	3	0	0	9	1	1	0	3	0
	3	7	33	27	25	0	0	0	18	16	16	0	4	1
	4	5	37	29	29	0	0	0	11	2	0	2	0	0
	5	4	41	29	29	0	0	0	7	5	5	0	1	0
	Total cells		135	103	97	4	0	0	50	27	24	3	9	2
Embryo B														
	1	3	40	36	28	8	0	0	8	6	3	3	0	0
	2	1	37	31	25	6	0	0	9	2	2	0	1	0
	3	7	36	28	26	2	0	0	11	6	3	3	2	0
	4	5	52	36	30	6	0	0	7	2	2	0	3	0
	5	4	35	34	28	6	0	0	7	6	5	1	2	1
	Total cells		200	165	137	28	0	0	42	22	15	7	8	1
Embryo C														
	1	8	56	38	34	4	0	0	7	3	3	0	12	0
	2	4	38	29	29	0	0	0	6	4	4	0	3	0
	3	6	50	24	24	0	0	0	3	2	2	0	3	2
	4	5	31	29	29	0	0	0	8	4	4	0	6	1
	5	1	41	23	23	0	0	0	0	0	0	0	1	0
	Total cells		216	143	139	4	0	0	24	13	13	0	25	3

Embryo C													
1	8	39	26	20	6	0	0	4	0	0	0	4	0
2	4	44	23	22	1	0	0	5	4	4	0	0	0
3	6	35	24	24	0	0	0	7	3	3	0	3	2
4	5	33	27	20	7	1	0	2	1	1	0	0	0
5	1	52	32	32	0	0	0	1	1	1	0	1	0
Total cells		203	132	118	14	1	0	19	9	9	0	8	2
Embryo D													
1	1	17	11	11	0	0	0	16	3	3	0	12	0
2	2	14	9	9	0	0	0	8	3	3	0	17	2
3	3	18	10	10	0	1	0	10	4	4	0	8	2
4	4	15	9	8	1	0	0	15	4	4	0	14	2
Total cells		64	39	38	1	1	0	49	14	14	0	51	6
Embryo E													
1	1	46	42	28	14	0	0	8	6	6	0	14	0
2	2	45	37	37	0	0	0	7	1	0	0	5	0
3	3	40	26	23	3	0	0	11	10	0	0	2	1
Total cells		131	105	88	17	0	0	26	17	6	0	21	1
Embryo F													
1	1	31	25	24	1	0	0	4	4	0	0	3	1
2	2	31	24	24	0	0	0	1	1	1	0	3	0
3	3	31	22	21	0	0	0	5	2	2	0	1	0
4	4	36	34	33	1	0	0	1	1	1	0	3	0
Total cells		129	105	102	2	0	0	11	8	4	0	10	1
Embryo F													
1	1	48	41	40	1	0	0	3	3	3	0	1	1
2	2	52	39	39	0	0	0	5	4	4	0	3	3
3	3	55	49	49	0	0	0	10	7	7	0	5	0
4	4	46	39	37	2	0	0	11	10	10	0	12	2
Total cells		201	168	165	3	0	0	29	24	24	0	21	6
Embryo G													
1	1	37	38	37	1	0	0	7	7	7	0	9	3
2	2	51	41	40	1	0	0	9	7	7	0	5	2
3	5	32	21	20	1	0	0	8	5	4	1	8	0
4	4	44	45	44	1	0	0	9	6	6	0	16	2
5	6	38	36	34	2	0	0	4	4	4	0	2	1
Total cells		202	181	175	6	0	0	37	29	28	1	40	8

# Pax3V1

7 Embryos		12 Placodes		Ectoderm					Mesenchyme				
	Section	Pax3	GFP	Pax3/ GFP	Untargeted GFP	Islet1	Pax3/ GFP/ Islet1	Pax3	GFP	Pax3/ GFP	Untargeted GFP	Islet1	Pax3/ GFP/ Islet1
		Embryo A											
	1	4	58	47	47	0	0	0	0	0	0	0	0
	2	3	41	32	32	0	0	0	1	3	1	2	0
	3	7	35	33	33	0	0	0	8	8	6	2	0
	4	8	43	49	42	7	0	0	2	4	1	3	0
	5	6	31	22	22	0	0	0	6	4	2	2	1
Total cells			208	183	176	7	0	0	17	19	10	9	1
Embryo A													
	1	4	38	38	34	4	0	0	10	4	3	1	16
	2	3	49	43	38	0	0	0	8	3	3	0	14
	3	7	60	70	10	0	0	0	1	1	1	0	0
	4	8	45	41	41	0	0	0	0	0	0	0	0
	5	6	42	17	17	0	0	0	6	0	0	0	19
Total cells			234	209	140	4	0	0	25	8	7	1	49
Embryo B													
	1	4	35	19	13	6	0	0	2	2	2	0	0
	2	3	30	23	20	3	0	0	4	2	2	0	3
	3	5	35	11	11	0	1	0	8	7	3	4	5
	4	6	35	17	17	0	0	0	7	4	4	0	6
	5	1	21	19	14	5	0	0	5	5	5	0	2
Total cells			156	89	75	14	1	0	26	20	16	4	16
Embryo B													
	1	4	38	34	25	9	0	0	7	5	4	1	3
	2	3	47	31	30	1	0	0	16	11	10	1	0
	3	5	34	28	26	2	1	0	11	7	6	1	4
	4	6	45	32	32	0	1	0	10	8	7	1	7
	5	1	22	20	15	5	0	0	8	8	6	2	1
Total cells			186	145	128	17	2	0	52	39	33	6	15
Embryo C													
	1	1	43	30	30	0	0	0	12	6	6	0	3
	2	10	24	28	27	1	0	0	7	1	1	0	6
	3	6	37	27	27	0	0	0	8	5	4	1	25
	4	2	55	47	47	0	0	0	16	5	4	1	11
	5	7	46	47	44	3	0	0	14	6	5	1	24
Total cells			205	179	175	4	0	0	57	23	20	3	69

Embryo C													
1	1	36	26	26	0	0	0	8	5	4	1	6	0
2	10	22	17	15	2	0	0	5	2	2	0	0	0
3	6	51	39	39	0	0	0	19	15	8	7	4	1
4	2	46	45	42	3	0	0	10	8	7	1	6	2
5	7	59	41	38	3	0	0	9	8	7	1	2	0
Total cells		214	168	160	8	0	0	51	38	28	10	18	3
Embryo D													
1	2	66	51	50	1	4	3	4	4	4	0	3	0
2	1	66	65	64	1	0	0	7	5	5	0	3	0
3	3	40	33	30	3	0	0	5	4	1	3	2	0
4	5	46	32	27	5	0	0	5	9	3	6	1	0
5	6	27	21	18	3	1	1	6	7	5	2	0	0
Total cells		245	202	189	13	5	4	27	29	18	11	9	0
Embryo D													
1	2	20	18	18	0	0	0	5	4	3	1	2	1
2	1	37	32	31	1	2	0	6	7	6	1	3	0
3	3	30	28	28	0	0	0	3	3	2	1	0	0
4	5	41	31	29	2	0	0	2	3	2	1	1	0
5	6	30	22	21	1	1	1	1	1	0	1	1	0
Total cells		158	131	127	4	3	1	17	18	13	5	7	1
Embryo E													
1	9	37	38	37	1	0	0	5	6	5	1	1	0
2	6	35	24	24	0	0	0	7	5	5	0	0	0
3	1	39	28	26	2	0	0	4	4	4	0	5	1
4	7	28	25	24	1	0	0	7	6	6	0	7	2
5	2	33	31	31	0	1	0	9	9	9	0	10	0
Total cells		172	146	142	4	1	0	32	30	29	1	23	3
Embryo E													
1	9	54	42	41	1	0	0	12	10	9	1	7	1
2	6	50	38	37	1	0	0	9	8	8	0	2	1
3	1	44	46	44	2	0	0	5	2	2	0	2	0
4	7	48	41	39	2	0	0	8	4	4	0	6	3
5	2	47	52	47	5	2	0	2	2	2	0	4	1
Total cells		243	219	208	11	2	0	36	26	25	1	21	6
Embryo F													
1	1	33	23	21	2	0	0	9	9	9	0	6	2
2	2	36	28	25	3	0	0	10	9	7	2	11	0

	3	3	36	28	26	2	0	0	14	10	9	1	9	0
	4	4	31	31	29	2	0	0	14	12	12	0	10	2
	5	5	36	27	26	1	0	0	7	6	6	0	13	1
Total cells			172	137	127	10	0	0	54	46	43	3	49	5
Embryo G														
	1	1	43	26	26	0	0	0	1	0	0	0	4	0
	2	2	34	28	27	1	0	0	0	0	0	0	5	0
	3	3	36	26	26	0	0	0	3	2	2	0	6	0
	4	4	44	31	30	1	1	0	5	5	5	0	3	0
	5	5	31	29	28	1	0	0	6	8	6	2	7	1
Total cells			188	140	137	3	1	0	15	15	13	2	25	1

## Pax3V2

7 Embryos		10 Placodes		Ectoderm					Mesenchyme					
		Pax3	GFP	Pax3/ GFP	Untargeted GFP	Islet1	Pax3/ GFP/ Islet1	Pax3	GFP	Pax3/ GFP	Untargeted GFP	Islet1	Pax3/ GFP/ Islet1	
Embryo A														
	Section													
	1	5	26	31	27	4	0	0	11	6	6	0	9	5
	2	7	27	22	20	2	0	0	12	6	5	1	12	5
	3	4	36	29	29	0	0	0	11	7	7	0	14	6
	4	6	24	26	19	7	0	0	11	12	9	3	17	7
	5	10	32	24	21	3	0	0	14	7	7	0	15	7
Total cells			145	132	116	16	0	0	59	38	34	4	67	30
Embryo A														
	1	5	21	13	12	1	0	0	4	2	2	0	7	1
	2	7	24	17	14	3	0	0	20	5	5	0	29	4
	3	4	23	17	14	3	0	0	6	4	4	0	6	4
	4	6	21	17	13	4	0	0	14	7	4	3	15	3
	5	10	0	0	0	0	0	0	11	10	9	1	9	5
Total cells			89	64	53	11	0	0	55	28	24	4	66	17
Embryo B														
	1	2	31	24	24	0	0	0	15	10	9	1	10	7
	2	6	46	20	20	0	0	0	11	8	6	2	18	5
	3	3	22	20	19	1	0	0	13	7	7	0	11	3
	4	1	27	20	15	5	0	0	15	6	5	1	5	1
	5	8	28	29	24	5	0	0	18	11	11	0	15	7
Total cells			154	113	102	11	0	0	72	42	38	4	59	23

## Embryo B

1	2	19	19	15	4	0	0	2	1	0	1	1	0
2	6	18	12	5	7	0	0	7	3	1	2	8	0
3	4	20	12	10	2	0	0	5	2	2	0	0	0
4	5	16	10	10	0	0	0	6	6	5	1	2	2
5	8	22	14	9	5	0	0	9	6	4	2	8	2
Total cells		95	67	49	18	0	0	29	18	12	6	19	4

## Embryo C

1	7	28	15	11	4	0	0	20	10	8	2	16	6
2	2	25	21	15	6	0	0	22	12	11	0	15	6
3	3	21	17	15	2	0	0	24	18	16	20	14	6
4	5	22	14	9	5	0	0	13	10	6	4	10	3
5	1	31	24	18	6	0	0	15	11	8	3	11	5
Total cells		127	91	68	23	0	0	94	61	49	29	66	26

## Embryo D

1	6	8	6	6	0	0	0	7	6	3	3	5	0
2	2	18	15	12	3	0	0	11	5	5	0	6	3
3	3	14	11	11	0	0	0	9	6	5	1	11	5
4	5	8	8	7	1	1	0	7	9	6	3	6	2
5	4	22	15	14	1	0	0	11	3	3	0	10	2
Total cells		70	55	50	5	1	0	45	29	22	7	38	12

## Embryo E

1	7	35	32	31	1	0	0	6	3	3	0	4	1
2	6	38	36	36	0	0	0	3	3	3	0	4	0
3	4	31	32	31	1	0	0	17	12	11	1	10	3
4	1	37	29	29	0	1	1	16	12	11	1	13	3
5	2	32	32	32	0	1	0	10	10	9	1	8	6
Total cells		173	161	159	2	2	1	52	40	37	3	39	13

## Embryo F

1	1	43	38	37	1	4	1	4	3	3	0	4	3
2	2	38	44	38	6	1	1	10	7	7	0	7	4
3	3	32	33	32	1	0	0	11	11	11	0	6	5
4	4	41	29	29	0	2	0	11	11	10	1	15	5
5	5	36	32	29	3	0	0	8	9	7	2	6	1
Total cells		190	176	165	11	7	2	44	41	38	3	38	18

## Embryo G

1	6	34	24	24	0	0	0	13	9	9	0	11	3
2	4	27	25	23	2	0	0	13	11	11	0	15	6



	3	2	36	25	25	0	0	0	17	11	10	1	16	8
	4	8	30	27	25	2	0	0	4	3	3	0	4	1
	5	5	40	28	24	4	0	0	23	13	13	0	19	6
Total cells			167	129	121	8	0	0	70	47	46	1	65	24
Embryo G														
	1	6	23	13	12	1	0	0	15	10	10	0	13	4
	2	4	22	19	18	1	0	0	6	4	4	0	7	3
	3	2	21	15	14	1	0	0	4	1	0	0	5	1
	4	8	25	14	14	0	0	0	13	10	9	1	17	4
	5	5	22	18	18	0	0	0	13	5	5	0	8	1
Total cells			113	79	76	3	0	0	51	30	28	1	50	13

Table 4 Cell counts of *in ovo* misexpression embryos at 14-16ss

pCIG		Ectoderm						Mesenchyme							
5 Embryos		9 Placodes		Pax3	GFP	Pax3/ GFP	Untargeted GFP	Islet1	Pax3/ GFP/ Islet1	Pax3	GFP	Pax3/ GFP	Untargeted GFP	Islet1	Pax3/ GFP/ Islet1
Embryo A															
	1	3	21	16	6	10	0	0	36	12	11	1	21	3	
	2	1	20	20	20	0	0	0	24	7	5	2	21	3	
	3	6	14	27	12	15	0	0	72	26	16	10	48	13	
	4	5	23	28	16	22	0	0	57	28	20	8	31	11	
	5	4	27	24	10	14	0	0	60	22	13	9	41	9	
Total cells			105	115	64	61	0	0	249	95	65	30	162	39	
Embryo A															
	1	4	17	37	10	27	0	0	75	19	16	3	58	10	
	2	6	5	20	1	19	0	0	59	17	12	5	42	8	
	3	7	0	17	0	17	0	0	23	17	9	8	27	6	
	4	1	26	22	9	13	0	0	36	7	3	4	6	0	
	5	3	12	25	6	19	0	0	67	17	13	4	37	11	
Total cells			60	121	26	95	0	0	260	77	53	24	170	35	
Embryo B															
	1	8	30	21	18	3	0	0	34	20	15	5	17	10	
	2	4	26	18	9	9	0	0	32	21	17	4	29	12	
	3	2	20	22	10	12	0	0	30	26	16	10	22	11	
	4	5	15	18	7	11	0	0	50	29	26	3	28	13	
	5	3	22	20	8	12	0	0	29	21	14	7	19	12	
Total cells			113	99	52	47	0	0	175	117	88	29	115	58	

Embryo B

1	2	24	21	13	8	0	0	32	18	17	1	27	9
2	10	17	27	9	18	0	0	28	23	18	5	17	11
3	1	24	21	8	13	0	0	22	11	11	0	9	6
4	5	24	22	9	13	0	0	32	11	11	0	20	6
5	9	13	35	11	24	0	0	34	21	18	3	20	10
Total cells		102	126	50	76	0	0	148	84	75	9	93	42

Embryo C

1	6	7	8	5	3	0	0	36	9	6	3	23	3
2	4	14	14	10	4	0	0	41	8	5	3	38	5
3	5	8	12	7	5	0	0	45	8	6	2	30	5
4	1	23	11	8	3	0	0	22	12	7	5	14	7
5	2	11	14	6	8	0	0	37	17	7	10	37	7
Total cells		63	59	36	23	0	0	181	54	31	23	142	27

Embryo C

1	1	8	30	6	24	0	0	13	13	10	3	9	6
2	2	12	27	7	20	0	0	18	16	11	5	15	8
3	3	7	21	6	15	0	0	15	15	8	7	8	7
4	4	9	25	5	20	0	0	19	21	15	6	19	14
5	5	10	15	7	8	0	0	23	20	14	6	18	13
Total cells		46	118	31	87	0	0	88	85	58	27	69	48

Embryo D

1	1	36	25	12	13	0	0	18	9	8	1	6	3
2	4	26	24	16	8	0	0	43	17	15	2	16	5
3	7	14	20	12	8	0	0	31	8	7	1	39	7
4	2	39	26	17	9	0	0	36	13	13	0	37	7
5	5	19	17	8	9	0	0	30	9	9	0	23	4
Total cells		134	112	65	47	0	0	158	56	52	4	121	26

Embryo D

1	1	21	19	11	8	0	0	13	14	14	0	17	10
2	2	17	18	10	8	0	0	15	18	14	4	21	12
3	3	15	28	15	13	0	0	9	7	6	1	13	6
4	4	8	18	7	1	0	0	14	13	11	2	11	7
Total cells		61	83	43	30	0	0	51	52	45	7	62	35

Embryo E

1	1	7	19	7	12	0	0	8	7	6	1	9	5
2	2	14	21	14	7	0	0	15	11	10	1	10	7
3	3	14	27	14	13	0	0	42	45	42	3	17	12

4	4	10	17	9	8	0	0	30	17	16	1	23	10
Total cells		45	84	44	40	0	0	95	80	74	6	59	34

### Pax3

4 Embryos		7 Placodes		Ectoderm				Mesenchyme					
		Pax3	GFP	Pax3/ GFP	Untargeted GFP	Islet1	Pax3/ GFP/ Islet1	Pax3	GFP	Pax3/ GFP	Untargeted GFP	Islet1	Pax3/ GFP/ Islet1
Embryo A													
1	4	36	24	24	0	0	0	2	2	2	0	4	0
2	8	26	20	20	0	0	0	7	4	3	1	46	2
3	2	32	15	15	0	0	0	12	7	7	0	5	0
4	1	35	29	25	4	0	0	9	7	7	0	8	3
5	6	24	17	17	0	0	0	2	2	2	0	8	0
Total cells		153	105	101	4	0	0	32	22	21	1	71	5
Embryo A													
1	5	19	15	15	0	0	0	17	10	10	0	18	0
2	2	38	22	22	0	1	0	11	9	8	1	7	0
3	6	13	12	12	0	0	0	8	8	8	0	25	0
4	4	18	15	15	0	1	0	5	5	5	0	16	0
5	3	27	16	16	0	0	0	4	2	2	0	14	1
Total cells		115	80	80	0	2	0	45	34	33	1	80	1
Embryo B													
1	2	45	27	24	0	0	0	2	2	2	0	5	0
2	3	40	24	23	1	0	0	9	9	3	6	6	0
3	6	30	20	18	2	0	0	9	8	6	2	10	0
4	8	28	6	6	0	0	0	13	7	5	2	6	0
5	4	54	27	22	5	0	0	8	4	3	1	7	1
Total cells		197	104	93	8	0	0	41	30	19	11	34	1
Embryo C													
1	4	52	44	42	2	0	0	21	9	8	1	25	1
2	1	51	33	33	0	0	0	25	17	17	0	19	2
3	6	38	30	30	0	0	0	12	8	7	1	18	1
4	3	36	31	31	0	0	0	26	16	16	0	23	2
5	2	42	30	30	0	0	0	12	9	9	0	26	2
Total cells		219	168	166	2	0	0	96	59	57	2	111	8
Embryo C													
1	7	14	10	10	0	0	0	17	12	10	2	13	0
2	3	23	19	16	3	0	0	12	9	7	2	21	1
3	5	24	19	16	3	0	0	10	7	6	1	14	0

4	6	21	10	10	0	0	0	18	13	13	0	13	0
5	2	19	11	11	0	0	0	17	15	8	7	29	0
Total cells		101	69	63	6	0	0	74	56	44	12	90	1

Embryo D

1	1	23	14	12	2	0	0	18	12	11	1	5	1
2	5	16	14	12	2	0	0	16	8	8	0	38	2
3	2	14	10	10	0	0	0	14	12	11	1	4	0
4	10	34	22	22	0	0	0	13	8	7	1	37	2
5	7	38	13	10	3	0	0	19	14	10	4	43	2
Total cells		125	73	66	7	0	0	80	54	47	7	127	7

Embryo D

1	1	48	37	36	1	0	0	2	2	2	0	33	0
2	5	39	33	33	0	0	0	3	2	2	0	2	0
3	6	34	27	27	0	0	0	5	5	5	0	37	2
4	3	33	32	31	1	0	0	5	3	3	0	26	0
5	4	27	24	24	0	0	0	3	2	2	0	15	0
Total cells		181	153	151	2	0	0	18	14	14	0	113	2

## Pax3V1

6 Embryos		11 Placodes		Ectoderm					Mesenchyme				
		Pax3	GFP	Pax3/ GFP	Untargeted GFP	Islet1	Pax3/ GFP/ Islet1	Pax3	GFP	Pax3/ GFP	Untargeted GFP	Islet1	Pax3/ GFP/ Islet1
Embryo A													
1	1	40	35	33	2	2	2	10	6	6	0	3	1
2	2	29	26	25	1	0	0	8	6	6	0	1	0
3	3	31	25	25	0	0	0	1	2	1	0	17	2
4	4	22	23	22	1	0	0	8	7	7	0	11	1
5	5	27	17	17	0	0	0	2	2	2	0	3	0
Total cells		149	126	122	4	2	2	29	23	22	0	35	4
Embryo A													
1	1	38	35	30	5	0	0	5	3	3	0	8	0
2	2	25	19	19	0	0	0	4	4	4	0	0	0
3	3	12	13	7	6	0	0	5	4	3	1	3	0
4	4	16	11	8	3	0	0	4	2	2	0	0	0
5	5	20	10	10	0	0	0	1	0	0	0	0	0
Total cells		111	88	74	14	0	0	19	13	12	1	11	0
Embryo B													
1	5	25	24	12	12	0	0	25	20	19	1	18	2
2	4	17	12	8	4	0	0	21	13	12	1	7	0

3	6	33	25	22	3	0	0	33	31	24	7	6	1
4	3	18	15	12	3	0	0	22	16	16	0	14	0
5	2	25	17	13	4	0	0	33	24	18	6	5	0
Total cells		118	93	67	26	0	0	134	104	89	15	50	3
Embryo B													
1	5	33	19	19	0	0	0	15	11	8	3	7	1
2	4	30	24	23	1	0	0	15	10	9	1	14	1
3	6	18	17	11	6	0	0	19	20	13	7	9	2
4	3	18	21	15	6	0	0	16	8	8	0	8	0
5	2	33	30	15	15	0	0	14	12	7	5	6	0
Total cells		132	111	83	28	0	0	79	61	45	16	44	4
Embryo C													
1	3	18	10	10	0	0	0	3	2	1	1	2	0
2	1	18	8	8	0	0	0	3	2	1	1	3	0
3	5	32	12	12	0	0	0	9	5	5	0	4	0
4	4	32	19	16	3	0	0	9	3	2	1	9	0
5	6	30	16	16	0	1	0	16	8	8	0	7	0
Total cells		130	65	62	3	1	0	40	20	17	3	25	0
Embryo C													
1	3	30	23	20	3	0	0	9	7	6	1	4	0
2	1	29	18	18	0	0	0	7	3	3	0	5	2
3	4	36	18	18	0	1	0	5	5	4	1	4	0
4	7	25	17	17	0	0	0	8	7	7	0	6	1
5	2	31	20	17	3	0	0	3	3	3	0	0	0
Total cells		151	96	90	6	1	0	32	25	23	2	19	3
Embryo D													
1	3	36	24	24	0	0	0	23	18	18	0	18	2
2	2	34	32	32	0	0	0	20	20	0	0	6	3
3	7	30	31	30	1	0	0	23	20	20	0	21	1
4	1	34	22	22	0	0	0	16	13	12	1	2	0
5	4	28	25	24	1	0	0	23	18	18	0	24	1
Total cells		162	134	132	2	0	0	105	89	68	1	71	7
Embryo D													
1	3	30	23	22	1	0	0	18	15	15	0	13	1
2	2	26	20	19	1	0	0	22	17	17	0	11	0
3	7	35	34	34	0	0	0	15	13	13	0	22	1
4	1	31	24	24	0	0	0	13	11	11	0	7	0
5	4	28	18	17	1	0	0	21	14	14	0	20	2
Total cells		150	119	116	3	0	0	89	70	70	0	73	4

Embryo E													
1	5	36	31	30	1	0	0	2	0	0	0	8	0
2	2	29	22	21	1	0	0	9	8	8	0	6	0
3	7	49	32	32	0	0	0	14	12	12	0	4	1
4	4	33	25	25	0	0	0	16	16	15	1	10	0
5	3	39	25	24	1	1	0	9	5	4	1	4	0
Total cells		186	135	132	3	1	0	50	41	39	2	32	1
Embryo F													
1	7	21	15	12	3	0	0	6	4	4	0	12	1
2	5	41	23	23	0	0	0	17	9	9	0	18	1
3	1	59	39	38	1	0	0	16	10	10	0	7	0
4	2	50	34	31	3	0	0	8	4	4	0	7	0
5	3	41	28	28	0	0	0	17	12	12	0	14	2
Total cells		212	139	132	7	0	0	64	39	39	0	58	4
Embryo F													
1	3	36	23	21	2	0	0	13	7	7	0	22	1
2	1	29	25	25	0	0	0	12	7	7	0	26	0
3	8	30	15	15	0	0	0	8	3	3	0	18	0
4	7	37	27	27	0	0	0	3	3	2	1	10	1
5	5	26	18	17	1	0	0	12	4	4	0	26	0
Total cells		158	108	105	3	0	0	48	24	23	1	102	2

## Pax3V2

5 Embryos		10 Placodes		Ectoderm				Mesenchyme					
		Pax3	GFP	Pax3/ GFP	Untargeted GFP	Islet1	Pax3/ GFP/ Islet1	Pax3	GFP	Pax3/ GFP	Untargeted GFP	Islet1	Pax3/ GFP/ Islet1
Embryo A													
1	7	23	17	17	0	0	0	11	14	9	5	46	2
2	2	19	14	13	1	0	0	32	38	33	5	34	4
3	5	13	9	8	1	0	0	11	8	8	0	35	4
4	1	16	16	10	6	0	0	16	17	14	3	11	4
5	3	17	11	8	3	0	0	25	23	16	7	40	4
Total cells		88	67	56	11	0	0	95	100	80	20	166	18
Embryo A													
1	7	26	18	14	4	0	0	17	14	13	1	23	5
2	2	31	19	14	5	0	0	26	23	19	4	27	9
3	5	32	21	16	5	0	0	22	21	19	2	27	8
4	1	32	27	23	4	0	0	17	21	13	8	15	4
5	3	37	26	25	1	0	0	24	19	15	4	32	7
Total cells		158	111	92	19	0	0	106	98	79	19	124	33

Embryo B														
1	5	27	24	19	5	0	0	14	10	10	0	5	0	
2	3	23	13	9	4	0	0	13	8	8	0	7	1	
3	6	20	11	7	4	0	0	1	1	0	0	3	1	
4	4	32	21	18	3	0	0	10	7	7	0	4	1	
5	2	18	19	12	7	0	0	8	7	5	2	4	3	
Total cells		120	88	65	23	0	0	46	33	30	2	23	6	
Embryo B														
1	5	17	16	12	4	0	0	5	4	4	0	8	0	
2	3	13	10	6	4	0	0	4	3	2	1	8	0	
3	6	11	9	8	1	0	0	4	4	4	0	12	3	
4	4	15	8	8	0	0	0	7	3	3	0	4	1	
5	2	17	11	10	1	0	0	3	2	2	0	2	0	
Total cells		73	54	44	10	0	0	23	16	15	1	34	4	
Embryo C														
1	1	14	9	6	3	0	0	6	8	6	2	15	2	
2	5	8	10	7	3	0	0	8	7	6	1	14	2	
3	4	7	6	5	1	0	0	6	8	4	4	10	0	
4	6	10	8	7	1	0	0	11	6	6	0	20	2	
5	3	17	13	8	5	0	0	14	9	9	0	18	3	
Total cells		56	46	33	13	0	0	45	38	31	7	77	9	
Embryo C														
1	5	21	21	16	5	0	0	14	21	12	9	14	3	
2	8	29	25	25	0	0	0	17	20	12	8	13	2	
3	6	42	36	33	3	0	0	36	35	27	8	27	8	
4	10	36	34	22	12	0	0	40	46	33	13	59	19	
5	2	40	40	28	12	0	0	15	15	14	1	12	2	
Total cells		168	156	124	32	0	0	122	137	98	39	125	34	
Embryo D														
1	4	51	38	35	3	0	0	26	30	21	9	39	9	
2	5	30	32	28	4	0	0	27	27	22	5	35	6	
3	1	26	26	20	6	0	0	14	17	12	5	11	3	
4	6	29	14	14	0	0	0	30	31	21	10	32	4	
5	2	52	48	42	6	0	0	15	16	12	4	19	8	
Total cells		188	158	139	19	0	0	112	121	88	33	136	30	

## Embryo D

1	4	22	21	16	5	0	0	29	27	25	2	43	8
2	8	14	15	14	1	0	0	17	17	15	2	16	6
3	5	23	14	13	1	0	0	28	27	24	3	32	7
4	6	19	12	11	1	0	0	35	29	29	0	44	11
5	1	22	25	21	4	0	0	18	20	18	2	23	8
Total cells		100	87	75	12	0	0	127	120	111	9	158	40

## Embryo E

1	1	26	24	24	0	0	0	11	13	11	2	22	7
2	2	21	15	15	0	0	0	11	9	9	0	12	3
Total cells		47	39	39	0	0	0	22	22	20	2	34	10

## Embryo E

1	3	29	16	16	0	0	0	15	11	10	1	19	4
2	6	16	19	15	4	0	0	10	12	10	2	18	7
3	2	27	21	21	0	0	0	20	13	13	0	23	5
4	5	21	19	19	0	0	0	11	14	11	3	16	5
5	1	36	22	17	0	0	0	17	17	14	3	29	8
Total cells		129	97	88	4	0	0	73	67	58	9	105	29

Table 5 Cell counts of cultured misexpression embryos in DMSO

## pCIG

6 Embryos	9 Placodes	Ectoderm						Mesenchyme					
		Pax3	GFP	Pax3/ GFP	Untargeted GFP	Islet1	Pax3/ GFP/ Islet1	Pax3	GFP	Pax3/ GFP	Untargeted GFP	Islet1	Pax3/ GFP/ Islet1
Embryo A													
1	40	13	15	4	11	7	2	8	4	4	0	9	4
2	43	3	13	2	11	0	0	8	9	7	2	12	6
3	46	4	20	1	19	2	0	7	9	5	4	10	4
4	53	10	9	6	3	0	0	4	3	1	2	11	1
Total cells		30	57	13	44	9	2	27	25	17	8	42	15
Embryos B													
1	61	13	18	11	7	4	1	1	3	1	2	5	1
2	64	15	19	13	6	3	3	3	5	5	0	8	5
3	67	13	18	7	11	4	1	5	3	3	0	5	3
Total cells		41	55	31	24	11	5	9	11	9	2	18	9



## Embryo C

1	99	15	29	13	16	2	2	11	9	6	3	17	6
2	105	14	15	9	6	1	1	12	11	6	5	17	5
3	108	20	18	16	2	2	1	15	10	8	2	16	8
4	111	22	17	15	2	2	2	8	5	3	2	17	3
5	114	22	10	9	1	2	1	5	7	5	2	13	5
Total cells		93	89	62	27	9	7	51	42	28	14	80	27

## Embryo D

1	117_1	15	27	15	12	5	3	8	7	4	3	10	4
2	120_1	9	14	7	7	0	0	10	18	4	14	17	3
3	123_1	19	25	16	9	3	3	9	8	4	4	19	3
4	126_1	11	16	6	10	1	1	11	5	3	2	17	3
5	129_1	12	11	2	9	0	0	7	6	2	4	10	3
Total cells		66	93	46	47	9	7	45	44	17	27	73	16

## Embryo D

1	117_2	19	10	9	1	4	3	6	4	3	1	17	3
2	120_2	23	5	5	0	2	0	6	2	2	0	15	2
3	123_2	14	9	7	2	0	0	7	3	3	0	13	3
4	126_2	14	11	8	3	2	0	7	0	0	0	10	0
5	129_2	4	10	3	7	3	0	5	4	2	2	6	2
Total cells		74	45	32	13	11	3	31	13	10	3	61	10

## Embryo E

1	148_1	10	21	8	13	0	0	3	5	2	3	8	2
2	151_1	12	21	12	9	0	0	6	8	4	4	9	4
3	154_1	15	21	11	10	0	0	4	4	4	0	5	4
4	157_1	22	17	16	1	1	0	3	5	3	2	4	3
5	161_1	5	15	4	11	2	1	2	2	2	0	5	2
Total cells		64	95	51	44	3	1	18	24	15	9	31	15

## Embryo E

1	148_2	14	24	11	13	0	0	3	3	3	0	3	2
2	151_2	16	26	13	13	0	0	4	3	2	1	5	2
3	154_2	19	19	12	7	1	0	4	7	3	4	5	3
4	157_2	14	19	13	6	1	1	3	4	2	2	5	2
5	161_2	7	18	6	12	0	0	3	4	3	1	4	3
Total cells		70	106	55	51	2	1	17	21	13	8	22	12

## Embryo F

1	57	27	29	26	3	2	2	9	10	9	1	25	8
2	61	29	32	26	6	0	0	7	8	6	2	11	6
3	64	17	15	13	2	2	2	5	7	4	3	11	4
4	67	13	9	7	2	1	0	6	6	5	1	10	5
Total cells		86	85	72	13	5	4	27	31	24	7	57	23

## Embryo F

1	72	24	15	15	0	3	2	6	7	4	3	10	4
2	73	15	30	15	15	0	0	7	7	5	2	12	5
3	76	19	33	17	16	0	0	1	3	1	2	6	1
4	82	19	20	15	5	8	8	7	8	6	2	9	6
Total cells		77	98	62	36	11	10	21	25	16	9	37	16

## Pax3

7 Embryos		11 Placodes		Ectoderm					Mesenchyme				
		Pax3	GFP	Pax3/ GFP	Untargeted GFP	Islet1	Pax3/ GFP/ Islet1	Pax3	GFP	Pax3/ GFP	Untargeted GFP	Islet1	Pax3/ GFP/ Islet1
Embryo A													
1	58	13	13	12	1	4	0	5	8	5	3	7	1
2	60	16	12	12	0	15	3	4	4	4	0	19	0
3	64	15	10	9	1	11	0	5	5	5	0	3	1
4	70	28	13	12	1	18	0	1	2	1	1	8	0
5	72	15	14	11	3	2	0	6	8	5	3	15	4
Total cells		87	62	56	6	50	3	21	27	20	7	52	6
Embryo B													
1	67	6	4	4	0	4	0	6	6	6	0	0	0
2	77	13	13	11	2	5	0	0	0	0	0	9	0
3	79	35	35	33	2	1	1	7	7	6	1	11	6
4	81	32	32	32	0	1	1	2	3	2	1	11	2
Total cells		86	84	80	4	11	2	15	16	14	2	31	8
Embryo C													
1	98	55	55	53	2	5	0	9	10	9	1	11	0
2	101	39	39	38	1	1	0	11	13	10	1	22	0
Total cells		94	94	91	3	6	0	20	23	19	2	33	0

## Embryo D

1	10	50	46	44	2	3	3	9	3	3	0	11	0
2	13	53	46	44	2	2	2	13	6	6	0	23	2
3	16	56	52	52	0	1	1	7	3	3	0	22	0
4	22	58	52	51	1	6	3	4	1	1	0	24	0
5	25	55	48	47	1	9	7	4	1	1	0	17	0
Total cells		272	244	238	6	21	16	37	14	14	0	97	2

## Embryo D

1	43	38	37	37	0	3	0	22	13	12	1	7	1
2	49	60	59	57	3	3	0	26	22	22	0	17	1
3	52	35	32	31	1	5	0	23	12	11	1	14	1
4	55	21	20	19	2	3	0	16	13	13	0	15	0
5	58	29	15	15	0	7	1	20	12	11	1	13	0
Total cells		183	163	159	6	21	1	107	72	69	3	66	3

## Embryo E

1	141	64	63	62	1	22	1	34	33	33	0	20	3
2	144	60	60	59	1	12	10	22	22	22	0	27	0
3	147	58	58	58	0	1	0	27	27	27	0	18	1
4	150	55	54	54	0	9	2	28	28	28	0	24	1
5	156	37	35	35	0	6	2	27	27	27	0	5	1
Total cells		274	270	268	2	50	15	138	137	137	0	94	6

## Embryo E

159	15	13	11	2	1	0	9	9	8	1	18	1
162	13	12	12	0	1	1	11	11	11	0	6	1
165	11	6	5	1	4	1	10	13	9	3	18	1
171	11	9	9	0	1	0	16	16	14	1	12	0
174	12	12	10	1	2	0	12	12	10	2	10	0
Total cells	62	52	47	4	9	2	58	61	52	7	64	3

## Embryo F

1	195	59	58	58	0	17	6	5	5	5	0	45	3
2	198	68	67	67	0	1	0	0	0	0	0	14	0
3	201	50	50	50	0	4	4	0	0	0	0	13	0
4	204	51	49	49	0	11	0	2	2	2	0	14	0
5	207	69	67	67	0	5	1	10	10	10	0	19	0
Total cells		297	291	291	0	38	11	17	17	17	0	105	3

Embryo F													
1	177	46	45	44	1	8	0	2	2	2	0	9	1
2	184	48	46	46	0	12	10	2	4	2	2	17	0
3	187	35	34	34	0	13	3	2	2	2	0	8	0
4	189	25	25	25	0	2	0	0	0	0	0	5	0
5	192	33	33	33	0	3	0	9	9	9	0	22	0
Total cells		187	183	182	1	38	13	15	17	15	2	61	1
Embryo G													
1	1	28	26	26	0	0	0	5	6	4	2	32	0
2	10	36	36	36	0	2	2	9	9	9	0	60	1
3	16	38	36	36	0	1	1	5	5	5	0	48	0
4	19	54	53	53	0	5	3	4	4	4	0	60	0
5	25	51	51	51	0	2	2	4	4	4	0	46	0
Total cells		207	202	202	0	10	8	27	28	26	2	246	1
Embryo G													
1	1	55	55	55	0	5	3	4	4	4	0	55	0
2	9	36	39	36	3	0	0	15	15	15	0	43	2
3	10	69	67	67	0	2	2	3	3	3	0	45	0
4	16	62	62	62	0	2	2	8	6	6	0	50	0
5	25	26	27	26	1	0	0	0	0	0	0	55	0
Total cells		248	250	246	4	9	7	30	28	28	0	248	2

## Pax3V1

4 Embryos	7 Placodes	Ectoderm						Mesenchyme					
		Pax3	GFP	Pax3/ GFP	Untargeted GFP	Islet1	Pax3/ GFP/ Islet1	Pax3	GFP	Pax3/ GFP	Untargeted GFP	Islet1	Pax3/ GFP/ Islet1
Embryo A													
1	20	40	38	37	1	8	5	10	9	8	1	27	3
2	23	39	37	37	0	4	1	8	6	6	0	25	4
3	29	44	44	44	0	3	0	3	3	3	0	16	1
4	33	62	62	61	1	3	0	8	8	8	0	17	1
5	42	44	42	42	0	4	2	1	1	1	0	14	0
Total cells		229	223	221	2	22	8	30	27	26	1	99	9
Embryo A													
1	29	22	19	18	1	1	0	1	1	1	0	4	0
2	33	28	25	25	0	0	0	2	2	2	0	24	0
3	42	20	16	16	0	3	3	1	1	1	0	7	0
Total cells		70	60	59	1	4	3	4	4	4	0	35	0

Embryo B													
1	1	33	32	32	0	1	1	5	7	5	2	6	3
2	4	23	23	23	0	0	0	9	8	7	1	14	1
3	7	21	22	21	1	4	0	12	10	9	3	12	1
4	16	20	20	20	0	1	0	2	1	1	0	6	0
5	22	38	36	36	0	4	1	7	7	5	2	10	1
Total cells		135	133	132	1	10	2	35	33	27	8	48	6
Embryo B													
1	1	13	11	10	1	1	0	6	7	3	4	0	0
2	4	14	13	13	0	0	0	12	12	10	2	5	0
3	7	16	14	14	0	4	0	12	14	12	2	8	0
4	16	16	15	15	0	0	0	6	8	6	2	11	1
5	22	23	22	22	0	4	1	8	7	7	0	20	2
Total cells		82	75	74	1	9	1	44	48	38	10	44	3
Embryo C													
1	28	31	30	28	2	1	0	7	4	4	0	11	3
2	31	33	30	30	0	4	1	9	4	4	0	6	3
3	34	21	21	21	0	0	0	2	2	2	0	30	0
4	37	36	35	35	0	1	1	9	4	4	0	11	4
5	41	27	24	24	0	5	3	9	6	6	0	7	3
Total cells		148	140	138	2	11	5	36	20	20	0	65	13
Embryo D													
1	50	50	49	48	1	6	3	13	15	12	3	2	0
2	53	41	38	38	0	1	1	7	8	5	3	5	0
3	59	49	46	45	1	2	0	10	9	9	0	3	0
4	65	36	34	34	0	0	0	14	12	11	1	4	0
5	68	36	34	33	1	4	2	8	9	7	2	8	2
Total cells		212	201	198	3	13	6	52	53	44	9	22	2
Embryo D													
1	50	31	26	26	0	11	0	14	19	13	6	20	1
2	53	21	19	19	0	3	0	10	8	7	1	18	1
3	59	19	13	13	0	0	0	13	9	9	0	24	5
4	65	12	9	9	0	4	0	7	7	5	2	13	1
5	68	19	14	14	0	2	1	9	4	3	1	12	2
Total cells		102	81	81	0	20	1	53	47	37	10	87	10

# Pax3V2

7 Embryos		14 Placodes		Ectoderm					Mesenchyme				
		Pax3	GFP	Pax3/ GFP	Untargeted GFP	Islet1	Pax3/ GFP/ Islet1	Pax3	GFP	Pax3/ GFP	Untargeted GFP	Islet1	Pax3/ GFP/ Islet1
Embryo A													
1	120	70	68	68	0	1	1	5	4	4	0	16	0
2	135	40	40	39	1	17	15	3	4	3	1	26	2
3	141	38	39	37	2	7	4	5	1	1	0	21	1
4	144	35	35	35	0	12	8	1	1	1	0	27	0
Total cells		183	182	179	3	37	28	14	10	9	1	90	3
Embryo A													
1	120	49	47	47	2	0	0	7	6	6	0	0	0
2	135	63	62	62	0	6	6	8	6	6	0	3	1
3	144	39	40	39	1	18	5	3	3	3	0	24	1
4	147	38	39	37	2	3	1	16	17	16	1	9	8
5	150	29	30	29	1	5	5	8	15	8	7	14	5
Total cells		218	218	214	6	32	17	42	47	39	8	50	15
Embryo B													
1	50	12	17	11	6	14	10	17	16	12	4	12	2
2	53	4	7	4	3	19	1	9	13	8	5	21	4
Total cells		16	24	15	9	33	11	26	29	20	9	33	6
Embryo B													
1	50	22	24	22	2	15	8	49	49	48	1	20	7
2	53	12	13	12	1	5	5	41	39	39	0	37	16
3	56	12	14	12	2	12	10	32	34	32	2	33	9
4	59	6	7	6	1	4	4	33	38	31	7	25	9
5	62	12	12	12	0	4	3	26	24	23	1	26	2
Total cells		64	70	64	6	40	30	181	184	173	11	141	43
Embryo C													
1	80	52	53	52	0	18	14	39	40	37	3	51	9
2	84	46	48	44	4	17	11	27	26	25	1	48	2
3	93	63	61	61	0	26	19	26	26	25	1	40	8
4	96	32	34	32	2	31	25	28	32	28	4	43	7
5	99	21	23	21	2	11	8	14	16	13	3	29	2
Total cells		214	219	210	8	103	77	134	140	128	12	211	28
Embryo C													
1	87	42	46	42	4	15	10	36	38	35	3	24	3
2	90	49	50	49	1	14	9	28	27	27	0	38	6
3	99	27	28	25	3	15	7	24	23	22	1	41	2

4	102	26	28	26	2	11	5	14	16	13	3	26	0
Total cells		144	152	142	10	55	31	102	104	97	7	129	11
Embryo D													
1	114	14	14	14	0	4	2	13	13	13	0	32	4
2	117	27	27	27	0	9	8	13	15	13	2	31	4
3	123	21	23	21	0	9	5	13	12	12	0	29	2
4	126	36	37	36	1	15	9	11	10	10	0	23	5
5	129	18	20	18	0	12	7	7	10	6	4	21	4
Total cells		116	121	116	1	49	31	57	60	54	6	136	19
Embryo D													
1	114	23	23	23	0	7	5	7	9	7	2	35	3
2	123	28	28	28	0	3	2	8	10	8	2	17	1
3	126	28	28	28	0	13	6	14	16	14	2	22	2
4	129	18	18	18	0	5	4	11	12	10	2	21	2
Total cells		97	97	97	0	28	17	40	47	39	8	95	8
Embryo E													
1	10	31	27	25	2	6	0	17	10	10	0	37	7
2	13	24	22	17	5	3	2	8	5	4	1	25	3
3	19	21	19	18	1	5	5	15	13	9	4	34	2
4	22	40	20	20	0	4	1	15	10	6	4	20	3
5	28	24	15	14	1	2	0	13	9	7	2	23	2
Total cells		140	103	94	9	20	8	68	47	36	11	139	17
Embryo E													
1	10	31	29	27	2	5	3	8	8	8	0	11	8
2	13	29	29	28	1	2	2	11	9	9	0	20	7
3	19	23	21	21	0	4	3	9	10	8	2	18	7
4	22	33	28	28	0	3	3	8	8	6	2	12	4
5	28	26	19	19	0	3	2	10	9	7	2	24	5
Total cells		142	126	123	3	17	13	46	44	38	6	85	31
Embryo F													
1	37	31	36	30	6	2	2	12	12	12	0	26	12
2	40	38	40	38	0	9	6	8	6	6	0	20	6
3	43	34	36	29	7	9	2	5	5	5	0	12	5
4	49	27	27	27	0	5	4	5	6	5	1	29	5
5	52	10	14	10	4	4	1	8	8	7	1	34	7
Total cells		140	153	134	17	29	15	38	37	35	2	121	35

Embryo F														
1	37	15	13	12	1	2	1	5	3	3	0	8	3	
2	40	18	15	15	0	3	2	4	3	3	0	7	2	
3	43	23	23	23	0	3	0	4	2	2	0	10	1	
4	49	22	22	22	0	1	1	4	3	2	1	4	1	
Total cells		78	73	72	1	9	4	17	11	10	1	29	7	
Embryo G														
1	57	22	24	22	2	1	1	7	9	7	2	8	5	
2	59	34	33	33	0	3	1	4	4	4	0	23	2	
3	62	34	34	34	0	8	5	6	6	6	0	20	6	
4	65	31	28	27	1	4	0	12	10	9	1	18	5	
5	68	21	20	19	1	9	4	5	5	5	0	23	4	
Total cells		142	139	135	4	25	11	34	34	31	3	92	22	
Embryo G														
1	74	29	27	27	0	5	2	10	9	8	1	10	4	
2	77	24	26	24	2	2	2	3	5	3	2	19	2	
3	80	25	24	23	1	6	0	5	7	5	2	19	5	
4	83	15	14	14	0	1	0	9	11	8	3	18	5	
5	87	32	35	29	6	11	1	8	13	7	6	27	5	
Total cells		125	126	117	9	25	5	35	45	31	14	93	21	

Table 6 Cell counts of cultured misexpression embryos in DAPT

pCIG

5 Embryos	10 Placodes	Ectoderm						Mesenchyme					
		Pax3	GFP	Pax3/ GFP	Untargeted GFP	Islet1	Pax3/ GFP/ Islet1	Pax3	GFP	Pax3/ GFP	Untargeted GFP	Islet1	Pax3/ GFP/ Islet1
Embryo A													
1	156	29	33	27	5	5	4	59	57	38	19	115	35
2	159	17	18	15	3	5	5	40	81	32	49	138	32
3	162	12	14	9	5	2	1	32	65	22	43	145	21
4	165	8	15	8	7	3	3	40	45	27	18	129	25
Total cells		66	80	59	20	15	13	171	248	119	129	527	113
Embryo A													
1	159	12	33	12	21	9	5	8	22	7	15	16	5
2	165	8	28	8	20	3	3	9	22	8	14	17	7
3	162	10	20	7	13	1	1	6	14	6	8	24	4
Total cells		30	81	27	54	13	9	23	58	21	37	57	16



Embryo B													
1	61	23	28	18	10	5	2	9	11	7	4	17	7
2	64	13	22	11	11	3	3	6	10	5	5	17	5
3	69	12	16	10	4	2	2	9	18	5	13	21	5
4	72	13	17	9	8	8	7	9	17	7	10	18	7
5	76	9	14	8	6	2	2	9	13	8	5	15	8
Total cells		70	97	56	39	20	16	42	69	32	37	88	32
Embryo B													
1	64	21	32	20	12	3	2	2	7	2	5	11	2
2	69	18	22	16	8	2	1	14	21	10	11	29	11
3	72	18	26	17	9	9	7	14	19	13	6	33	12
4	76	15	24	13	11	4	2	13	18	10	8	24	10
5	80	15	18	14	4	12	4	13	18	11	7	22	10
Total cells		87	122	80	44	30	16	56	83	46	37	119	45
Embryo C													
1	86	20	25	17	8	11	7	18	23	15	8	64	13
2	89	21	28	16	12	10	5	12	32	8	24	74	8
3	92	11	16	9	7	7	3	10	15	6	9	76	6
4	95	14	30	13	17	7	4	18	19	14	5	40	14
5	98	11	15	6	9	1	0	12	23	9	14	59	9
Total cells		77	114	61	53	36	19	70	112	52	60	313	50
Embryo C													
102		14	3	2	1	7	0	12	6	6	0	31	6
105		21	2	2	0	6	0	14	9	8	1	40	7
108		17	5	5	0	10	0	19	10	9	1	45	9
114		30	2	2	0	14	1	24	11	10	1	65	8
117		36	32	29	3	9	3	14	9	6	3	29	4
Total cells		118	44	40	4	46	4	83	45	39	6	210	34
Embryo D													
1	1	9	7	3	4	5	1	18	7	6	1	27	5
2	7	16	5	3	2	8	3	29	9	5	4	81	5
3	17	17	10	5	5	3	0	28	21	2	19	90	2
4	23	11	22	15	7	5	2	35	30	10	20	101	10
Total cells		53	44	26	18	21	6	110	67	23	44	299	22

Embryo D													
1	7	5	10	5	5	0	0	15	9	8	1	19	8
2	10	4	18	4	14	2	2	19	7	5	2	26	5
3	17	13	22	16	8	2	2	11	19	7	12	35	7
4	23	17	14	14	0	4	4	13	21	7	14	54	7
Total cells		39	64	39	27	8	8	58	56	27	29	134	27
Embryo E													
1	26	14	0	0	0	4	0	47	16	9	7	87	9
2	30	13	6	0	6	4	0	48	13	10	3	75	10
3	33	18	14	12	2	6	1	43	16	12	4	75	11
4	37	14	20	13	7	4	0	37	14	10	4	67	10
5	44	9	4	0	0	2	0	17	20	11	9	62	9
Total cells		68	44	25	15	20	1	192	79	52	27	366	49
Embryo E													
1	30	19	22	16	6	14	5	4	4	2	2	8	2
2	33	20	17	17	0	15	8	7	5	3	2	8	3
3	37	11	19	16	3	12	4	9	4	3	1	17	3
4	44	9	20	12	8	6	2	17	21	13	8	26	8
Total cells		59	78	61	17	47	19	37	34	21	13	59	16

## Pax3

8 Embryos	14 Placodes	Ectoderm						Mesenchyme					
		Pax3	GFP	Pax3/ GFP	Untargeted GFP	Islet1	Pax3/ GFP/ Islet1	Pax3	GFP	Pax3/ GFP	Untargeted GFP	Islet1	Pax3/ GFP/ Islet1
Embryo A													
1	36	58	45	43	2	7	2	6	6	5	1	21	0
2	40	35	36	35	1	0	0	9	12	9	3	9	1
3	44	24	28	23	5	0	0	10	12	10	2	10	2
Total cells		117	109	101	8	7	2	25	30	24	6	40	3
Embryo A													
1	36	38	30	28	2	7	3	19	12	11	1	143	2
2	40	30	32	29	3	0	0	26	24	24	0	88	2
Total cells		68	62	57	5	7	3	45	36	35	1	231	4
Embryo B													
1	123	34	34	32	2	2	1	2	2	2	0	22	0
2	128	28	26	26	3	4	0	12	8	8	4	13	0
3	133	21	22	18	3	1	0	12	12	12	0	30	7
Total cells		83	82	76	8	7	1	26	22	22	4	65	7

Embryo B													
1	123	39	37	36	2	2	0	18	11	11	0	55	2
2	128	34	33	33	1	2	0	10	3	3	0	73	2
3	133	11	10	9	2	0	0	16	6	6	10	145	1
Total cells		84	80	78	5	4	0	44	20	20	10	273	5
Embryo C													
1	5	32	26	23	3	2	2	1	0	0	0	6	0
2	16	60	58	58	0	0	0	17	16	16	0	23	5
3	20	44	40	37	3	4	4	20	14	11	3	31	3
4	28	36	36	33	3	2	1	15	13	13	0	33	1
5	32	44	45	42	2	1	1	15	15	15	0	84	3
Total cells		216	205	193	11	9	8	68	58	55	3	177	12
Embryo C													
1	16	48	47	47	0	2	2	14	15	14	1	9	2
2	20	34	36	33	3	0	0	19	13	13	0	6	2
3	32	37	37	35	2	4	0	27	27	27	0	10	1
Total cells		119	120	115	5	6	2	60	55	54	1	25	5
Embryo D													
1	92	54	50	50	0	0	0	28	27	27	0	53	2
2	97	39	38	35	3	2	0	21	23	21	2	51	4
3	104	56	56	54	2	7	0	16	16	15	1	87	1
4	109	34	34	33	1	3	1	4	7	4	0	95	1
5	112	37	38	35	2	6	1	17	17	17	0	90	0
Total cells		220	216	207	8	18	2	86	90	84	3	376	8
Embryo D													
1	92	66	62	62	0	0	0	27	27	27	0	9	3
2	97	58	57	56	1	3	2	30	30	30	0	20	5
3	104	42	40	40	0	2	0	28	27	26	1	55	2
4	109	34	34	34	0	0	0	6	6	6	0	62	1
5	112	56	57	54	2	1	0	9	9	9	0	75	0
Total cells		256	250	246	3	6	2	100	99	98	1	221	11
Embryo E													
1	38	69	70	67	2	11	7	33	36	31	5	9	2
2	41	73	75	73	2	9	3	28	28	26	2	14	1
3	44	71	73	68	5	15	4	12	10	8	2	23	0
4	53	46	47	42	3	4	2	30	30	28	1	36	1
5	65	61	63	61	2	5	3	29	29	29	0	42	1
Total cells		320	328	311	14	44	19	132	133	122	10	124	5

Embryo E														
1	38	77	80	75	5	6	2	28	28	20	5	35	4	
2	41	64	64	62	2	4	3	29	30	19	5	54	5	
3	44	66	69	64	4	0	0	23	23	20	3	44	6	
4	53	65	65	63	2	8	2	29	33	28	5	45	0	
5	65	87	88	87	1	14	2	31	32	31	1	62	3	
Total cells		359	366	351	14	32	9	140	146	118	19	240	18	
Embryo F														
1	71	15	9	9	0	15	1	19	0	0	0	38	0	
2	74	17	6	6	0	14	1	23	1	1	0	35	1	
3	77	15	12	12	0	9	1	14	4	4	0	24	1	
4	80	16	12	12	0	15	1	5	2	2	0	28	0	
5	83	15	15	15	0	4	1	6	8	6	2	28	0	
Total cells		78	54	54	0	57	5	67	15	13	2	153	2	
Embryo G														
1	99	43	45	43	2	6	2	20	22	18	4	42	5	
2	102	33	36	32	3	4	1	11	13	11	2	31	3	
3	105	37	38	37	1	10	7	21	20	20	0	37	3	
4	108	22	19	19	2	2	0	10	7	7	0	56	1	
5	111	44	44	40	2	8	2	37	37	34	3	109	5	
Total cells		179	182	171	10	30	12	99	99	90	9	275	17	
Embryo G														
1	99	20	21	20	1	16	1	16	16	16	0	17	2	
2	102	36	42	35	6	13	7	15	16	15	1	19	0	
3	105	48	50	48	2	15	7	25	23	23	0	23	1	
4	108	5	6	5	1	13	1	24	14	14	0	49	1	
5	111	25	26	23	2	27	4	13	15	13	2	24	5	
Total cells		134	145	131	12	84	20	93	84	81	3	132	9	
Embryo H														
1	143	32	29	29	0	0	0	8	7	6	1	41	1	
2	146	14	12	10	2	0	0	11	11	11	0	47	0	
3	149	27	26	25	1	0	0	6	7	6	1	46	2	
4	152	18	14	14	0	2	2	10	8	8	0	13	5	
5	155	14	14	13	1	2	1	11	7	7	0	18	2	
Total cells		105	95	91	4	4	3	46	40	38	2	165	10	

# Pax3V1

6 Embryo	11 Placode	Ectoderm						Mesenchyme					
		Pax3	GFP	Pax3/ GFP	Untargeted GFP	Islet1	Pax3/ GFP/ Islet1	Pax3	GFP	Pax3/ GFP	Untargeted GFP	Islet1	Pax3/ GFP/ Islet1
Embryo A													
1	3	35	35	35	0	5	1	3	3	3	0	17	0
2	9	39	38	38	0	3	1	1	1	0	1	24	0
3	12	43	43	43	0	3	3	3	3	3	0	23	2
4	18	40	39	39	0	0	0	4	2	2	0	36	2
5	24	40	40	40	0	1	1	5	4	3	1	29	3
Total cells		197	195	195	0	12	6	16	13	11	2	129	7
Embryo A													
1	3	31	33	30	3	2	2	13	11	10	1	32	4
2	9	48	48	47	1	2	2	7	3	2	1	27	1
3	12	54	54	54	0	3	3	11	6	5	1	39	1
4	18	46	45	45	0	0	0	18	20	16	2	45	10
5	24	52	40	40	0	1	1	16	10	10	0	35	6
Total cells		231	220	216	4	8	8	65	50	43	5	178	22
Embryo B													
1	51	9	11	9	0	0	0	2	3	2	1	25	0
2	54	10	10	10	0	2	1	2	4	2	2	12	0
Total cells		19	21	19	0	2	1	4	7	4	3	37	0
Embryo B													
1	39	27	28	27	1	0	0	3	3	2	1	38	2
2	42	31	31	31	0	3	3	1	3	1	2	17	1
3	51	23	24	23	1	1	1	2	2	2	0	78	0
4	54	30	30	30	0	3	3	4	5	3	2	83	2
5	45	21	22	21	0	0	0	0	0	0	0	20	0
Total cells		132	135	132	2	7	7	10	13	8	5	236	5
Embryo C													
1	60	37	35	35	0	2	2	2	2	2	0	50	0
2	63	33	33	33	0	5	5	5	5	5	0	52	2
3	66	45	45	45	0	3	3	3	3	3	0	35	2
4	69	46	43	43	0	2	2	3	2	1	1	32	0
5	72	36	36	36	0	2	2	2	2	2	0	25	1
Total cells		197	192	192	0	14	14	15	14	13	1	194	5

Embryo C														
1	78	43	43	43	0	7	4	3	3	3	0	27	0	
2	75	26	26	26	0	1	1	4	4	4	0	27	1	
Total cells		69	69	69	0	8	5	7	7	7	0	54	1	
Embryo D														
1	1	37	35	35	0	6	2	11	11	8	3	64	1	
2	4	36	36	35	1	3	2	13	12	11	1	44	3	
3	7	25	24	24	0	4	1	6	6	5	1	20	1	
4	10	27	28	26	2	5	1	9	10	8	2	44	0	
5	13	39	35	35	0	3	1	7	7	6	1	44	0	
Total cells		164	158	155	3	21	7	46	46	38	8	216	5	
Embryo E														
1	105	29	30	29	1	5	3	5	6	5	1	18	0	
2	108	39	39	39	0	7	7	12	12	12	0	18	0	
3	111	39	38	38	0	4	2	9	8	8	0	8	0	
4	120	56	58	55	3	2	2	15	17	14	3	2	0	
Total cells		163	165	161	4	18	14	41	43	39	4	46	0	
1	105	28	28	28	0	11	9	14	15	14	1	8	1	
2	108	43	43	42	1	10	4	23	21	21	0	26	2	
3	111	45	44	44	0	6	3	21	21	21	0	14	1	
4	120	51	48	48	0	2	0	24	23	23	0	30	3	
5	123	40	40	40	0	4	4	19	17	17	0	12	2	
Total cells		207	203	202	1	33	20	101	97	96	1	90	9	
Embryo F														
1	95	41	36	35	1	1	1	4	2	2	0	75	0	
2	107	53	53	53	0	6	2	2	2	2	0	53	1	
3	110	46	45	45	0	5	5	7	5	5	0	62	0	
4	113	46	45	44	1	3	1	6	6	6	0	59	1	
5	116	37	36	36	0	8	5	10	15	9	6	43	0	
Total cells		223	215	213	2	23	14	29	30	24	6	292	2	
Embryo F														
1	104	54	54	54	0	5	2	2	2	1	1	12	0	
2	116	31	31	31	0	0	0	4	3	3	0	23	1	
3	119	37	38	37	0	2	2	7	4	4	0	32	2	
4	122	36	36	36	0	11	6	9	8	6	2	36	6	
5	125	32	27	26	1	7	3	9	1	0	1	43	0	
Total cells		190	186	184	1	25	13	31	18	14	4	146	9	

# Pax3V2

7 Embryo		13 Placodes		Ectoderm					Mesenchyme				
		Pax3	GFP	Pax3/ GFP	Untargeted GFP	Islet1	Pax3/ GFP/ Islet1	Pax3	GFP	Pax3/ GFP	Untargeted GFP	Islet1	Pax3/ GFP/ Islet1
Embryo A													
1	6	16	18	14	4	0	0	4	6	3	3	11	3
2	14	9	13	8	5	2	2	28	30	27	3	55	26
3	21	12	10	10	0	2	2	10	10	9	0	61	2
4	25	25	25	25	0	2	2	8	8	8	0	25	8
5	29	15	17	15	2	0	0	11	11	11	0	24	8
Total cells		77	83	72	11	6	6	61	65	58	6	176	47
Embryo A													
1	14	18	20	18	2	0	0	24	24	23	1	36	16
2	33	13	15	12	3	2	0	7	6	6	0	16	5
3	17	15	17	14	3	2	1	14	14	14	0	26	10
Total cells		46	52	44	8	4	1	45	44	43	1	78	31
Embryo B													
1	52	24	25	21	4	1	0	8	7	5	2	10	5
2	56	24	24	22	2	0	0	12	11	10	1	28	10
3	60	35	38	34	4	2	2	23	21	18	3	95	18
4	64	18	16	16	0	4	0	16	15	14	1	38	13
Total cells		101	103	93	10	7	2	59	54	47	7	171	46
Embryo B													
1	68	38	39	38	1	0	0	17	16	15	1	98	14
2	72	13	12	12	0	3	0	26	28	26	2	76	21
3	76	23	23	23	0	3	3	19	21	19	2	85	17
Total cells		74	74	73	1	6	3	62	65	60	5	259	52
Embryo C													
1	171	34	34	23	11	9	6	24	14	12	2	26	9
2	174	25	33	24	9	4	3	31	24	17	7	38	15
3	178	32	43	31	8	3	1	20	18	11	7	20	6
4	180	26	34	25	9	8	2	16	12	5	7	27	5
5	183	19	15	14	1	1	0	13	8	8	0	23	4
Total cells		136	159	117	38	25	12	104	76	53	23	134	39
Embryo C													
1	183	33	36	33	3	0	0	53	20	18	2	65	15
Total cells		33	36	33	3	0	0	53	20	18	2	65	15

Embryo D														
1	192	39	39	37	2	2	1	6	6	6	0	2	0	
2	20	45	47	45	2	0	0	7	5	3	2	5	0	
3	208	50	47	45	2	3	3	5	7	5	2	9	1	
4	225	55	55	53	2	8	6	6	8	5	3	3	1	
5	199	40	37	37	0	0	0	2	0	0	0	4	0	
Total cells		229	225	217	8	13	10	26	26	19	7	23	2	
Embryo D														
1	192	34	34	34	0	5	4	14	8	8	0	19	7	
2	202	32	30	27	3	9	4	36	14	14	0	60	13	
3	208	22	21	19	2	3	2	50	30	30	0	99	29	
4	225	14	12	11	1	7	1	44	30	29	1	78	29	
5	199	30	30	27	3	3	2	26	19	18	1	42	18	
Total cells		132	127	118	9	27	13	170	101	99	2	298	96	
Embryo E														
1	1	29	30	28	2	2	1	31	35	25	10	44	21	
2	7	72	72	72	0	2	1	32	25	23	2	54	16	
3	10	53	57	54	3	7	7	21	24	20	4	33	12	
4	16	68	67	67	0	2	2	49	59	47	12	97	28	
5	22	62	62	62	0	8	8	37	41	37	4	80	26	
Total cells		284	288	283	5	21	19	170	184	152	32	308	103	
Embryo E														
1	1	14	0	0	0	16	0	20	12	10	2	38	8	
2	7	14	2	1	1	8	1	25	6	6	0	57	6	
3	10	6	1	1	0	12	1	26	12	12	0	63	11	
4	22	5	0	0	0	7	0	15	6	5	1	42	5	
Total cells		39	3	2	1	43	2	86	36	33	3	200	30	
Embryo F														
1	161	42	45	42	3	11	8	21	23	21	2	45	19	
2	164	43	45	43	2	11	6	21	20	20	0	57	17	
3	167	54	55	53	2	8	5	21	23	21	2	51	17	
4	176	30	33	30	3	5	4	18	20	18	2	59	16	
5	179	32	33	32	1	12	5	20		19	4	48	17	
Total cells		201	211	200	11	47	28	101	86	99	10	260	86	



Embryo F														
1	161	43	44	42	2	0	0	17	20	16	4	15	9	
2	164	48	51	48	3	0	0	17	17	17	0	30	15	
3	167	52	53	51	2	0	0	18	18	16	2	37	11	
4	176	40	44	40	4	0	0	19	18	18	0	20	16	
5	179	47	53	47	6	3	0	31	32	31	1	56	27	
Total cells		230	245	228	17	3	0	102	105	98	7	158	78	
Embryo G														
1	173	25	27	25	2	4	1	23	23	23	0	44	19	
2	185	55	55	55	0	18	8	51	49	47	2	54	41	
3	188	46	54	46	8	12	7	36	40	36	4	51	29	
4	191	61	63	61	2	6	5	38	38	38	0	39	34	
5	194	54	59	54	5	12	7	39	38	38	0	50	36	
Total cells		241	258	241	17	52	28	187	188	182	6	238	159	

## CURRICULUM VITAE

**Jason Samuel Adams**

801-691-8987  
adamsj@byui.edu

---

### EDUCATION

Brigham Young University, Provo, UT, 2008-present  
Projected graduation date is April 2012, Physiology and Developmental Biology,  
Doctorate of Philosophy (Dissertation abstract located at the end of CV)  
Boise State University, Boise, ID, 2005-2008  
3.50 GPA, Biology, Master of Science  
Palmer College of Chiropractic, Davenport, IA, 1999-2003  
3.81 GPA, Doctorate of Chiropractic  
Brigham Young University, Provo, UT, 1993-1999  
3.33 GPA, Pre-Physical Therapy, Bachelor of Science

### TEACHING EXPERIENCE

Online Instructor, Brigham Young University Idaho, 2010- present.  
Courses: Anatomy and Physiology (BIO264, BIO265) and Medical Terminology (HS280). I was the instructor for the pilot course of each of these online courses.  
Teaching Assistant, Brigham Young University, 2009-present.  
Courses: Advanced Physiology lab (PDBIO363) and Developmental Biology (PDBIO482)  
Teaching Assistant, Boise State University, 2005-2008.  
Courses: Anatomy and Physiology labs (BIOL264, BIOL265) and Developmental Biology lab (BIOL344)  
Physiology Instructor, Wellspring School for Healing Arts, Boise, ID, 2008.  
Course: Physiology  
Adjunct Faculty, Treasure Valley Community College, Ontario, OR, 2005.  
Course: Anatomy and Physiology (BIO231) This was an online course with an on-campus lab.  
Teaching Assistant, Palmer College of Chiropractic, 2000-2002.  
Course: Gross Anatomy I and II lab, Neuroanatomy lab, Histology lab, and Microbiology lab

### RELATED TEACHING EXPERIENCE

Curriculum Improvement Council Member, Brigham Young University Idaho, 2010-present.  
Recommend improvement in the online courses of Anatomy and Physiology (BIO264, BIO265) and Medical Terminology (HS280).

Biology Teaching Group Leader, Brigham Young University Idaho, 2011

Participate in biweekly meetings with online directors on teacher improvement and instruction. Conduct biweekly meetings with online biology instructors to teach techniques in improving online instruction.

Boise State Teaching Scholars Program Participant, Boise State University, 2007-2008.

This particular teaching scholar group was made up of six faculty members and a facilitator at Boise State University who met regularly throughout the school year. Our purpose was to stimulate dialogue and innovation in teaching, specifically on the topic of engaging first year students in their learning. As a group we combined our dialogue and innovation in a wiki, which was available to other faculty members at Boise State University as a resource.

## **RESEARCH EXPERIENCE**

Doctoral Research Assistant, Department of Physiology and Developmental Biology, Brigham Young University, Provo, UT, 2008-present (research advisor: Michael R. Stark).

Identification of isoforms for the transcription factor, Pax3

Analysis of the spatiotemporal expression patterns of the Pax3 isoforms

Experimentation in understanding the function of Pax3 isoforms in sensory neurogenesis

Understand the roles of signaling molecules in the differentiation of sensory neurons

Masters Research Assistant, Department of Biology, Boise State University, Boise, ID, 2005-2008 (research advisor: Julia T. Oxford).

Identification of isoforms for the Col11a1 protein

Analysis of the spatiotemporal expression patterns of the Col11a1 isoforms

Experimentation in understanding the necessity of Col11a1 isoforms in craniofacial development

## **RELATED RESEARCH EXPERIENCE**

Ph.D. Dissertation Research Assistant, Brent Feland, Department of Exercise Science, Brigham Young University, Provo, UT, 1999.

As an undergraduate, I participated with a Ph.D. candidate in stretching hamstrings of an elderly population, and measuring and recording the range of motion within this population at different time points.

Feland JB, Myrer JW, Schulthies SS, Fellingham GW, Measom GG. The effect of duration stretching of the hamstring muscle group for increasing range of motion in people 65 years or older. *Physical Therapy*, 2001; 81(5): 1110-1117.

## **PUBLICATIONS**

Lassiter RN, Ball MK, Adams JS, Wright BT, Stark MR. Sensory neuron differentiation is regulated by notch signaling in the trigeminal placode. *Developmental Biology*, 2010 Aug. 15;344(2):836-48.

Fang M, Adams JS, McMahan BL, Brown RJ, Oxford JT. The expression patterns of minor fibrillar collagens during development in zebrafish. *Gene Expression Patterns*, 2010 Oct-Dec; 10(7-8):315-22.

## **WORKS IN PROGRESS**

Identification of a Novel Pax3 Isoform and its Function in the Differentiation of Sensory Neurons in the Ophthalmic Trigeminal Placode.  
FGF and Notch Signaling in the Differentiation of Sensory Neurons in the Ophthalmic Trigeminal Placode.

## **POSTER PRESENTATIONS**

Pax3 splice form expression and isoform function in the trigeminal placode, Jason Adams and Michael Stark, Society for Neuroscience, 2010  
Sensory neuron differentiation is regulated by notch signaling in the trigeminal placode, Rhonda Lassiter, Matthew Ball, Jason Adams, Brian Wright, and Michael Stark, Society for Developmental Biology, 69<sup>th</sup> Annual Meeting, 2010  
Collagen type XI in zebrafish axial skeletal development, Jason S. Adams, Brian L. McMahan, Linda Mercer, Raquel J. Brown, and Julia T. Oxford, American Society for Matrix Biology Biennial Meeting 2008  
Developmental expression and function of collagen type XI in zebrafish (*Danio rerio*), Jason Adams, Lane McMahan, Raquel Brown, Jeremiah Maschmann, Linda Mercer, Julia Oxford, AAAS Pacific Division, Boise, ID, 2008  
Developmental expression of collagen type XI in zebrafish (*Danio rerio*), Jason Adams, Raquel Brown, Jeremiah Maschmann, Katey Irwin, Luke Woodbury, Linda Mercer, Julia Thom Oxford, AAAS Pacific Division, Boise, ID, 2007

## **WORK EXPERIENCE**

Chiropractor, Sole Proprietor, Nampa, ID 2003-2007

## **PROFESSIONAL QUALIFICATIONS**

Chiropractic license, 2003-2007, State of Idaho

## **PROFESSIONAL MEMBERSHIPS**

Society of Developmental Biology, 2009-current  
Idaho Association of Chiropractic Physicians, 2003-2004

## **AWARDS**

Doctoral Research Assistant, Department of Physiology and Developmental Biology, Brigham Young University, Provo, UT, 2008-present (research advisor: Michael R. Stark).

Teaching Assistant, Department of Physiology and Developmental Biology, Brigham Young University, 2009-present.

Graduated Magna cum laude at Palmer College of Chiropractic, 2003

## **GRANTS RECEIVED**

Recipient of Graduate Mentoring Award 2010-2011, Brigham Young University

Recipient of Graduate Mentoring Award 2009-2010, Brigham Young University

Recipient of Biology Department grant, 2007, Boise State University

Recipient of NASA-ISGC Graduate Student Fellowship, 2006-2007

Recipient of Ferguson Scholarship, 2001, Palmer College of Chiropractic

Recipient of departmental scholarship, 1999, Brigham Young University

## **COMPUTER SKILLS**

Blackboard, I-Learn, BrainHoney, Microsoft Windows, Excel Spreadsheet, PowerPoint, Photoshop, SAS statistical program, Adobeconnect, Microsuite

## **LANGUAGES**

Excellent Spanish reading and speaking abilities

## **PRINCIPAL TEACHING INTERESTS**

Anatomy, cell and molecular biology, developmental biology, embryology, general biology, histology, human biology, neurobiology, physiology

## **PRINCIPAL RESEARCH INTERESTS**

Identifying spatiotemporal expression of splice variants and understanding their function within an organism.

## **VOLUNTEER EXPERIENCE**

BSA Assistant Scoutmaster, Rock Canyon District, Provo UT, Unit 651, 2011.

Flag Football Coach, Utah Parks and Recreation, Provo, UT, 2011.

Assistant Football Coach, Utah Valley Football League, Provo, UT, 2010.

Soccer Coach, Utah Parks and Recreation, Provo, UT, 2009.

Chiropractic Clinic Abroad, Palmer College of Chiropractic, Cochabamba, Bolivia, 2002.

Volunteer Representative, Church of Jesus Christ of Latter-day Saints, Venezuela Caracas Mission, 1994-1996.